

Copyright is owned by the Author of the thesis. Permission is given for a copy to be downloaded by an individual for the purpose of research and private study only. The thesis may not be reproduced elsewhere without the permission of the Author.

Flow Control of Agricultural Spraying Machines

A Thesis in partial fulfilment of the requirements for the Degree of

Master of Engineering in Mechatronics

Massey University,
Palmerston North,
New Zealand.

Tobin Hall

2016

Abstract

New Zealand relies heavily on its agricultural industry. A large portion of this industry is pastoral farming, where livestock are raised to graze on pasture. This includes beef, sheep and dairy farming. An important aspect of this style of farming is maintaining pasture quality. In order to increase growth fertilisers are often applied to the pastures. This increases yields in both meat and milk production. However, the increased application of fertiliser is linked with diminishing water quality. While the effects of nitrogen leaching and the best ways to manage fertiliser use are still being investigated, it is clear that control over the application will become more and more important.

The Tow and Fert is a range of fertiliser machines designed and built in New Zealand by Metalform Dannevirke. The Tow and Fert range is capable of spraying a wide range of fertilisers including both soluble and non-soluble fertilisers. The Tow and Fert is unique in its ability to spray fertiliser slurries consisting of mixture ratios of up to three-parts fine particle fertiliser to one-part water. This is achieved by the use of a recirculating system. Currently there is next to no control on the flow rate of the machines and the application rate is determined by the speed the operator maintains.

The purpose of this thesis is to design and build a flow control system for the Tow and Fert product range and investigate the effect of the changing flow rate on the spray characteristics. The ability to spray such a wide range of fluids with drastically different properties presents many challenges.

Many flow meters were considered and a low cost ultrasonic sensor (TUF2000M) was installed and investigated. After limited success of the ultrasonic sensor, a simple turbine flowmeter was installed. A flow controller was developed and tuned. Based off a PID control loop, the controller was able to maintain flowrate well between 10 L/min and 25 L/min depending on the installed nozzle.

After flow control had been achieved, methods for assessing the impact of flow rate on spray characteristics and specifically spray distribution were investigated. Several prototypes were created and tested. A stationary patternator capable of continuous measurement was developed and tested. The patternator does not correctly measure the flowrates in low flow sections. Only half of the flow being applied to the platform is being measured. This causes highly nonlinear results in spray distribution measurement. The testing did show an increase of spray area with increasing flowrate. However, the true distribution can be improved when the low flow issues have been resolved.

Acknowledgements

I would like to thank my supervisor Dr. Gourab Sen Gupta for his help and guidance throughout my research and undergraduate studies.

Campbell and Geoff Easton of Metalform with whom it has been a pleasure to work. The Metalform assembly team for their help and putting up with the lengthy, loud periods of testing.

The Massey University workshop staff: Morio Fukuoka, Anthony Wade, Ian Thomas and Clive Bardell for their friendship, guidance and lengthy discussions about anything and everything.

Finally, I would like to thank my friends and family for their unconditional support and love.

Table of Contents

Abstract.....	i
Acknowledgements.....	ii
List of Figures	vi
List of Tables	viii
1 Introduction	1
1.1 Pastoral Farming and Soil Health	1
1.2 Precision Agriculture	1
1.3 Fertiliser Application Technology.....	2
1.4 Research Challenges and Objectives.....	3
2 Sprayers in Agriculture.....	4
2.1 Traditional Field Sprayer Setup.....	4
2.1.1 Booms and Boom Components	4
2.1.2 Nozzles	5
2.1.3 Control of Multi-Nozzle Boom Sprayers	7
2.2 C-Dax Sprayers	8
2.2.1 Trailed Units	8
2.2.2 Tractor Mounted Units	8
2.3 The Tow and Fert Range	10
2.4 The Tow and Fert 1000	10
2.4.1 Tow and Fert System Overview	10
2.4.2 Motor and Pump.....	11
2.4.3 Tank Agitation and Premixer.....	12
2.4.4 Retractable Spray Booms.....	13
2.4.5 Detachable Spray Heads	14
2.4.6 Spray Control and Electronics	14
2.4.7 Load Cells and Weight Measurement	15
2.5 Tow and Fert Nozzles	15
3 Volumetric Flowrate Measurement.....	18
3.1 Types of Flowmeters.....	18
3.1.1 Differential Pressure Flow Metering.....	18
3.1.2 Turbine and Related Flow Meters.....	19
3.1.3 Positive Displacement Meters	20
3.1.4 Electromagnetic Flow Meters	21
3.1.5 Ultrasonic Flow Meters	22

3.1.6	Summary of Flowmeters	24
3.2	TUF2000M Ultrasonic Flow Meters	24
3.2.1	About the TUF2000M.....	24
3.2.2	Installation of TUF2000M Flow Meters	25
3.2.3	Testing of the TUF2000M Flow Meters	28
3.2.4	Investigating TUF2000M Noise sources.....	31
3.2.5	Conclusions of TUF2000M	33
3.3	ZD1200 Impeller Flow Sensor	34
3.3.1	About the ZD1200 Flow Sensor.....	34
3.3.2	Installation of the ZD1200 Flow Meter onto the Tow and Fert	35
3.3.3	Measurement of Flow from ZD1200 Meter.....	35
3.3.4	Testing and Calibration of the ZD1200	36
3.3.5	System Nozzle Flow Characteristics	37
3.3.6	Motor Speed / Pump Pressure:.....	37
3.3.7	Nozzle Flow Characteristics.....	38
3.3.8	Testing Diaphragm Valve Consistency	38
4	Hardware and Software Design of Flow Controller	40
4.1	Controller Design and Specifications:	40
4.1.1	Microcontroller selection (ATmega2560)	40
4.1.2	Additional Electronics and Modules	41
4.1.3	Controller PCB Design	42
4.2	Prototyping Code Development	44
4.2.1	TUF2000M Communication Library.....	44
4.2.2	Linear Actuator Class Development.....	46
4.3	Controller Tuning	48
4.3.1	Actuator Positioning Tuning.....	48
4.3.2	Flow Control Overview.....	48
4.3.3	Ultimate Gain Tuning	49
4.3.4	Testing Proportional Flow Control.....	52
5	Spray Area Distribution	53
5.1	Spray Area Measurement	55
5.1.1	Vision Based Measurement	55
5.1.2	Mechanical Patternators.....	55
5.1.3	Scanning Patternators.....	56
5.2	Scanning Load Cell Panel.....	56
5.2.1	Design and Construction.....	57

5.2.2	Electronics and Code Development	58
5.2.3	Calibration and Signal Conditioning	60
5.2.4	Testing and Results	62
5.2.5	Evaluation and Conclusion	66
5.3	Stationary Patternator	67
5.3.1	Design and Construction	67
5.3.2	Flow Measurement and Calibration	67
5.3.3	Spray Characterisation Testing and Results	72
6	Conclusions and Future Work	76
	References	78
	Appendices	81

List of Figures

Figure 1 Precision Farming Cycle [5]	2
Figure 2 - Comparison of Dry and Wet Boom Types [8]	4
Figure 3 - Left: Teejet QJ200 Dry Boom Nozzle Body Right: Teejet Q17560A Wet Boom Nozzle Body [9]	5
Figure 4 - Left: TeeJet QJ360 Nozzle Body Right: TeeJet QJS-B3-AAA Stackable Nozzle Body [9].....	5
Figure 5 - Nozzle Geometry and Spray Pattern [11]	6
Figure 6 - Nozzle Configuration with 100% Overlap [11].....	6
Figure 7 – Example of Automatic Section Control [7]	7
Figure 8 - C-Dax Goldline 1500L Trailed Sprayer [18]	8
Figure 9 - C-Dax GoldLine Hi-Spec [19]	9
Figure 10 - C-Dax Promotional Content Showing Goldline Options [19]	9
Figure 11 - Tow and Fert Series [20]	10
Figure 12 - Tow and Fert System Overview	11
Figure 13 - Tow and Fert Front View	12
Figure 14 - Tow and Fert Boom Actuator.....	13
Figure 15 - Tow and Fert Manual Boom Operation	13
Figure 16 - Spray Head with Rubber Diaphragm Valve.....	14
Figure 17 - Existing Flow Control Overview	15
Figure 18 - Metalform TF40 Nozzle.....	16
Figure 19 - Importance of Nozzle Rotation for Spray Evenness	17
Figure 20 - Common Types of Differential Pressure Meters [25]	18
Figure 21 - Comparison of Axial and Radial Turbines [23]	19
Figure 22 - Comparison of Singe and Multi Jet Radial Turbine Meters [26]	20
Figure 23 - Left: Paddlewheel Meter Concept [28] Right: Example of Pelton Wheel Geometry [29] 20	
Figure 24 - Left: Elliptical PD Meter Flow Process [31] Right: Round Gear PD Meter	21
Figure 25 - Left: Fundamental EM Meter Setup Left: ABB Brand EM Flowmeter [33]	22
Figure 26 - Left: Ultrasonic Transit Time Meter Principle Right: Sono-Trak Ultrasonic Flowmeter [34]	23
Figure 27 - Doppler Flowmeter Working Principal [27]	23
Figure 28 - TUF2000M Flow Meter [36].....	25
Figure 29 - TUF2000M Pipe Installation Requirements [36].....	26
Figure 30 - Ultrasonic Transducer Z Installation [36].....	27
Figure 31 - Ultrasonic Transducer V Installation [36]	27
Figure 32 - Ultrasonic Transducer W Installation [36]	27
Figure 33 - TUF2000M Raw Flow Data - Closed Loop Testing	29
Figure 34- TUF2000M Filtered, Offset Corrected Flow Data - Closed Loop Testing	30
Figure 35 - TUF2000M Calculated Nozzle Flowrate - Closed Loop	30
Figure 36 - Oscilloscope Trace of TUF2000M Operation	31
Figure 37 - Trace of TUF2000M Pulse and Response.....	32
Figure 38 - Trace of TUF2000M Pulse and Response with Transducer Disconnected.....	33
Figure 39 - ZD1200 Flow Sensor Calibration Plot.....	34
Figure 40 - ZD1200 Installed	35
Figure 41 - ZD1200 Calibration Data	37
Figure 42 - Effect of Pump Pressure on Nozzle Flow Characteristics.....	38
Figure 43 - Nozzle Flow Characteristics	39
Figure 44 - Diaphragm Valve Testing	39
Figure 45 - Arduino Mega Microcontroller Development Board [40]	41
Figure 46 - SP483 Pinout [41].....	41

Figure 47 - VNH2SP30 pinout and chip as implemented on Pololu MD01B [42]	42
Figure 48 - HC05 Module (front and back) [43]	42
Figure 49 - Flow Controller PCB Layout	43
Figure 50 - Flow Controller and TUF2000M Meters	43
Figure 51 - Basic TUF2000M Query.....	45
Figure 52 - findLimits() Function Flow	47
Figure 53 - Control System Overview	49
Figure 54 - Flowrate Control – Rough Ultimate Gain Tuning.....	50
Figure 55 - Flowrate Control - Rough Gain Tuning	50
Figure 56 - Flowcontrol Tuning - Refinement	51
Figure 57 – Flowrate Control Tuning – Refinement.....	51
Figure 58 - Flowrate Proportional Control Testing - Simulated Speed Variation	52
Figure 59 - Ideal Spray Application	53
Figure 60 - Areas of no spray caused by reduced spray width	54
Figure 61 - Areas of excessive spray caused by increased spray width	54
Figure 62 - Example of Horizontal Spray Patternator [44].....	55
Figure 63 - Scanning Patternator [47].....	56
Figure 64 - Scanning Platform Experimental Setup	57
Figure 65 - Scanning Element.....	58
Figure 66 - Scanning Element Spacers	58
Figure 67 - TAL201 Load Cells	58
Figure 68 - Load Cell Scanner Electronics Overview	59
Figure 69 - Load Cell Scanner Electronics Schematic.....	59
Figure 70 - Load Cell Scanner Electronics PCB Layout	60
Figure 71 – Load Cell Calibration Raw Data	61
Figure 72 - Load Cell Calibration Filtered Offset-Corrected Data	61
Figure 73 - Effect of Filtering on Impulse Response	62
Figure 74 - Scan Platform Test Path.....	63
Figure 75 - Initial Scanning Patternator Testing.....	63
Figure 76 - Scanning Element Water Accumulation	64
Figure 77 - Scanning Patternator - Typical Pattern One	65
Figure 78 - Scanning Patternator - Typical Pattern Two	65
Figure 79 - Visual Indication of Spray Pattern.....	66
Figure 80 - Segmentation of Spray Pattern by Scanning Element	66
Figure 81 - YF-S401 Flow Sensor	67
Figure 82 - Stationary Patternator Flow Sensor Installation.....	68
Figure 83 - Patternator Flow Calibration Variance	69
Figure 84 - Patternator Discharge Characteristics	71
Figure 85 - Totalised Patternator Platform Flow	72
Figure 86 - Flowrate of first six spray sections.....	73
Figure 87 - Flowrate of central spray sections.....	73
Figure 88 - Reported Spray Distributions – TF20 Nozzle at 10, 12, 14, 16 and 18 Litres per minute ...	75

List of Tables

Table 1 - Tow and Fert 1000 Specifications	11
Table 2 - Metalform Nozzle Spray Rate and Spray Area	16
Table 3 - ZD1200 Calibration Data	34
Table 4 - ZD1200 CalibrationTest Data	36
Table 5 - Modbus Protocol Example Transaction	44
Table 6 - TUF2000M Relevant Registers	45
Table 7 - Patternator Flow Calibration Variance.....	69
Table 8 - Sensor Calibration Factors	70
Table 9 - Tow and Fert Nozzle Spray Density.....	71
Table 10 -Proportion of Flow Measured.....	74

1 Introduction

Farming is a huge part of New Zealand's history and contributes a large proportion of New Zealand's revenue [1]. The most popular form of farming in New Zealand is pastoral farming (also known as livestock farming or grazing), where pasture is grown to feed livestock. This type of farming includes production of meats like beef, lamb and mutton as well as the production of wool and milk. As of 2007, pastoral farmland made up 40% of the land in New Zealand [2]

1.1 Pastoral Farming and Soil Health

An important aspect of pastoral farming is maintaining good soil health. Soil nutrients levels are controlled to ensure sustainable production. Fertilisers are used to increase the nutrient content of the soil and increase fertility [3]. Nitrogen, phosphate and potassium are needed in large quantities and are commonly used fertilisers. Nitrogen is often applied in the form of urea. Phosphate is often applied in an artificial fertiliser called Superphosphate. Mixtures of these fertilisers as well as trace elements are also extremely common.

The use of fertilisers can increase pasture growth which affects the yields of both meat and dairy. However, excessive application can cause potential toxicities from excessive fertility [3]. Another issue associated with excessive application is the runoff and leeching into waterways. High nitrogen levels in waterways substantially stimulate plant growth and can have severely detrimental effects on water quality. In the Waikato region, during the 2002-2003 period, the average dairy farm applied 125kg of nitrogen per hectare per year. By comparison, sheep and beef farms applied only 9kg/ha/yr [4].

Another important aspect of maintaining soil health is the process of liming. Liming is the application of materials with high calcium and magnesium content [3]. This can neutralise soil acidity and increases soil bacteria activity. This is particularly important because the use of nitrogen fertilisers increase the acidity of the soil. Most liming products are not water-soluble and liming is typically performed by spreaders. Most spraying machines are not capable of spraying lime. There are however, a range of machines designed and built in New Zealand called the Tow and Fert range. The Tow and Fert range have been specifically designed to be able to spray both soluble fertilisers and non-soluble fertilisers in suspension. These machines are capable of spraying a much wider variety of fertilisers and pesticides than traditional boom sprayers. The Tow and Fert uses only one or two nozzles mounted much higher than traditional boom sprayers.

1.2 Precision Agriculture

Precision Agriculture has been defined in many ways. In simple terms, it can be defined as a holistic and environmentally friendly strategy in which farmers can vary input use and cultivation methods to match varying soil and crop conditions across a field [5]. There are several commonalities in the various definitions of the term precision agriculture: subfield spatial division, variability within the spatial divisions, efficiency of resource use, and the use of technology [6].

Precision agriculture relies heavily on the use of spatial data often stored and interpreted in geographical information systems (GIS). Spatial data is often collected using global positioning system (GPS) data. The process of precision agriculture has been represented as a five-step cycle shown in Figure 1.

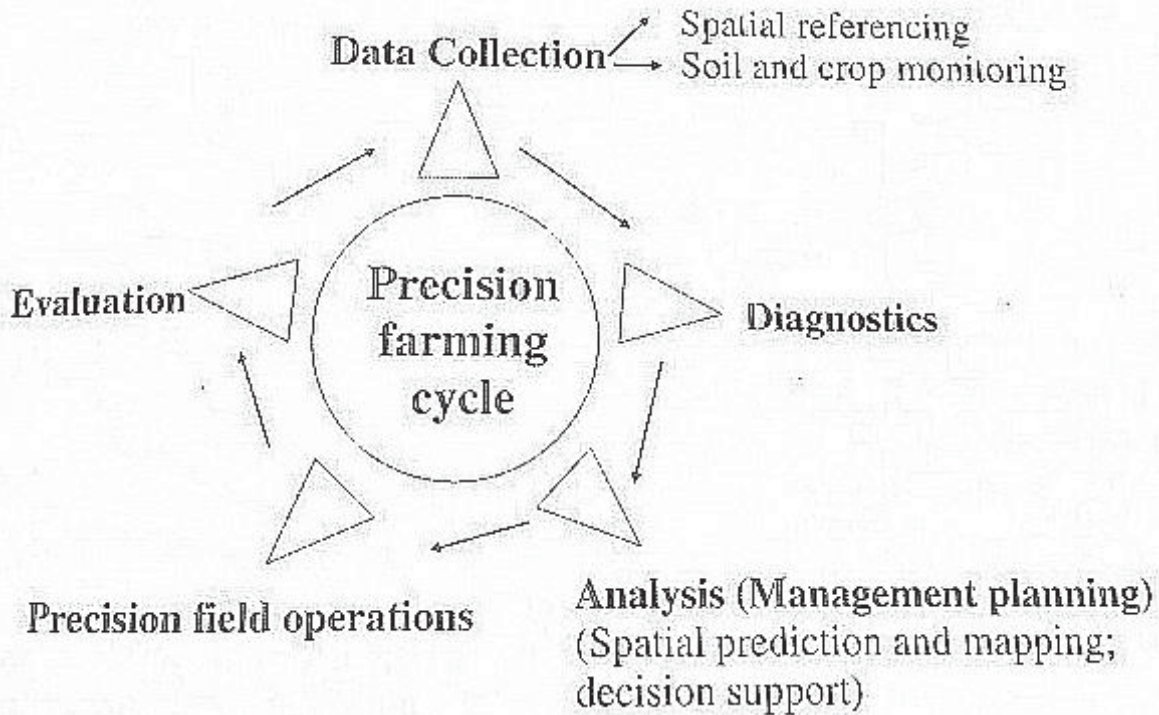


Figure 1 Precision Farming Cycle [5]

Three criteria are required for a precision agriculture implementation [5]:

1. Clear evidence of spatial variability in soil and crop conditions within a field or region.
2. Ability to identify and quantify the variability.
3. Ability to reallocate inputs and adjust management practices to improve productivity and reduce environmental degradation.

The work presented in this thesis is concerned with the third requirement, the ability to reallocate inputs. Control of application rate of fertiliser machines allow nutrients to be applied in a more cost-effective manner with less environmental impact.

1.3 Fertiliser Application Technology

Most fertiliser application is performed by spraying machines which spray water-soluble fertilisers. Aerial and ground application are both common practices. Aerial application includes spray from helicopters and aeroplanes.

A wide range of ground sprayers is available. Some sprayers are self-propelling machines built specifically for spraying but units that attach to tractors are common. Trucks and Utes are sometimes outfitted with a tank and booms for spraying. Ground sprayers consist of a tank for the fertiliser, one or more pumps, and one or more spray booms. These booms usually consist of a series of spray nozzles spaced around 380 to 750 mm apart. Many different styles of nozzles are available, with different spray characteristics. Boom height is typically around 500 mm from the ground depending on the nozzles and the required overlap etc. Spray nozzles come with tables relating nozzle spacing, nozzle spray angle, desired overlap and boom height. These boom sprayers work well with water-soluble fertilisers and pesticides but are not typically capable of handling insoluble fertilisers at all.

Because of the varied terrain of a lot of New Zealand farmland spraying machine in New Zealand tend to be smaller and more manoeuvrable than machines used on large areas of flat terrain. Retrofitted Utes, small trucks and trailed units are more common than large specially built sprayers.

An area of research on ground application sprayers is automatic section control. This involves turning on and off nozzles or sections of nozzles on the boom [7]. Coupled with electronic controllers and GPS information this can be used to reduce over application by turning off boom sections when they pass an already treated region. They could also be used to automatically stop application near waterways.

Currently the application rate of Tow and Fert sprayers is controlled purely by the traveling speed of the machine. This is achieved through the use of cruise control or simply by the operator. This can cause issues especially in irregular shaped or hilly paddocks where terrain dictates the travel speed. Often this will mean that the maximum speed of any section of the paddock becomes the speed of the entire paddock to ensure consistent application.

1.4 Research Challenges and Objectives

The aim of this research is to investigate methods in which the application rate of the fertiliser mixture can be decoupled by vehicle speed. This would remove the requirement of maintaining vehicle speed from the operator. It would also add the capability of adjusting the application rate based on location.

The Tow and Fert system was used during this research as a test platform. This platform offers an extremely versatile spray setup, but also presents several unique challenges.

Initially, flow meters were investigated for their suitability on the Tow and Fert System. Then a flow controller was developed and tuned. Once flow control had been implemented, a method for characterising spray width was sought. Because of the nature of the spray system, the flowrate has a large effect on the spray (or swath) width. The wide spray area of a single nozzle made traditional methods of measuring nozzle spray pattern infeasible. Several methods were explored to measure spray pattern in a continuous fashion. This thesis is split into six sections:

Chapter 2 investigates agricultural spraying machines. It contrasts traditional boom spraying machines and the Tow and Fert product range developed by Metalform. The Tow and Fert 1000 machine is described in detail.

Chapter 3 concerns the volumetric flowrate measurement of liquids with regards to fine-particle suspension slurries. The first part of this section is a review of flowrate measurement technology. The rest of this section describes the installation, calibration and testing of two different flowmeters that were investigated for use on the Tow and Fert machine.

Chapter 4 documents the creation of a flow controller for the Tow and Fert. The first part of this section describes the requirements of the controller, the selected electronic hardware, and the electronic circuit board design. The second part details the development of the code for the prototype controller. The final part of this section describes the testing and tuning of the controller.

Chapter 5 concerns spray distribution measurement. The first part of the section explores the issue of spray distribution measurement and investigates the existing technologies. The second and third parts detail the design, construction, and testing of two new concepts for continuous and semi-continuous spray distribution measurement.

Chapter 6 concludes the thesis and discusses potential future work and research possibilities.

2 Sprayers in Agriculture

Aerial and ground based spraying is common practice in agriculture. Sprayers are used to apply fertilisers, herbicides, fungicides and insecticides. Most sprayers used in agriculture use booms with numerous evenly spaced nozzles.

2.1 Traditional Field Sprayer Setup

2.1.1 Booms and Boom Components

Booms can be split into two broad groups, dry booms and wet booms. In dry booms the mechanical structure of the boom is independent of the spray carrying section of the boom. Additional piping or tubing is attached to the booms to deliver the spray solution to the nozzles. In wet booms the spray solution is carried through one of the structural members of the boom. Wet booms tend to be made of stainless steel, while the spray carrying section of dry booms is commonly made up of plastic tubing. Dry booms tend to accumulate more contaminants than wet, and are typically harder to clean [8].



Figure 2 - Comparison of Dry and Wet Boom Types [8]

Booms are typically split into sections and are actuated so that they can travel through gates etc. This actuation may be folding horizontally in toward the vehicle or folding vertically upwards.

Nozzles are attached to the booms using fittings that manufacturers call boom components or nozzle bodies. Nozzle bodies for dry boom setups are quite different from wet boom setups. In dry booms tubes are attached to the nozzle bodies. In wet booms, a hole is drilled into the boom, the nozzle body is inserted and clamps around the pipe. Figure 2 shows an example of a wet and dry boom nozzle body from the manufacturer TeeJet.



Figure 3 - Left: TeeJet QJ200 Dry Boom Nozzle Body Right: TeeJet Q17560A Wet Boom Nozzle Body [9]

Boom components are available that allow more than one nozzle to be attached. Some allow the operator to select which nozzle is currently in use by manually rotating each nozzle body. The TeeJet QJ360 is an example of such a nozzle body and is shown on the left in Figure 4.

TeeJet also has a stackable nozzle body series. This series allows multiple nozzle body modules to be attached together. These modules can be independently controlled by pneumatic, electric, spring loaded or manual check valves [9]. An example of a triple stacked nozzle body manifold with three air actuated nozzles is shown on the right of Figure 4.



Figure 4 - Left: TeeJet QJ360 Nozzle Body Right: TeeJet QJS-B3-AAA Stackable Nozzle Body [9]

2.1.2 Nozzles

A huge variety of nozzles is available from many manufacturers. Sometimes manufactures split nozzles into two groups, nozzles designed for herbicides, insecticides and fungicides, and fertiliser application nozzles. The reason for this separation is that herbicide, insecticide and fungicide application is almost always foliar (applied to the leaves of crops), whereas for fertiliser application typical application is soil-based. There is some research to suggest that foliar application of fertiliser (and more specifically nitrogen) can increase yields compared to soil application. However other research suggests that the difference is insignificant and can cause plant damage by scorching [10].

The geometry of nozzles varies greatly, each shape of nozzle produces a different spray pattern. The nozzle design also greatly impacts droplet size which is an important factor on spray drift. Figure 5 shows a range of nozzle geometries and their corresponding spray patterns.

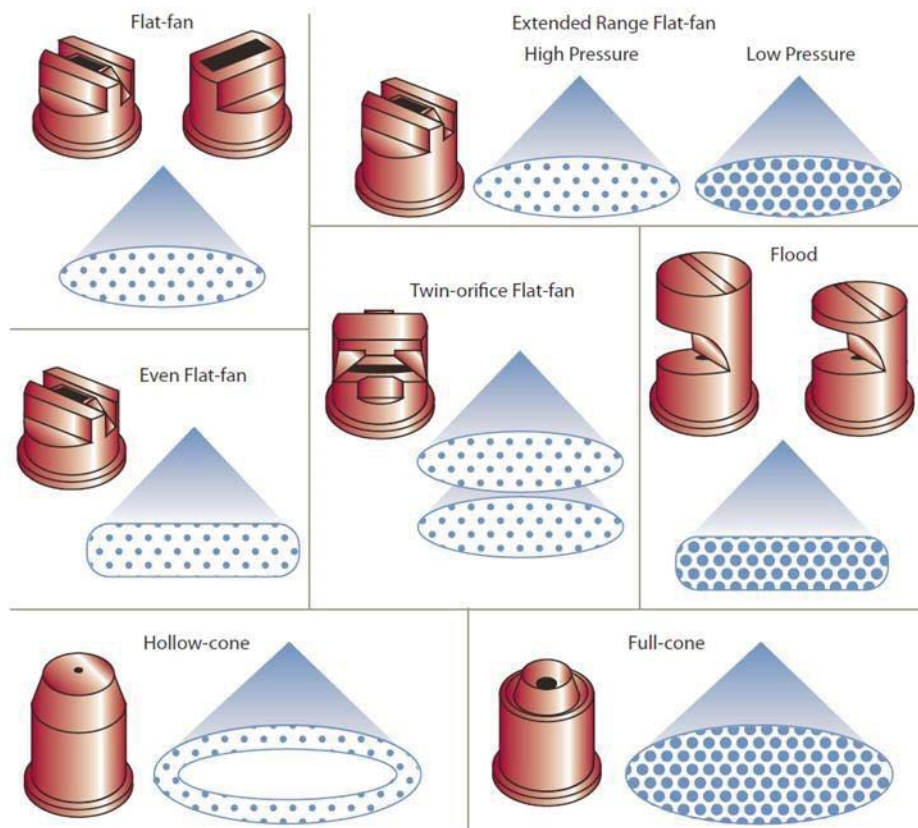


Figure 5 - Nozzle Geometry and Spray Pattern [11]

Nozzles are characterised by their geometry, rated pressure range and spray angle. The spray angle combined with the nozzle spacing can be used to determine boom height in order to maintain the correct amount of spray overlap. This data, and recommendations are provided by nozzle manufacturers for each nozzle or nozzle series.

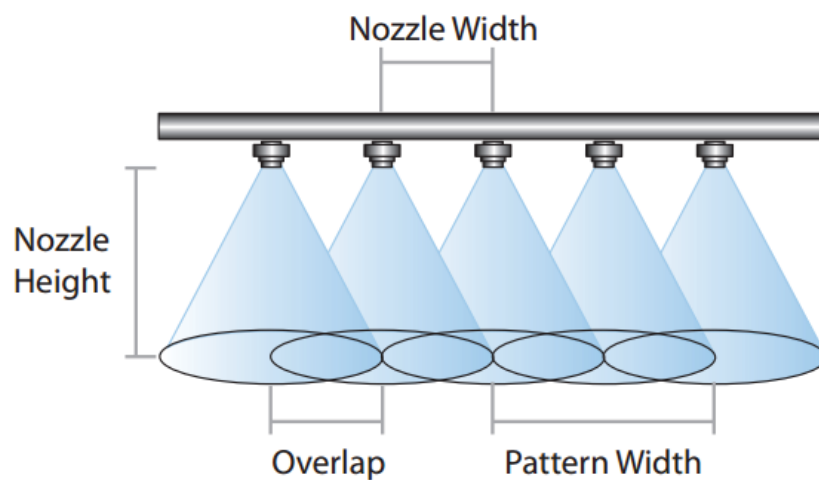


Figure 6 - Nozzle Configuration with 100% Overlap [11]

2.1.3 Control of Multi-Nozzle Boom Sprayers

There are two primary methods for controlling the flow rate of traditional sprayers, pressure based flow control and PWM based control [12]. Altering the pressure of the fluid in the boom changes the flowrate through the nozzles. This can be achieved by increasing pump speed etc. While the flow can be controlled in this manner, altering the pressure also changes the characteristics of the spray [13].

Another method of controlling flowrate is the use of pulse-width modulation (PWM). In PWM control the flow is switched on and off by the use of solenoid valves. Typical frequencies for the PWM signals used in flowrate controllers is around 10Hz [14]. The ratio between on time and total time of the valve is referred to as the duty cycle. Typically, the duty cycle for these types of controllers is varied between 10% and 100% [15].

PWM control can be implemented on entire booms, boom sections or individual nozzles. Obviously, control over boom sections or individual nozzles allows for more flexibility in the application. This comes at the expense of additional solenoid valves, requiring more control lines and more complicated controllers.

Having control over subsections of the booms allow for many otherwise impossible control systems. There has been research into a wide range of aspects including: compensating for horizontal boom oscillation [16], boom height oscillation [14] and sprayer turn compensation [17].

One of the control systems used industrially is automatic section control. Automatic section control uses GPS technology and mapping to turn on and off sections of the booms when approaching areas that have already been sprayed or are designated as no spray areas [7]. This reduces chemical use and reduces issues associated with over application. An example automatic section control application is demonstrated in Figure 7. It shows a 3 section sprayer in a spray zone approaching a no-spray zone at an angle.

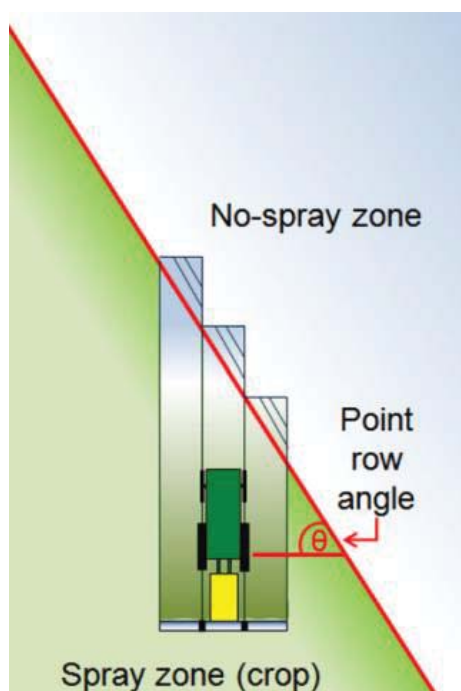


Figure 7 – Example of Automatic Section Control [7]

2.2 C-Dax Sprayers

C-Dax limited is a New Zealand based company that produce a range of agricultural equipment including sprayers, spreaders and pasture measurement systems. Within their sprayer range there are tractor-mounted, quad-bike-mounted and trailed units.

2.2.1 Trailed Units

Amongst the trailed units are the Goldline 1500L and 2500L machines. These machines have a main tank capacity of 1500 Litres and 2500 Litres respectively, but are otherwise very similar [18].

Standard Features Include:

- 100L foam marker tank with single foam marker
- 100L chemical rinse tank
- 10L fresh water tank
- 12m Hydraulic folding boom
- Adjustable length drawbar with swivel tow hitch
- 120L/min D123 pump
- Hydraulic parallelogram lift mast with suspension
- Max boom lift 1350mm—great for fence lines
- Geoline three section valve bank with electronic in-cab control

Several boom length options are available for both units: 12 meters, 14 meters, and 16meters. These booms can be fitted with a hydraulic folding option to allow remote boom closing for traveling through gates etc. Figure 8 shows the C-Dax Goldline 1500L Trailed Sprayer, on the right the hydraulic boom lifting feature is demonstrated.



Figure 8 - C-Dax Goldline 1500L Trailed Sprayer [18]

2.2.2 Tractor Mounted Units

C-Dax have a wide range of tractor-mounted options available. These options are mostly different combinations of tank sizes, boom lengths, pump options, and control systems. These are shown graphically in the promotional content shown in Figure 10



Figure 9 - C-Dax GoldLine Hi-Spec [19]

The parallelogram lift booms on both the trailed and tractor-mounted units are able to be lifted to navigate around uneven terrain, this can be seen in Figure 9. The lifting of the booms is controlled manually from inside the cab of the tractor.

Configure your own Goldline

Boom Components

- Boomjet Converters
- Induction Nozzle Tips
- Boom Suspension Frame

Controllers

- Electric Spray Control Kits
- TeeJet CentreLine 220
- CD50
- CD7

Booms

- I-Boom
- Superline
- CDA
- Manual som i-Boom
- Agri 5 Series Crossover
- Horticultural

Hose Reels & Kits

- 50m
- 100m
- 150m

Components

- Chemical Rinse Tank
- Chemical Induction Probe
- Foam Markers
- Foldaway Inspection Strip

Pumps

- M35
- M50
- M75
- D82
- D123

Tanks

- 600L Tank
- 800L Tank
- 1000L Tank
- 1200L Tank

CONFIGURE IT

LIMITED OFFER FROM C-DAX:

TeeJet CentreLine 220 Option at an incredibly low price!

The compact CentreLine 220 is designed to let you profit from GPS lightbar guidance with any field operation. Inside the compact guidance system is a high-quality GPS receiver and the guidance capabilities that make TeeJet leaders in lightbar guidance. This compact unit is fully portable, easy to install, and very quick to get going with—just enter your swath width and drive. Straight line (parallel) and curved AB modes available.

2190-1790

CALL 0800 230 230 FOR A QUOTE

C-Dax Goldline PASTURE SOLUTIONS

Figure 10 - C-Dax Promotional Content Showing Goldline Options [19]

2.3 The Tow and Fert Range

The Tow and Fert series is a series of spraying machines developed by Metalform (Dannevirke). There are three systems in the Tow and Fert range, the Multi 1200, the Multi 1000, and the Multi 4000. The number corresponds to each unit's capacity in litres.

The Multi 1200 has a three-point linkage for attachment to tractors while the Multi 1000 and Multi 4000 are trailed units. The Multi 1200 has a single boom and spray nozzle, the Multi 1000 and Multi 4000 have two retractable booms and nozzles. The Multi 1000 and Multi 4000 are similar conceptually, however the Multi 4000 has a hydraulically driven pump powered by a tractor while the Multi 1000 has a petrol driven motor so the unit can be used in with a Ute or tractor.



Figure 11 - Tow and Fert Series [20]

The biggest feature of the Tow and Fert range is that it is designed to be capable of spraying a large range of different fertiliser products. The mixing tanks are fitted with a patented agitation system and the booms are designed to have constant recirculation back into the tank. This allows the system to handle fine particle non-soluble fertilisers as well as liquid or soluble fertilisers simultaneously. Mixtures of one-part water to three parts fine particle fertilisers are possible. The Tow and Fert range can handle four forms of materials [20]:

- Water soluble fertilisers - Urea, Sulphate of Ammonia, etc.
- Fine particle insoluble fertilisers (100 micron or less) – Lime, RPR, Humates, etc.
- Liquid fertilisers – Liquid Seaweed Solutions, Fish Emulsions, etc.
- Biologically active fertilisers – Compost Teas, etc.

The capability of mixing and spraying this wide variety of materials makes the Tow and Fert range an extremely flexible system that can be used in both organic as well as traditional farming.

The range was developed out of the need for farmers to have the ability to apply fine particle/dissolved/slurry/biological fertilisers themselves. As such the Tow and Fert range is primarily marketed toward farmers however the line is also popular with contractors. Initially dairy farmers were the sole market for the range however, Metalform recently discovered additional opportunities in the avocado and macadamia nut farming industries in Australia.

2.4 The Tow and Fert 1000

2.4.1 Tow and Fert System Overview

The Tow and Fert 1000 is a trailer unit with standalone petrol driven pump. Table 1 shows the specifications of the Tow and Fert 1000 [21].

Table 1 - Tow and Fert 1000 Specifications

MODEL	Multi 1000
TANK-VOLUME	1000 litres (255 gallons)
APPLICATION-RATE	70 – 800 litres/hectare
AREA-PER-LOAD	approx. 6-12hectares
SPRAY-WIDTH	14-24metres
PUMP-MODEL	Metalform Stainless 3" Centrifugal Trash Pump
PUMP-PERFORMANCE	1300litres per minute at 0 metres lift. Max lift = 4 metres
ATTACHMENT-STYLE	Trailed
ATTACHMENT-VEHICLE	Tractor or 4wd Ute
PUMP-POWERED-BY	On board Petrol Engine
AGITATION-POWERED-BY	On board Petrol Engine
DRY-WEIGHT	650kg
FULL-WEIGHT	2,200kg
SIZE	4.30m (L) x 1.80m (W) x 1.70m (H)

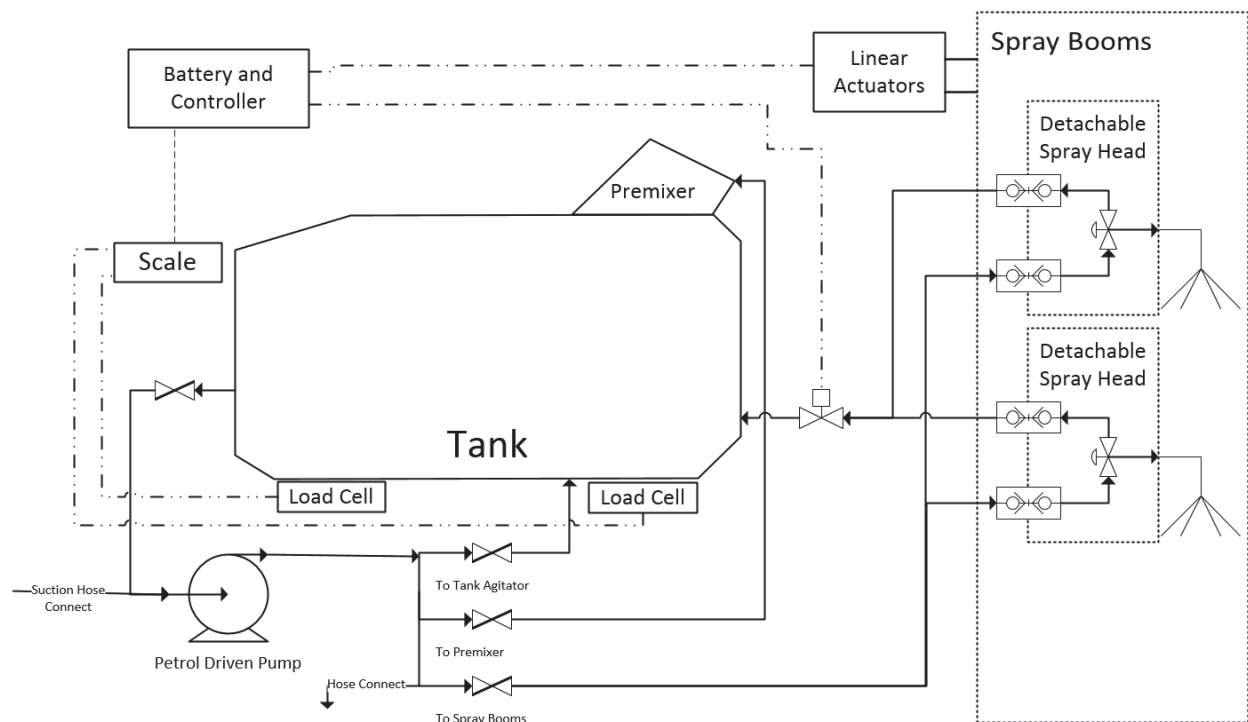


Figure 12 - Tow and Fert System Overview

2.4.2 Motor and Pump

The Tow and Fert 1000 is fitted with a 7HP petrol motor that drives a centrifugal pump designed and created by Metalform. The motor has both a pull start mechanism and an electric starter motor. The motor also charges the battery and provides additional power to run the electrics of the machine.

The pump pumps fluid from the tank into a distribution manifold. The manifold has valves to control fluid flow to the tank agitator, the spray booms and the premixer.

The pump is a centrifugal trash pump capable of pumping at 1300 litres per minute and maximum lift of 4 meters.

2.4.3 Tank Agitation and Premixer

The tanks of the Tow and Fert range have been specifically designed to enable recirculation and constant agitation of the fluid. This ensures that fine particles remain in suspension.

The premixer is a section of the tank where solids can be added that are gradually mixed into the main tank by a fluid stream. This premixing is essential to ensure a homogenous mixing of particles into the fluid.



Figure 13 - Tow and Fert Front View

2.4.4 Retractable Spray Booms

The Tow and Fert has two spray booms that can be automatically extended and retracted by a pair of linear actuators. This feature allows for the Tow and Fert to be moved through gates without the need to leave the vehicle to retract the booms.



Figure 14 - Tow and Fert Boom Actuator

In case of power or electrical failure, the booms can be opened or closed manually because of a mechanism on the spray booms. This is important, as the linear actuators cannot be moved manually because they are self-locking.



Figure 15 - Tow and Fert Manual Boom Operation

If the booms are forced to move the ramp forces the booms to be lifted up (overcoming gravity and the force of the springs) and allows the boom to be moved to the next position where they lock into position again. The boom should be replaced in the original position again before using the linear actuator mechanism again otherwise damage may occur.

2.4.5 Detachable Spray Heads

The Tow and Fert has a detachable spray head on the end of each spray boom. The spray heads have a pressure controlled diaphragm valve and removable nozzles. The valve has a spring-loaded mechanism with three positions. In the locked position, the lever forces the rubber diaphragm closed so that no fluid can flow.

In the open position, the lever forces the valve open and fluid can flow from the nozzle.

In the spray position, the spring applies a load to keep the valve closed however, when sufficient pressure is reached the valve opens and spray commences.

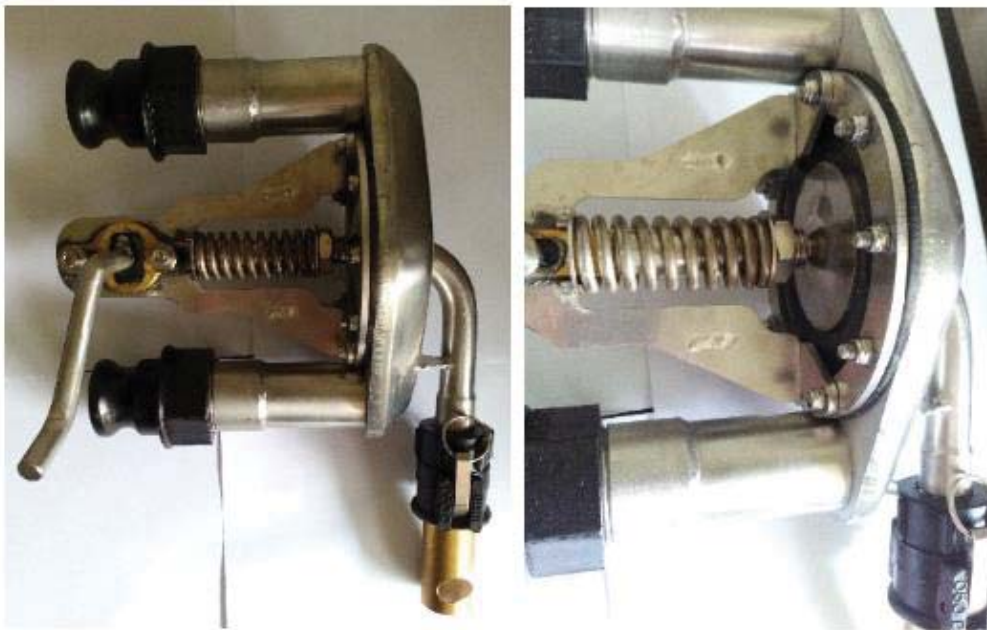


Figure 16 - Spray Head with Rubber Diaphragm Valve

2.4.6 Spray Control and Electronics

A wireless controller on the Tow and Fert is able to open and close the spray booms and also start and stop the spray if the spray heads are in the spray position. The wireless is implemented using an off the shelf four channel LR8824 wireless relay unit. The two boom extending linear actuators are wired to a single channel of the unit, with one button press on the wireless remote, both booms extend. They are retracted when the button is pressed again. Another channel is used to extend and retract the linear actuator attached to the flow control butterfly valve.

As mentioned in section 2.4.5, when the spray heads are in the spray position once a certain pressure is reached the diaphragm valve open and spray begins. This pressure is altered by a butterfly valve on the return lines of the booms back to the tank.

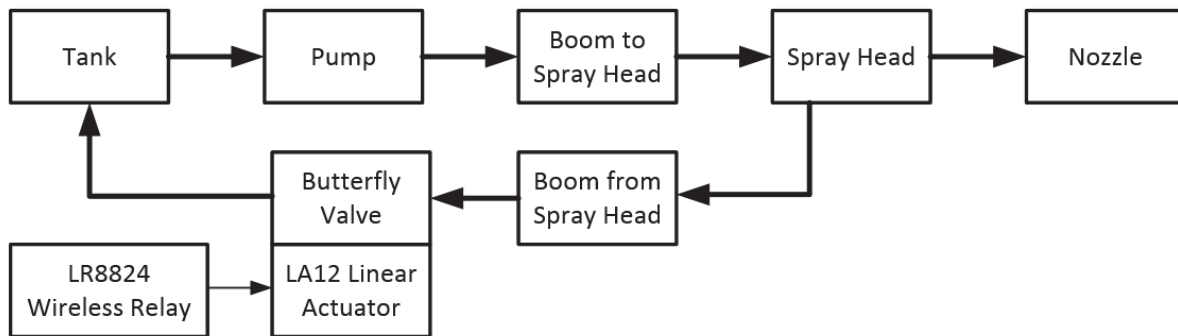


Figure 17 - Existing Flow Control Overview

When the valve is open the pressure drop in the booms is fairly low (coming only from fluid friction in the pipes). When the valve is closed the pressure increases drastically and the diaphragm opens allowing fluid to the nozzles. There is a hole in the disc of the butterfly to ensure that the majority of fluid is still circulated back into the tank. This flow helps to ensure that particles remain in suspension in the fluid.

It is important to note that the desired flow rate is controlled by the pressure at the manifold. This pressure is controlled crudely by the speed of the pump. The desired flow rate and pressure are related to the fluid properties by a calculator developed by Metalform based off empirical data.

2.4.7 Load Cells and Weight Measurement

To better control the composition of the fluid mixture the Tow and Fert tank is suspended entirely on four load cells. These load cells are wired back to a PT200X unit where the weight is displayed.

Knowing the weight of each element as it is added into the machine allows for an easy way to measure out the components of the mixture. It also allows for confirmation of application rate. The difference of weight divided by the spray area will give an average application rate of mixture.

2.5 Tow and Fert Nozzles

During the development process of the Tow and Fert range Metalform also developed specialised spray nozzles. The nozzles are designed to be inverted compared to a traditional nozzle. The reason for this unusual requirement is the slurry mixtures the Tow and Fert range is capable of spraying. When the slurry mixture ceases to be agitated, the fine particles previously distributed in suspension settle down. Depending on the mixture, these solids can form solid slugs that harden and block the flow is started again. With inverted nozzles when the fluid flow is removed, the nozzles and connecting tubes self-drain and no blockage is formed.

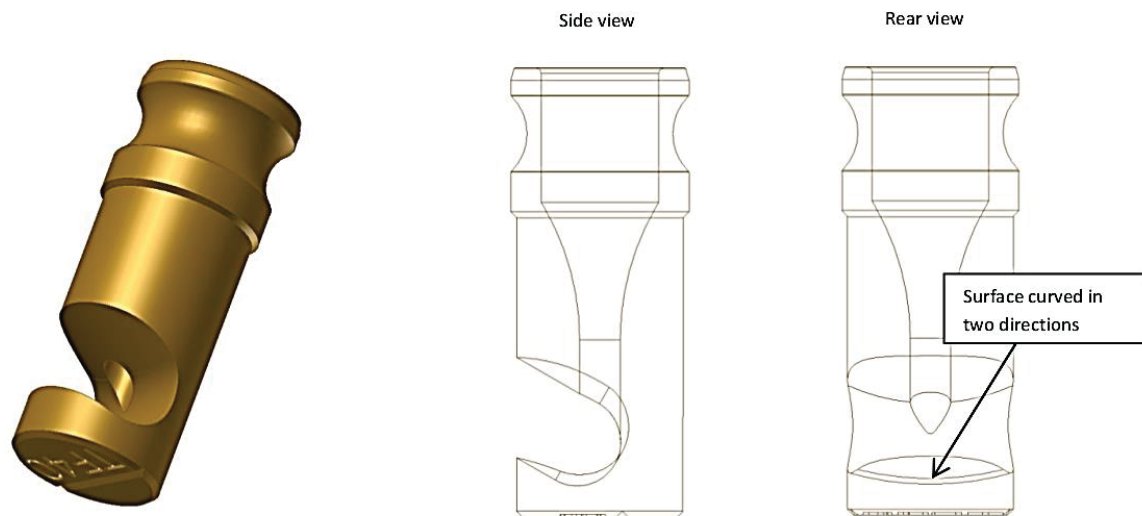


Figure 18 - Metalform TF40 Nozzle

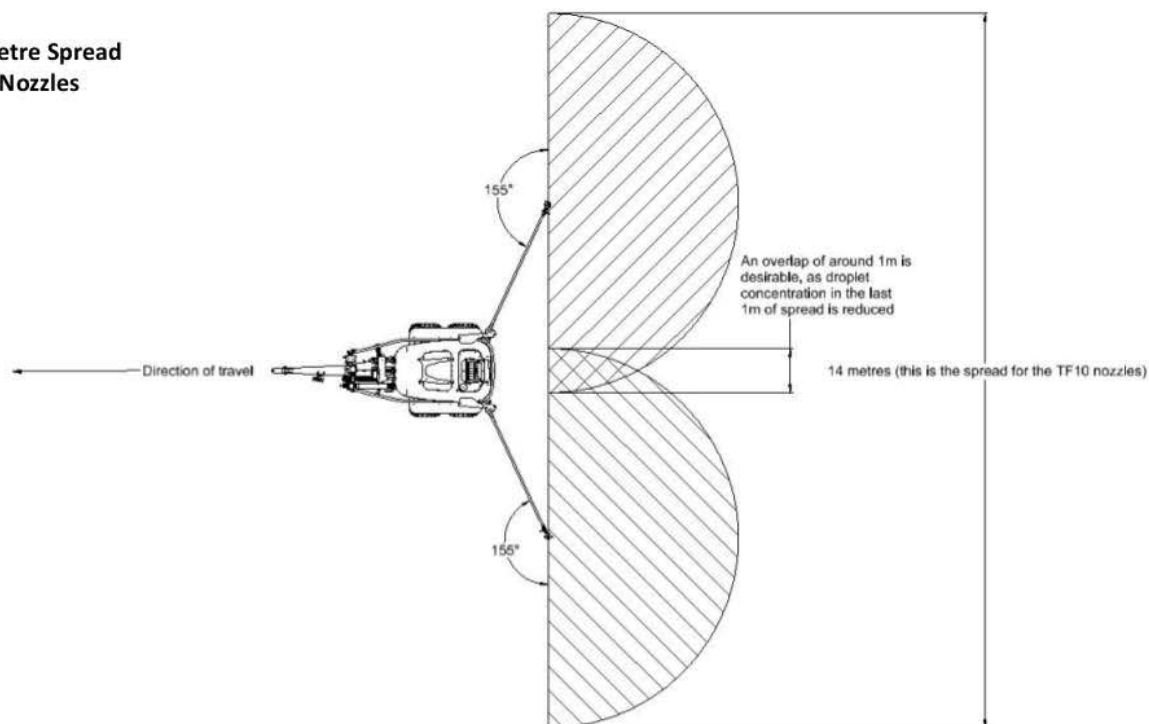
Metalform has developed a range of these nozzles. The nozzles range in flowrates from 10L/min up to 80L/min. As well as spraying fluid at a higher flow rate, the larger nozzles also have a wider spray width. However, the distance between the nozzles is fixed by the geometry of the machine. As a result, the user must rotate the spray nozzle to ensure an acceptable overlap in the centre of the machine. Figure 19 illustrates the requirement for rotating the nozzles to control the overlap.

Table 2 lists the different nozzle sizes with corresponding flow rates and spread widths with water. This data was measured by Metalform using a procedure described in section 5.

Table 2 - Metalform Nozzle Spray Rate and Spray Area

Nozzle	Spray Rate(L/min)	Spread Width(metres)
TF10	10	14
TF15	15	14.5
TF20	20	15
TF30	30	16
TF40	40	17
TF50	50	18
TF60	60	19
TF70	70	20
TF80	80	21

14 Metre Spread TF10 Nozzles



18 Metre Spread TF50 Nozzles

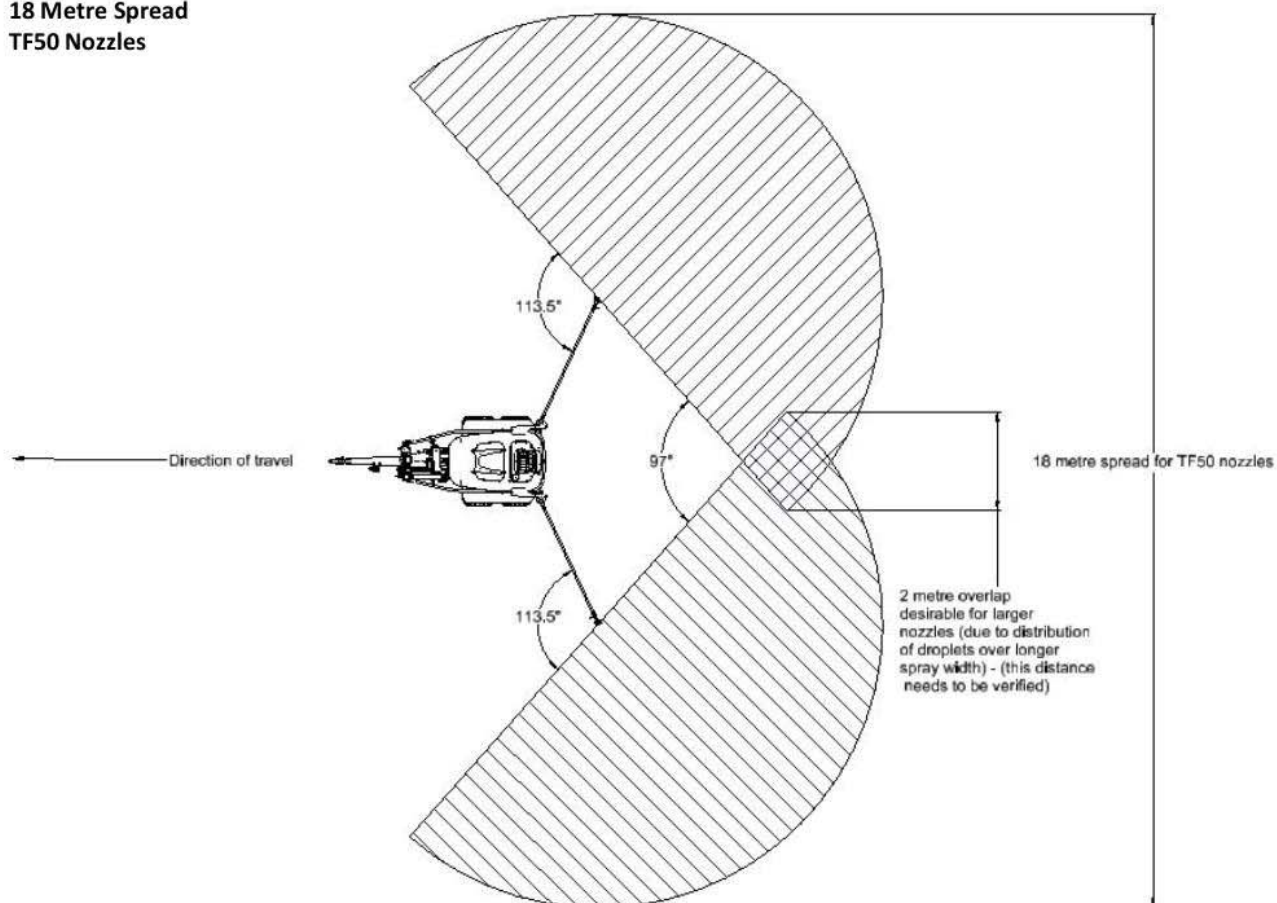


Figure 19 - Importance of Nozzle Rotation for Spray Evenness

3 Volumetric Flowrate Measurement

This chapter is concerned with the measurement of volumetric flowrate - the volume of fluid passing a point per unit time. The first part of this chapter provides an overview of industrially available volumetric flowrate technologies. The second and third parts of this chapter detail the specifics of two different flow meters that were tested for use in this research.

3.1 Types of Flowmeters

Many types of flow meters are available for measuring volumetric flow rate. This section explores many of the main types of meters and how they relate to this project.

3.1.1 Differential Pressure Flow Metering

Differential pressure flowmeters utilise a change in pressure to determine fluid flow rate. These meters use a restriction in the pipe to increase the fluid velocity. This increased velocity changes the pressure of the fluid at that section of the pipe and the difference in pressure can be measured [22].

Theoretically, the relationship between pressure and flowrate can be found by the application of the Bernoulli's equation. In practice, the equation needs to be adjusted in order to account for frictional losses in the pipe [23]. In general, the flow (Q) is proportional to the square root of the change in pressure (P):

$$Q \propto \sqrt{\Delta P} \quad (3.1)$$

Several variations of differential pressure meters are available, the difference is in the type of constriction used to create the pressure drop. Common types are: orifice plate, venturi and flow nozzle [24].

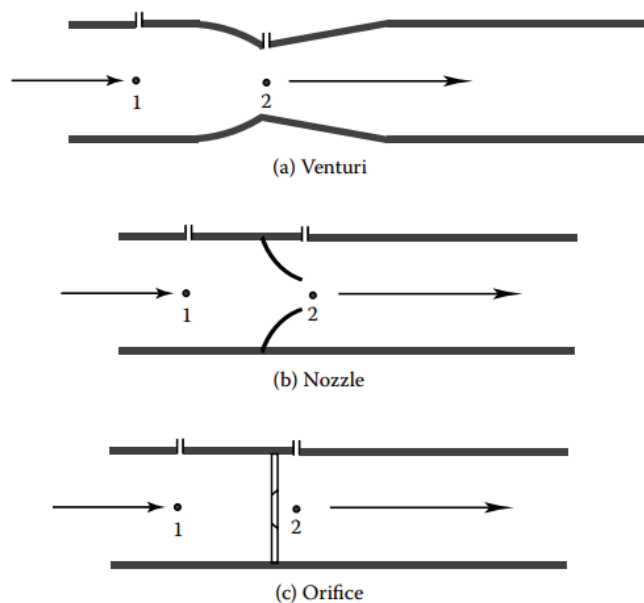


Figure 20 - Common Types of Differential Pressure Meters [25]

In general, there are several advantages to differential pressure meters:

- Simple
- Inexpensive
- Calibration can be inferred from mechanical construction
- Rugged

- No moving parts

The biggest disadvantage in this application is that the relationship between flowrate and pressure difference is dependent on fluid density. Because the fluid density of the slurry mixture can vary greatly, it is difficult to quantify the flow unless the fluid density is well known.

3.1.2 Turbine and Related Flow Meters

Turbine flow meters make use of bladed rotors or fans in the pipe that turn due to fluid flow. The hydrodynamic force on the rotor blades is converted into angular momentum, which rotates the rotor. The rotation frequency is then detected by an external sensor, such as a Hall Effect device. The flowrate is proportional to the speed of the turbine [25]. While the concept is simple there are several variations used. They can be broadly grouped into two categories, meters where the flow is applied radially to the turbine and meters where the flow is applied axially to the flow. Axial meters are more suitable for low flow measurement.

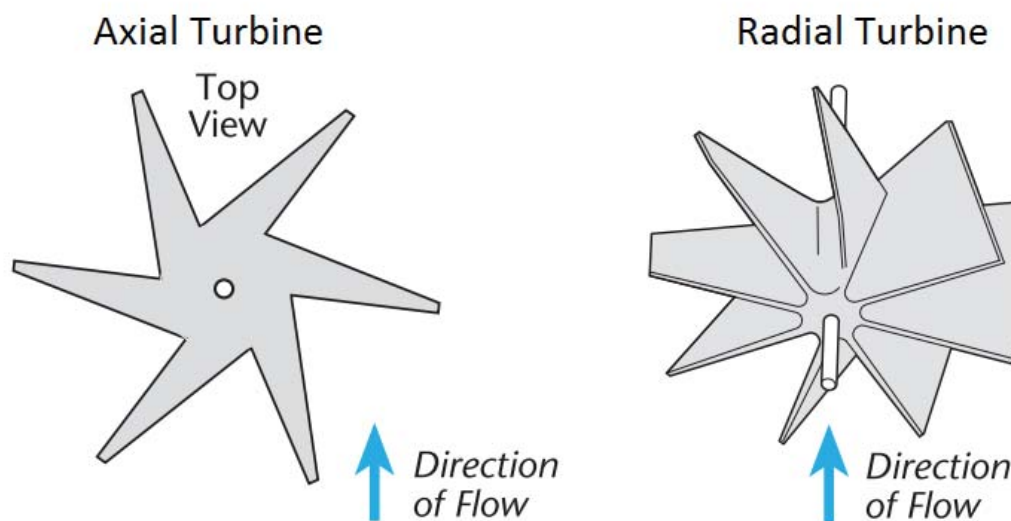


Figure 21 - Comparison of Axial and Radial Turbines [23]

Radial turbines vary somewhat in the shape of the turbine blades and the proportion of pipe area they cover. Often the diameter of the turbine is close to the internal diameter of the pipe, meaning the turbine works like a ducted fan. Although, sometimes the turbine is significantly smaller than the pipe diameter, which reduces the pressure drop of the meter. The Woltmann meter is a common type of axial turbine meter that uses helical blades.

Several variations of axial turbines are used industrially to measure water flow. Common types are single-jet, multi-jet, paddle wheel and Pelton wheel. The single and multi-jet variations are similar, both use a constriction to create jets of fluid, which radially strike a flat bladed turbine. The difference is that one uses a single jet of fluid, while the other uses multiple jets [25].

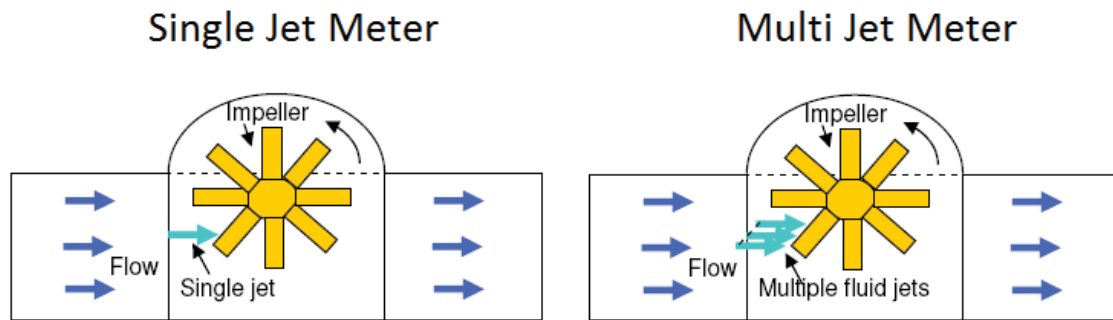


Figure 22 - Comparison of Single and Multi Jet Radial Turbine Meters [26]

Paddle wheel meters are similar to the single jet meter but the size of the wheel is small compared to the pipe diameter. Sometimes they are mounted in such a way that only a portion of the turbine is inserted into the fluid flow. Paddle wheel meters are mounted perpendicular to the flow and the shaft and bearings are often not within the fluid flow. Paddle meters are flat bladed.

Pelton wheel meters have concave blades designed to increase the force that the fluid flow imparts onto the turbine [27].

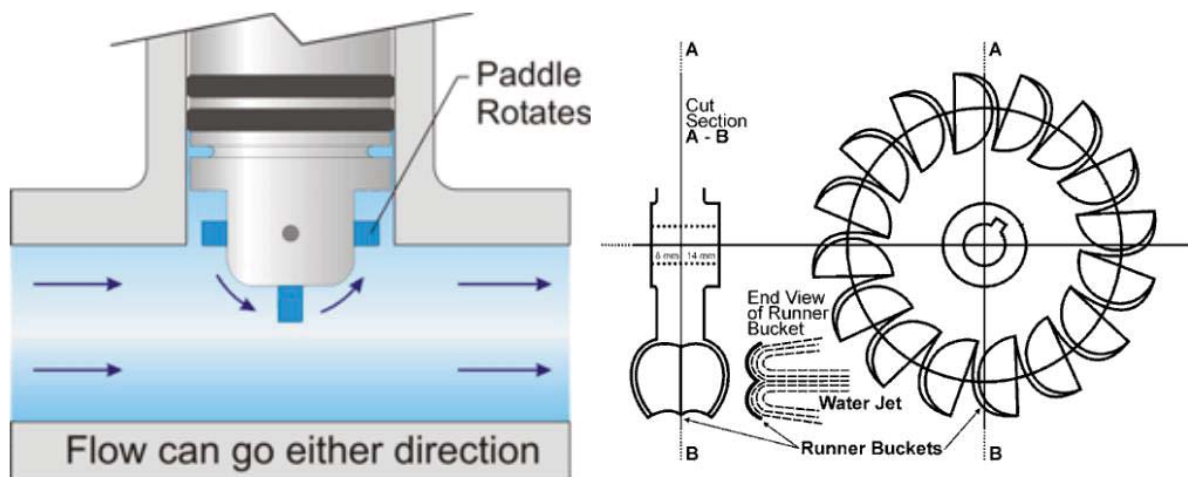


Figure 23 - Left: Paddlewheel Meter Concept [28] Right: Example of Pelton Wheel Geometry [29]

3.1.3 Positive Displacement Meters

Positive displacement (PD) meters are meters in which the fluid mechanically displaces meter components to measure the flowrate. PD meters divide the fluid flow into discrete, metered volumes. The number of volumes per unit time is used to determine the flowrate. This is very close to the concept of measuring the time to fill a bucket or measuring flask [30].

The division into discrete volumes is achieved using rotating or reciprocating mechanisms. Reciprocating meters use one or more pistons to discretise the fluid. There are many variations on rotation-based mechanisms. Some of these are: nutating disk, rotary vane and gear based types. The gear based types use round, elliptical or helical shaped gears.

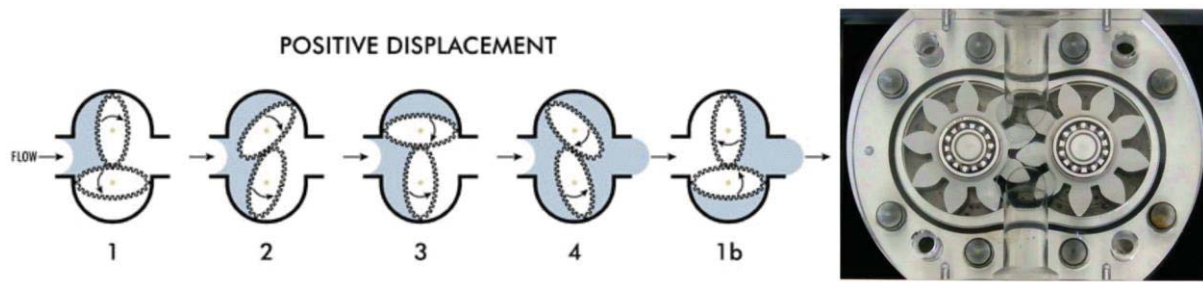


Figure 24 - Left: Elliptical PD Meter Flow Process [31]

Right: Round Gear PD Meter

There are several advantages from positive displacement meters [27]:

- Wide flow range (high turndown)
- Can handle high viscosity fluids
- Require no flow stream conditioning
- Very high volumetric accuracy

However, in this application there are many significant drawbacks:

- Bulky
- Relatively expensive
- Moving parts are prone to wear
- Create an extremely high pressure drop
- Do not deal well with larger impurities

3.1.4 Electromagnetic Flow Meters

Electromagnetic flowmeters (or 'magmeters') are based around Faraday's law of electromagnetic induction. When a conductor moves through a magnetic field a force is exerted onto the conductor. A magnetic field is created inside the pipe by external electrical coils. When a conducting fluid flows through the magnetic field, charged particles experience a force and are deflected. This deflection of charge causes a potential difference which can be measured by electrodes in the fluid stream. The potential difference is proportional to magnetic field strength and fluid velocity.

There are some requirements for this method of measurement to be effective [32]:

- The fluid must be conductive
- The pipe must be non-magnetic
- An insulating pipe liner must be used for conductive pipes

These restrictions can easily be overcome.

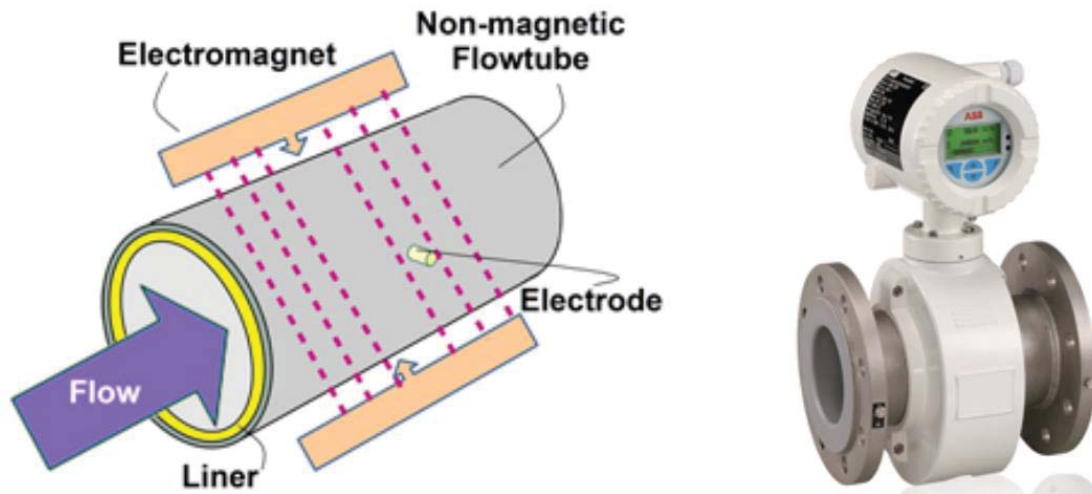


Figure 25 - Left: Fundamental EM Meter Setup Left: ABB Brand EM Flowmeter [33]

Two types of magnetic field generation are used, fields created by alternating current and fields created by direct current. AC excitation has a very high signal to noise ratio however it can be prone to drift. Pulsed DC excitation has the advantage of having no field for part of the cycle. This allows the meter to compensate for the drift. Any measured voltage during the down time of the excitation is clearly not caused by the fluid flow and can be compensated for.

Advantages to electromagnetic meters include:

- Low fluid obstruction – only two electrodes are exposed to the fluid
- Very low pressure drop
- Wide flow range measurement
- Capable of measuring slurry flowrate

Disadvantages of electromagnetic flowmeters in this application:

- Bulky
- Expensive
- Electrodes prone to corrosion and wear

3.1.5 Ultrasonic Flow Meters

Ultrasonic flow meters rely on the use of ultrasonic vibrations generated and received by one or more transducers. There are two primary types of ultrasonic sensors in industrial use, time of flight-based flow meters and Doppler Effect based meters.

Time of flight meters use a pair of transducers commonly referred to as the upstream and downstream transducers. First an ultrasonic signal is sent from the upstream transducer to the downstream transducer, the time taken is measured. Then a signal is sent from the downstream transducer to the upstream transducer, again the time is measured. If the transducers are stationary relative to the pipe the distance travelled by each signal is the same. If the speed of sound in the fluid is constant, any change in time measured between upstream and downstream paths must be attributed to the velocity of the fluid.

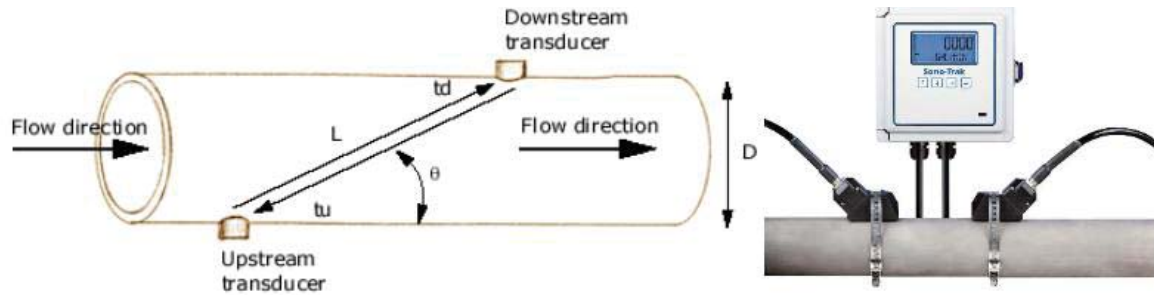


Figure 26 - Left: Ultrasonic Transit Time Meter Principle Right: Sono-Trak Ultrasonic Flowmeter [34]

For a constant fluid velocity, it can be shown that:

$$V_{Fluid} = \frac{L^2 \cdot (t_d - t_u)}{2 \cdot D \cdot t_d \cdot t_u} \quad (3.2)$$

Where:

L is the length of the acoustic path of the ultrasonic signal and D is the axial separation of the transducers, t_u and t_d are the upstream and downstream transit times shown in Figure 26.

The $t_d \cdot t_u$ term in the denominator eliminates the effect of the speed of sound in the fluid. The velocity of the fluid can be determined without knowing the speed of sound in the fluid. This means that the fluid properties can change without having an effect on the flow measurement [27].

Doppler Effect flow meters measure the Doppler shift of sound waves reflected off particles in a fluid. Using a transducer mounted to the exterior of the pipe an ultrasonic signal is sent into the fluid at a known frequency. As the signal propagates through the fluid, the signal is reflected by particles in the fluid. If the particles (and fluid) are moving, the observed frequency of the reflected signal will be different to the original signal [27].

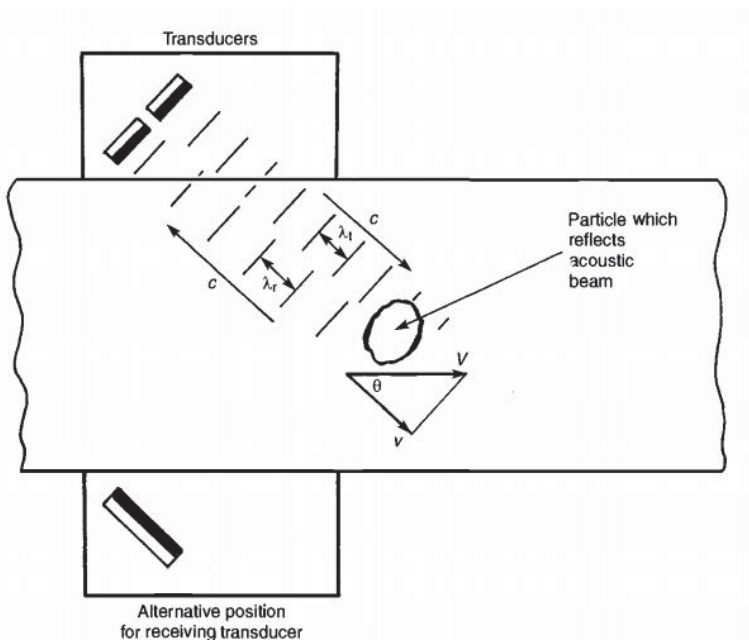


Figure 27 - Doppler Flowmeter Working Principal [27]

In the most basic terms, when the particles are assumed to be traveling parallel to fluid flow:

$$\Delta f = 2 \cdot f_T \cdot \frac{V_{Fluid}}{c} \cdot \cos \theta \quad (3.3)$$

Where:

Δf is the apparent frequency change, f_T is the frequency of the transmitted wave, V_{Fluid} is the fluid velocity, c is the velocity of sound in the fluid, θ is the angle between the transmitter and fluid flow direction shown in Figure 27.

The equation above shows a reliance on a known speed of sound in the fluid. This will be an issue with the variety of fluids that the Tow and Fert is capable of spraying.

3.1.6 Summary of Flowmeters

There are a set of requirements for metering nozzle flow on the Tow and Fert. These requirements change slightly between flowmeters that can be used for testing and flowmeters that could be potentially used for consumer machines.

The meter needs to be fitted to a moving machine near the end of the spray booms. This means that bulky meters like the positive displacement meters and the electromagnetic meters are not suitable.

Differential meters rely on knowledge of the fluid properties to determine flowrate. There are also concerns that the pressure transducer holes may quickly become blocked when spraying lime slurries.

This leaves turbine based meters and ultrasonic meters. Turbine meters are very simple and inexpensive devices, however, they need to be exposed to the fluid flow. In this application, the meters are unlikely to last very long when exposed to erosive and potentially corrosive fluids. Slurries may also clog the meters and prevent free rotation if the meter cannot be properly cleaned [35].

Transit time ultrasonic sensors have many attributes that make them ideal for this application. They are completely unobstructive, they do not require any contact with the fluid. They can readily be fitted to the Tow and Fert machines without any modification. They are not dependant on fluid properties to measure the flowrate. This means that they should be capable of measuring the flow of the wide range of fluids that the Tow and Fert can spray without recalibration.

3.2 TUF2000M Ultrasonic Flow Meters

3.2.1 About the TUF2000M

In order to be viable for production the flow measurement fitted to the Tow and Fert machines must be affordable. As discussed in section 3.1.6 the numerous advantages of ultrasonic flow meters would make them ideal for this application. Most ultrasonic flow meters would be prohibitively expensive however, the TUF-2000M flow meter is available from several Chinese manufacturers and distributors for around \$400. Two units were purchased for experimentation in this project. A TUF-2000M flow meter is show below in Figure 28.

The TUF2000M uses external transducers. Several transducer types are available; some transducers are designed for working at elevated temperatures however primarily the differences allow for

different sizes of pipes. The transducers used in this project are TS-2 transducers designed for pipes 15mm to 100mm in diameter and rated to temperatures between -40°C and 90°C.

The TUF2000M is based on the Texas Instruments MSP430FG4618 microprocessor and is a time of flight flow meter. There are three main interfaces available: an LCD panel and buttons, an RS485 Serial port and a 4-20mA analog output. The RS485 serial port supports 4 different communication protocols the most widely used being the MODBUS protocol.

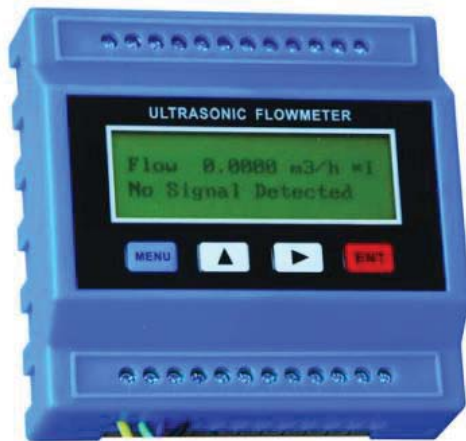


Figure 28 - TUF2000M Flow Meter [36]

In addition to the flow measurement capabilities, the unit has several additional features. Three analog inputs and two open collector outputs are available. The outputs are typically used for switching alarms and indicator lights etc. The unit is also able to read the signals from two PT100 RTD temperature sensors. The temperature and flow measurement combination allow the unit to monitor energy flow, something that is not needed in the application of this project.

3.2.2 Installation of TUF2000M Flow Meters

In order to minimise modification to the Tow and Fert the flow meters (and flow controller) were installed onto a removable boom extension. Metalform supplies these boom extensions when extremely wide spray is required. The extension extends the booms where the spray head is detached and extends the length of the booms.

The datasheet specifies restrictions for the installation of the transducers around things that alter fluid flow such as valves, pumps, pipe enlargement and reduction, and bends. This is to ensure laminar flow in the section of pipe where the transducers are installed. This is referred to as flow conditioning [37]. These restrictions are shown in Figure 29.

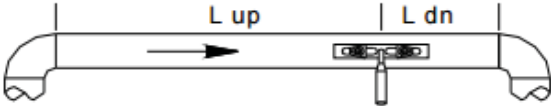
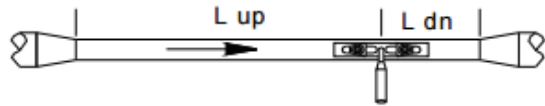
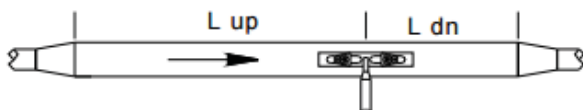
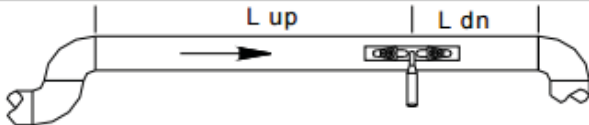
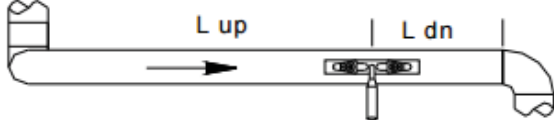
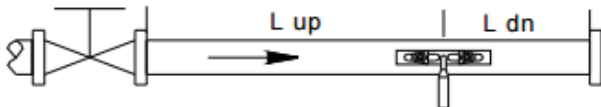
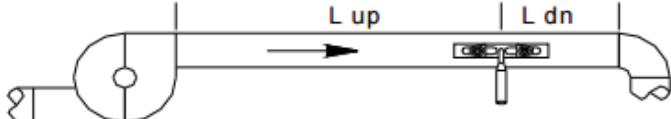
Piping Configuration and Transducer Position	Upstream Dimension	Downstream Dimension
	L up x Diameters	L dn x Diameters
	10D	5D
	10D	5D
	10D	5D
	12D	5D
	20D	5D
	20D	5D
	30D	5D

Figure 29 - TUF2000M Pipe Installation Requirements [36]

In this case, the diameter of the pipe is 38mm. The transducers are installed horizontally to avoid any air bubbles that may form and rise to the top.

There are several methods of mounting the transducers onto the pipe, the Z, V and W methods. The name of the installation method refers to the shape of the ultrasonic signal path from one transducer to another. An example of Z type installation is shown in Figure 30.

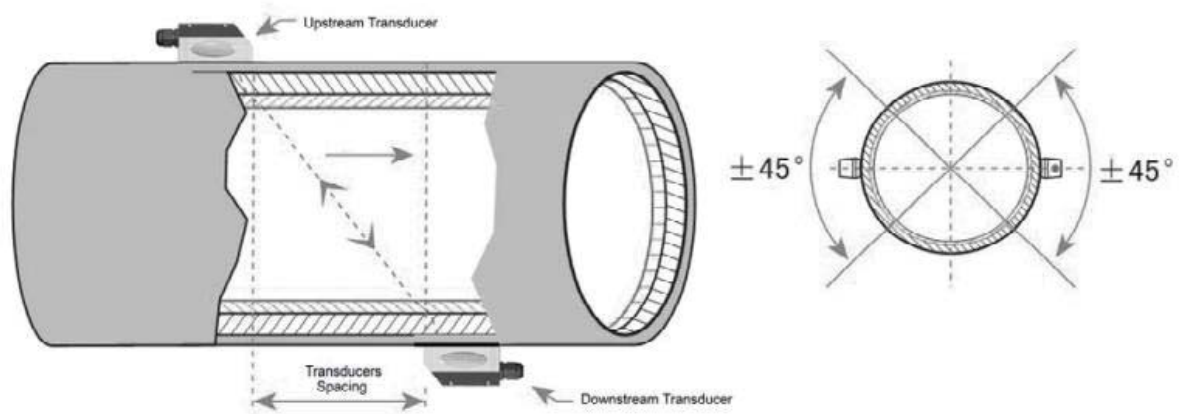


Figure 30 - Ultrasonic Transducer Z Installation [36]

Figure 31 shows a V type installation:

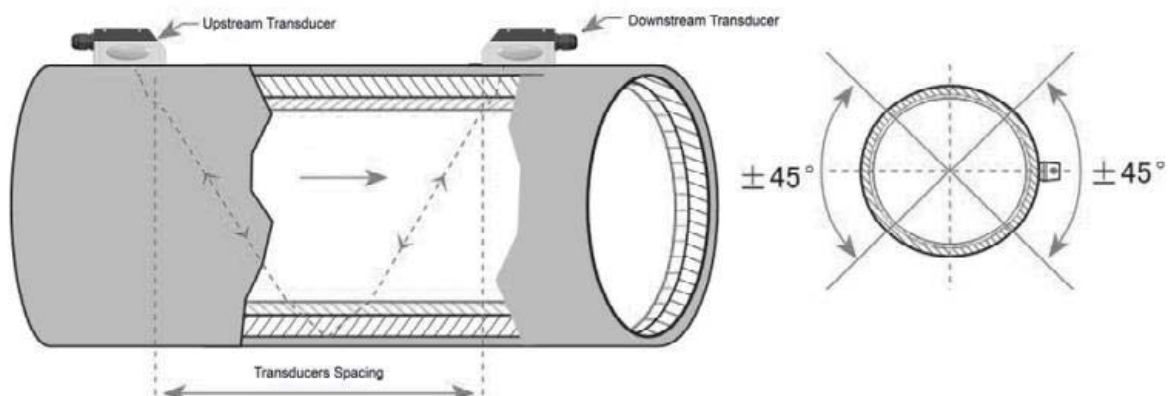


Figure 31 - Ultrasonic Transducer V Installation [36]

Finally, Figure 32 shows a W type installation:

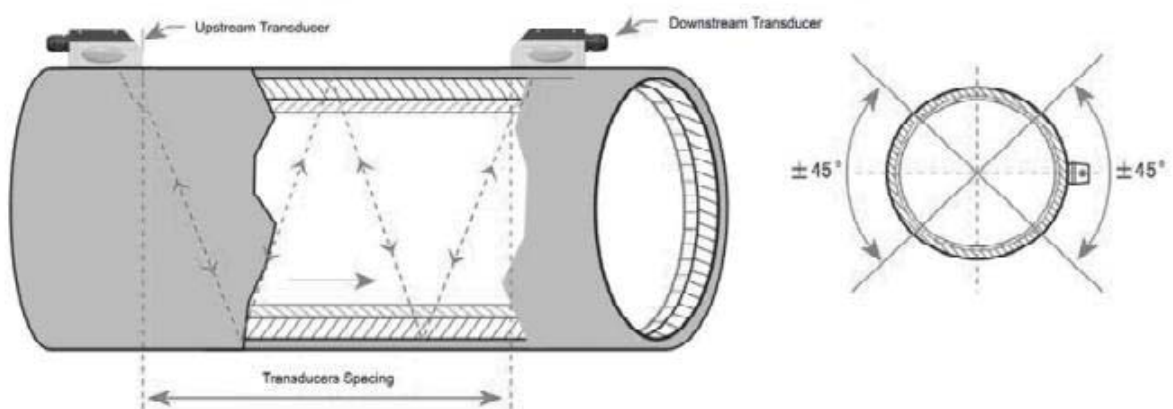


Figure 32 - Ultrasonic Transducer W Installation [36]

As the figures show, the path length relative to the pipe diameter increases when moving from a Z type to V type to W type installation. The increase in ultrasonic signal path increases accuracy of the flow measurement as long as the signal is not degraded and dispersed too much when it reaches the secondary transducer [27].

Because the relationship between the path length and diameter the different types of installation are typically used on different sized pipes. The Z method is usually only used on pipes with a diameter greater than 200mm. The w method is used with pipes between 15mm and 50mm. The V method is used with pipes between 30mm and 200mm [27]. The diameter of the boom pipes on the Tow and Fert is 38mm, meaning either the V or the W method could be used.

The installation procedure used is as follows:

1. Clean and polish the surface of the pipe in the region the transducers will be applied.
2. Enter the pipe diameter, transducer type and installation type into the flow meter.
3. Get the spacing information from the flow meter.
4. Add acoustic coupling agent to the area where the transducers will be installed to the pipe.
5. Lightly clamp the transducers to the pipes at the spacing suggested in step 3.
6. Use the signal strength and signal quality feedback of the flow meter to fine-tune the position of the transducers.
7. Tightly clamp the transducers to avoid movement.

The interaction with the flowmeters can be done with either the built in LCD and button interface or using the RS485 interface.

The signal strength is an indication of the amplitude of the signal received by the destination transducer. The strength is presented as a percentage. The manual suggests that a strength of at least 50% should be used.

The signal quality is an indication of the signal to noise ratio. A higher value indicates a higher signal to noise ratio. The signal quality is also expressed as a percentage and the suggested minimum is 60%.

3.2.3 Testing of the TUF2000M Flow Meters

Extensive testing of the TUF2000M was conducted. Primarily this testing was performed using water as a test fluid. During installation, both TUF2000M meters installed reported a signal of at least 80% well above the minimum 60% suggested in the product manual.

One of the tests performed was a closed loop test. This involved forcing the diaphragm valve closed (described in section 2.4.5). When the valve is forced closed no fluid can flow through the nozzle meaning that the fluid exiting the tank through the boom must also flow back through the other boom to the tank. Thus, the flow rate from one flowmeter should be the same as the flow from the other meter.

In this test, the manifold pressure was set to 5PSI by adjusting the throttle on the motor. This is much lower than the 20PSI the machine is typically set to. During the test, the butterfly on the return to the tank (described in section 2.4.6) was slowly opened. This increased the flowrate of fluid through the booms and therefore meters. Figure 33 shows a plot of the raw flow data obtained from both the meters. During operation, the meter reported total transit times around 60 microseconds.

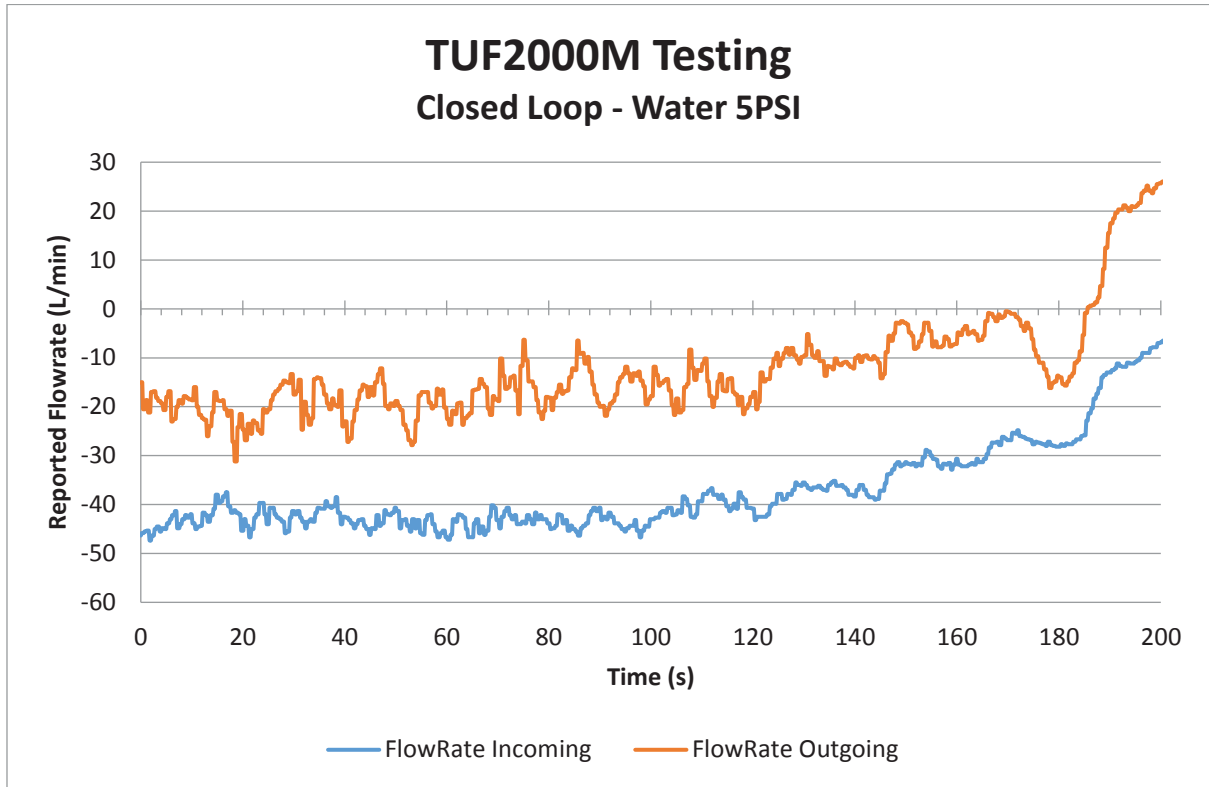


Figure 33 - TUF2000M Raw Flow Data - Closed Loop Testing

There is a reasonable amount of noise on the signal. To reduce the noise a cumulative moving average filter was used:

$$Flow_{CMA} = \frac{Flow_{New} + n \cdot Flow_{CMA}}{n+1} \quad (3.4)$$

Where:

$Flow_{New}$ is the newly obtained flow rate value, $Flow_{CMA}$ is the cumulative moving average of the flowrate, n is an integer filter factor.

The signals are also clearly offset. The meters support a zero offset, which can be set on the device. To correct for it both signals were shifted by the average of the data points of each set of data. The offset was corrected and the signals were filtered with an n -value of 50. This is shown in Figure 34.

After filtering and correcting for the offset the signals, the difference between the two signals was found. This difference was intended to be used to find the flow through the nozzle. Because this test was performed such that no fluid could flow through the nozzle, this difference is ideally zero. The calculated nozzle flow for this test is shown in Figure 35.

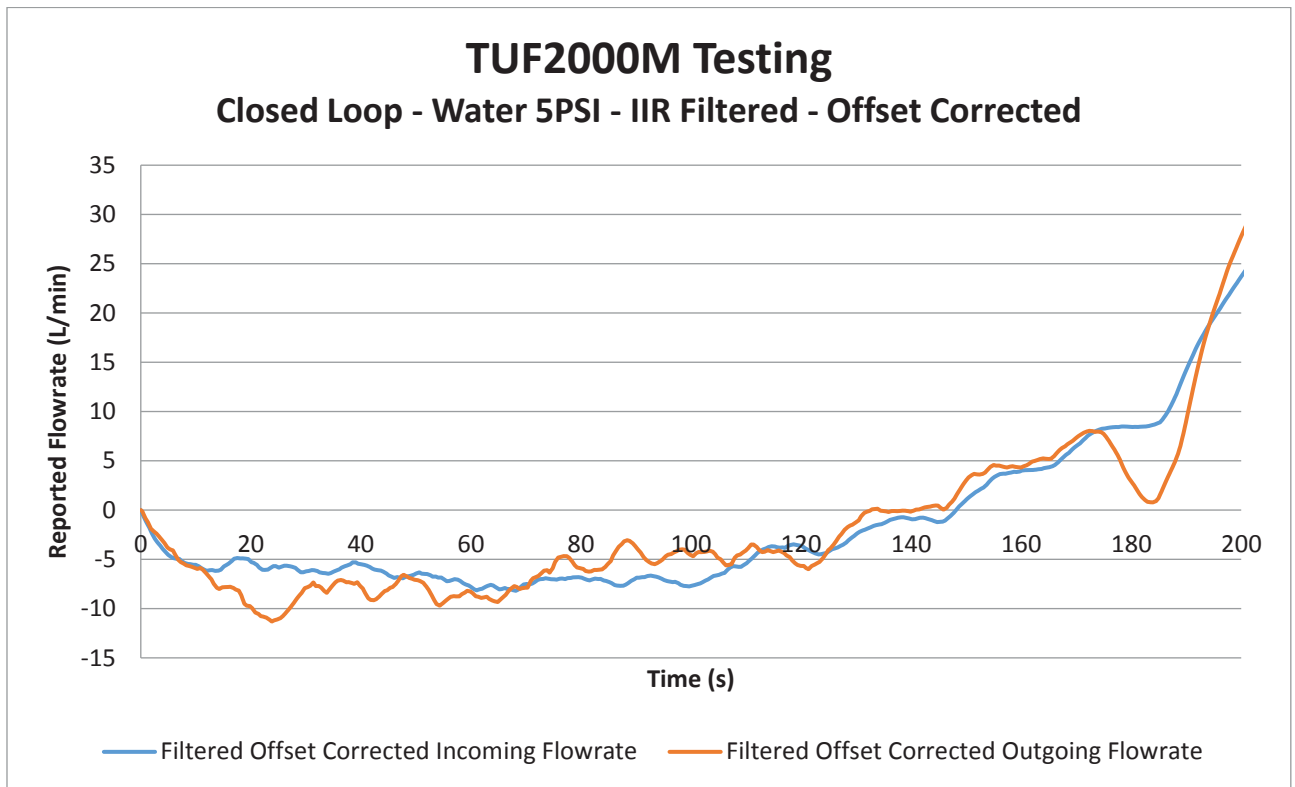


Figure 34- TUF2000M Filtered, Offset Corrected Flow Data - Closed Loop Testing

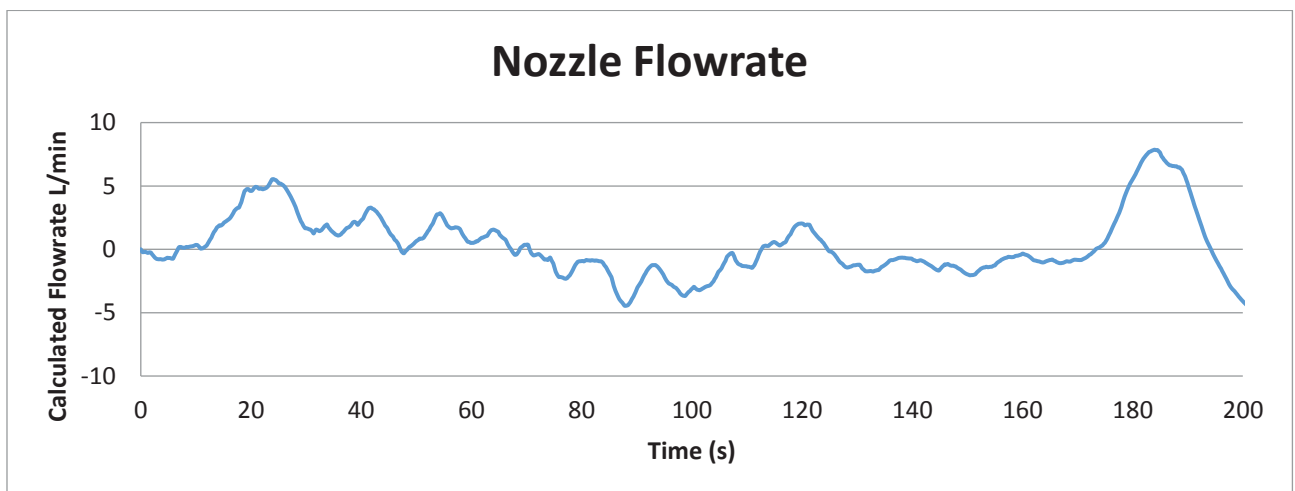


Figure 35 - TUF2000M Calculated Nozzle Flowrate - Closed Loop

The difference in the two flowrates (which ideally should be zero) had a range of around 14L/min. This range is higher than the maximum flowrate of the TF10 nozzle Tow and Fert nozzle. Clearly, this would not be suitable for measuring let alone controlling the flowrate of the machine.

Several similar tests were conducted under various conditions. This test was indicative of the results of all the tests that were performed.

3.2.4 Investigating TUF2000M Noise sources

The flow data obtained from the TUF2000M meters was not as expected. The noise level was too great to properly quantify the flow. To try to get better results an oscilloscope was used to investigate potential noise sources. The oscilloscope used was a 2-channel deep storage digital oscilloscope with a bandwidth of 100MHz and a sample rate of 1GS/s.

The two channels were connected to each of the upstream and downstream transducers. To get an overview of how the flowmeter was operating a trace with a long period was obtained. All of the tests were conducted with AC coupling. For some reason the reported flow signal intermittently stopped being available while the oscilloscope was connected.

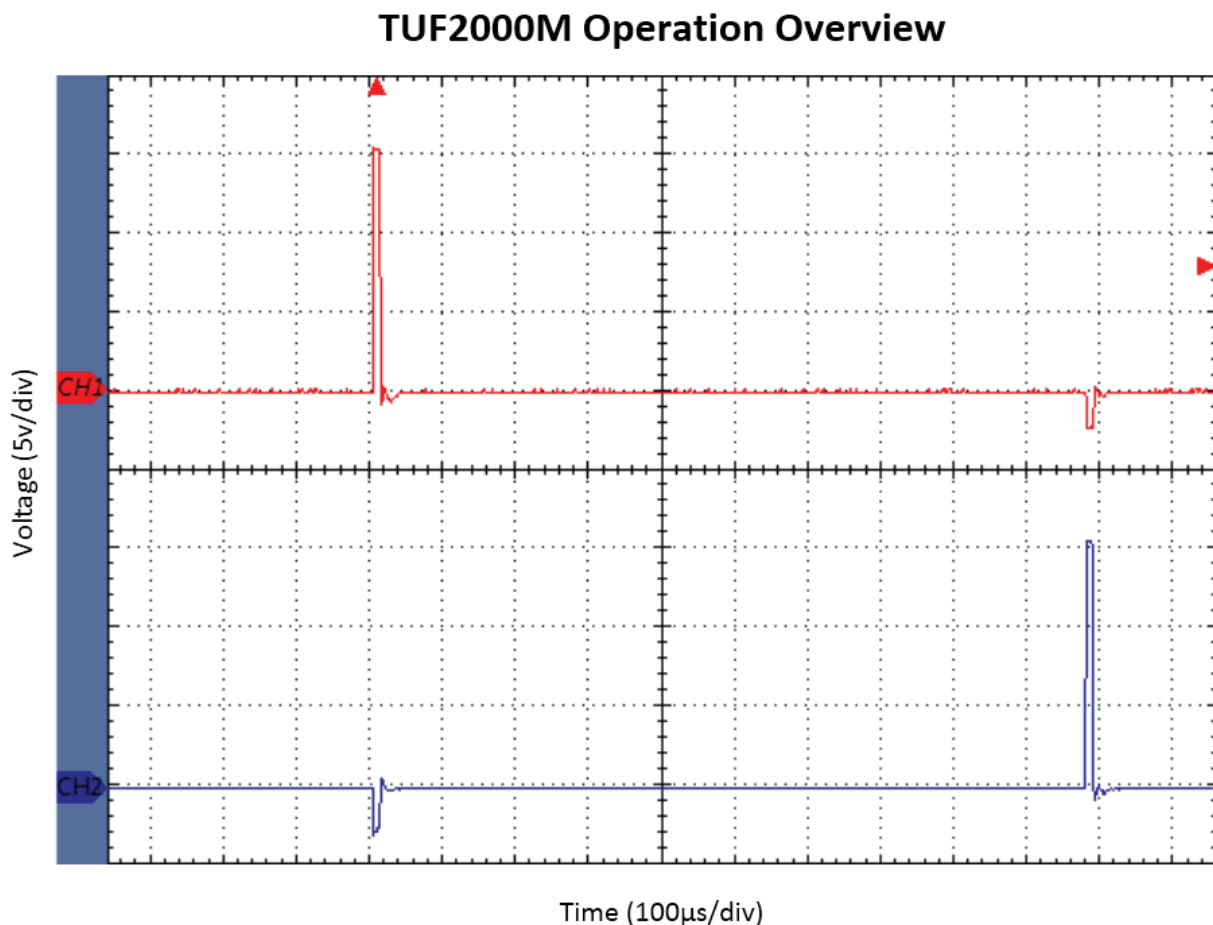


Figure 36 - Oscilloscope Trace of TUF2000M Operation

Figure 36 shows the obtained oscilloscope trace. The vertical axis scale is 5V/div and the horizontal is 100µs/div. Channel 1 shows a 15v signal being generated that lasts around 10 µs. Channel 2 immediately shows a voltage drop of around -2.4v. Nothing further is observed until channel 2 generates another 10µs 15v pulse. The second pulse is generated around 975µs after the first and affects channel 1 in a similar way with a 2.4v drop.

During flow measurement, operation the flowmeter reported a transit time of 60µs. This would presumably cause some change to occur on channel 2 at 60µs or 30µs if the reported transit time was a total transit time. No signal like this is visible in this trace.

This pulse and its response were then examined more closely. The trace is shown in Figure 37.

TUF2000M Pulse and Response

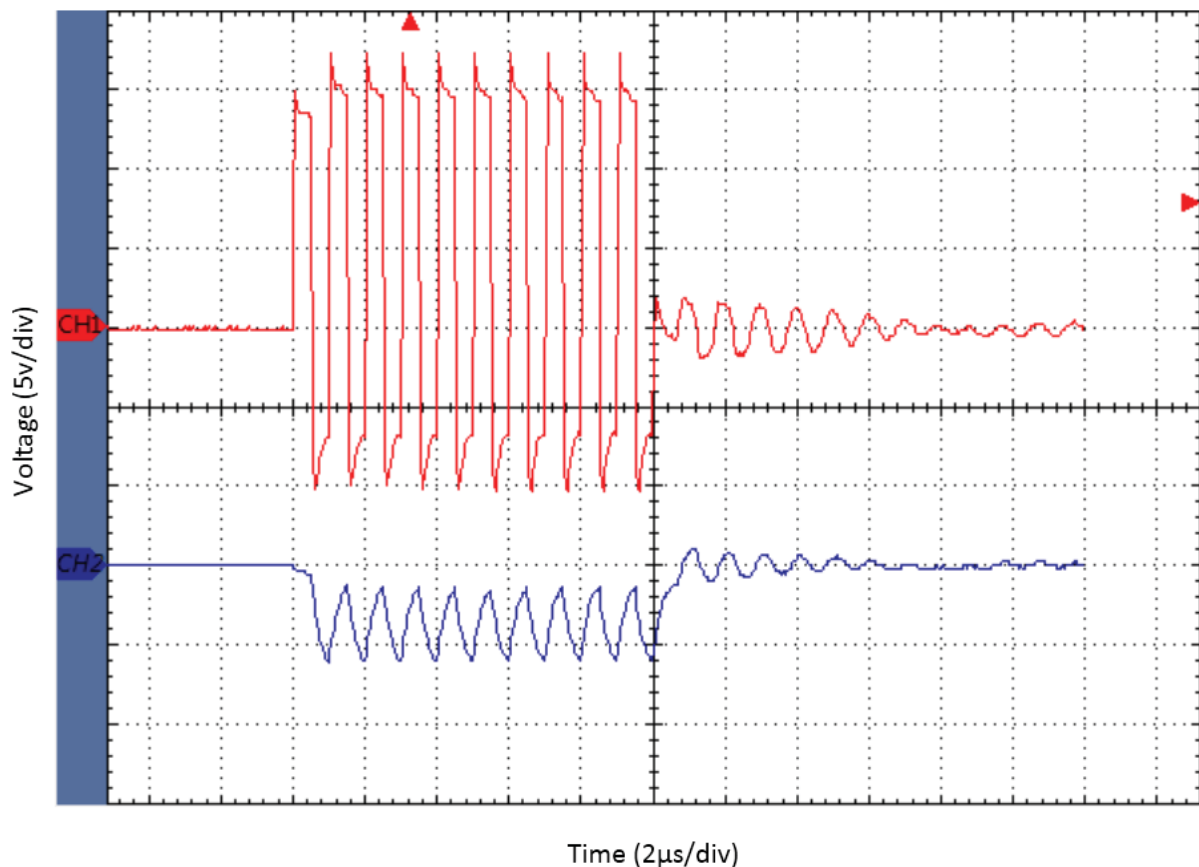


Figure 37 - Trace of TUF2000M Pulse and Response

In this test, the vertical axis scale remained at 5v/div however, the time scale was reduced to 2μs/div. The apparent pulse observed in Figure 36 was actually a pulse train of ten pulses with a frequency of 1MHz. Some residual ringing is observed after the pulse train ends.

The trace shows that channel 2 almost immediately drops by around 5v when the pulse is generated on channel 1. This is definitely not caused by an ultrasonic signal transiting through the fluid inside the pipe.

Initially it was suspected that this was caused by the ultrasonic signal being transmitted through the pipe wall. To confirm this theory, the downstream transducer was removed from the pipe. The test was conducted again. The results are shown in Figure 38.

TUF2000M Pulse and Response with Transducer Disconnected

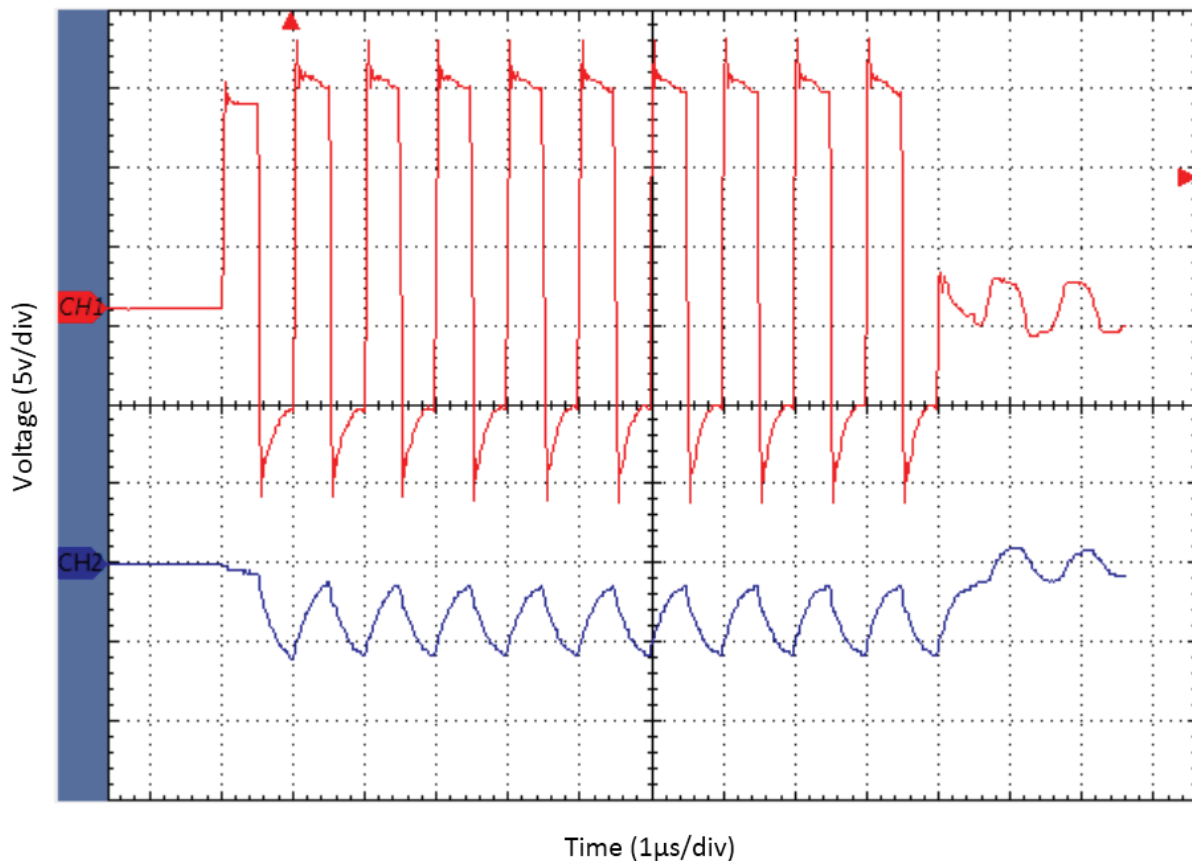


Figure 38 - Trace of TUF2000M Pulse and Response with Transducer Disconnected

The signal did not change significantly. The noise is still present. This means that the noise was not a signal being transmitted through the pipe wall. The noise must then come from another source. The transducers are wired to the meters using shielded cables, decreasing the likelihood of electromagnetic noise being induced on the lines. The oscilloscope probe lines are similarly shielded. It was concluded to noise source is most likely therefore within the meter itself.

3.2.5 Conclusions of TUF2000M

While possessing many attributes that would make these meters near perfect in this application, the flow signals obtained are simply not accurate enough. After investigating the meters using an oscilloscope, the source of the noise was not definitively determined. It is suspected that the noise is internal to the meters themselves. However, because the flow signal was not always available while the oscilloscope was connected, it is not possible to confirm this. It is possible that the signals are being altered in some way by the connection of the oscilloscope probes.

The result of this testing is that the TUF2000M are not suitable for measuring the nozzle flowrate of the Tow and Fert machine.

3.3 ZD1200 Impeller Flow Sensor

3.3.1 About the ZD1200 Flow Sensor

The ZD1200 is a low cost, plastic, axial-turbine style flow sensor. This sensor is capable of measuring flow rates from 1.5 to 25 Litres per minute. The device is based around a Hall Effect sensor and has a simple open collector digital output. The impeller inside the device is driven by fluid flow and the Hall Effect sensor provides a pulse every revolution of the impeller. The rate at which the device pulses is proportional to the flowrate through the device. This style of flowmeter is discussed in section 3.1.2 According to the devices datasheet [38] the orientation of the meter changes the coefficient of proportionality. Two calibration tables are given for the meter shown in Table 3.

Table 3 - ZD1200 Calibration Data

Flowrate (L/min)	Frequency	
	Horizontal Orientation(Hz)	Vertical Orientation(Hz)
1.5	5.1	7.8
3	13.5	15.9
6	28.7	29.8
9	42.1	42
15	71.4	70.4
20	93.9	93.5

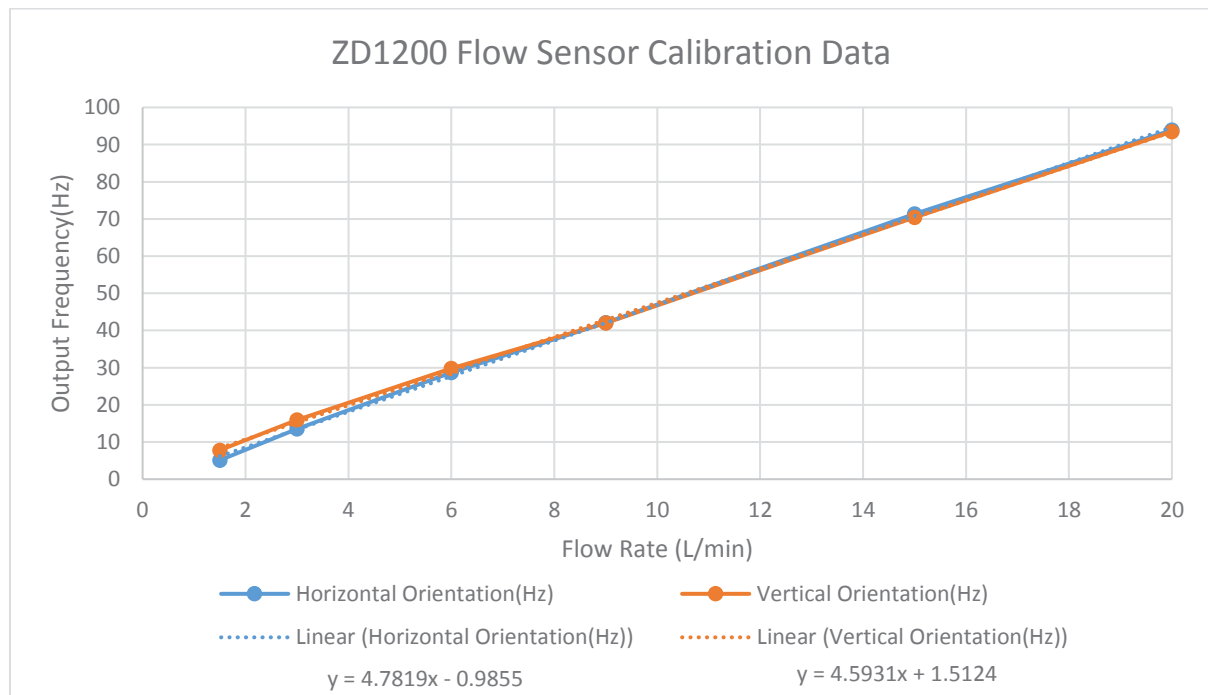


Figure 39 - ZD1200 Flow Sensor Calibration Plot

Figure 39 shows the data from Table 3 plotted with linear trend lines applied. The plot shows a strong linear relationship between the flow rate and output pulse frequency for both mounting orientations.

3.3.2 Installation of the ZD1200 Flow Meter onto the Tow and Fert

The ZD1200 has two male ½" BSP threads allowing for easy installation onto the Tow and Fert system. Unlike the ultrasonic flow meters described in section 3.1.5, there is no requirement for straight lengths of pipe. This means that this sensor could be plumbed directly in line with the spray nozzle. An image of a spray head with a flow meter fitted is shown in Figure 40.



Figure 40 - ZD1200 Installed

Because of the two male threads on the ZD1200, a simple female-to-female adaptor was required. The addition of the flow meter reduced the nozzle height by around 120mm.

3.3.3 Measurement of Flow from ZD1200 Meter

The output of the ZD1200 flow meter is a series of pulses generated by a Hall Effect device inside the device. The frequency is proportional to flowrate. In order to convert these pulses to a meaningful flow value, either the time between successive pulses or number of pulses per some time step must be measured [39]. Because of the relatively low frequency of the output it was decided that the time between successive pulses would be measured. This is implemented in the controller described in section 4.

The signal from the sensor is noisy. In order to reduce the effect of noise the signal is digitally filtered in the controller. The filter used is a cumulative moving average filter, which has an infinite impulse response:

$$Flow_{CMA} = \frac{Flow_{New} + n \cdot Flow_{CMA}}{n+1} \quad (3.5)$$

Where:

$Flow_{New}$ is the newly obtained flow rate value, $Flow_{CMA}$ is the cumulative moving average of the flowrate, n is an integer filter factor.

This type of filter is implemented extremely easily in a microcontroller. Higher n-values increase the smoothness of the obtained flowrate. However, this comes at the cost of responsiveness. High n-values introduce a delay to measured changes in flowrate.

3.3.4 Testing and Calibration of the ZD1200

After the ZD1200 flow sensor was installed to the Tow and Fert machine experiments were conducted to ensure the measured flow rate was accurate. The experiment setup was very simple:

1. The machine was started and the throttle of the motor was set such that 20PSI of pressure was measured on the distribution manifold.
2. The flow control butterfly valve was closed fully (to allow maximum nozzle flow)
3. A 72L bucket was used to collect the fluid. A stopwatch was started as the bucket began to fill and stopped when the bucket began to flow.
4. The bucket was emptied, steps 2 and 3 were repeated to obtain three readings for each valve position
5. The valve position set in step 2 was adjusted and the experiment repeated to obtain data for several flow rates.

The results comparing the ZD1200 flow sensor data to the bucket test data is shown in Table 4 and Figure 41. These tests show that the calibration of the ZD1200 flowmeter is good. There is little deviation between the manually measured flow rate and the flowrate reported by the ZD1200.

Table 4 - ZD1200 Calibration Test Data

Capacity: 72L			
Time to fill(s)	Average Flowrate (L/min)	ZD1200 Average Flowrate (L/min)	
180.48	23.94	23.99	
177.02	24.40	24.43	
183.48	23.55	24.62	
213.05	20.28	19.72	
214.28	20.16	20.40	
221.53	19.50	20.43	
257.91	16.75	17.02	
252.20	17.13	17.59	
247.94	17.42	16.78	
372.39	11.60	12.10	
368.08	11.74	12.21	
360.88	11.97	11.86	

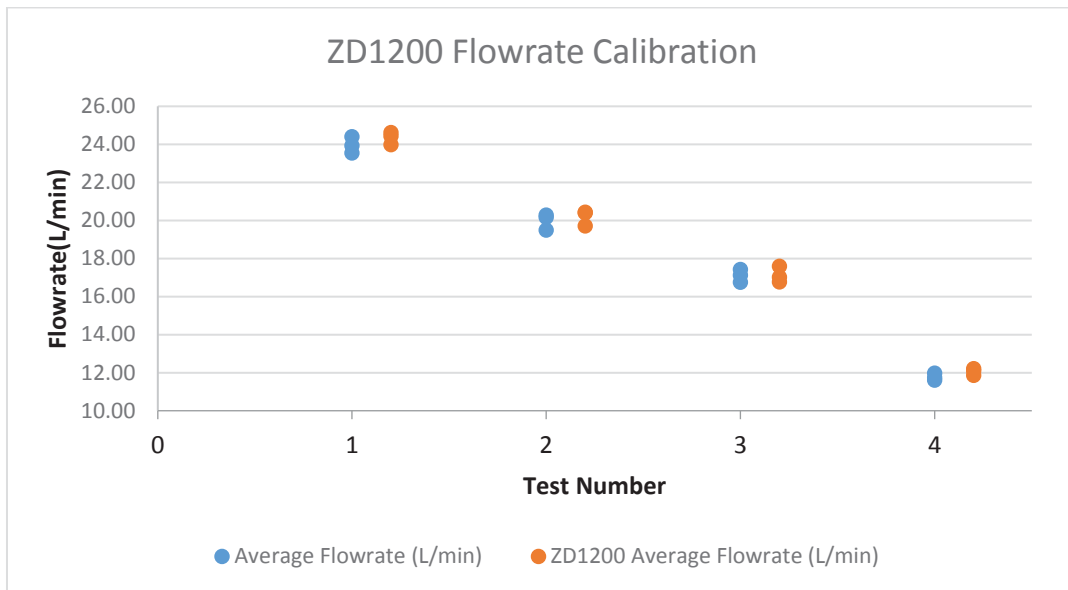


Figure 41 - ZD1200 Calibration Data

3.3.5 System Nozzle Flow Characteristics

Once the ZD1200 flowmeter was calibrated, the nozzle flow characteristics of the system could be found. The flowrate depends on several factors:

- Pump speed / manifold pressure
- Fluid properties
- Installed nozzle
- Flow valve position

This section presents several plots to show the effect of these factors with respect to flow valve position.

3.3.6 Motor Speed / Pump Pressure:

To determine the effect of the manifold pressure on nozzle flowrate tests were performed. These tests involved setting the pressure at the manifold by adjusting the throttle of the petrol motor. The flow controller was then used to slowly close the butterfly control valve increasing the nozzle flowrate. During these tests a return hose was used to return the nozzle spray back into the tank.

The plot in Figure 42 shows the effect of motor speed on the flowrate and the relationship to valve position.

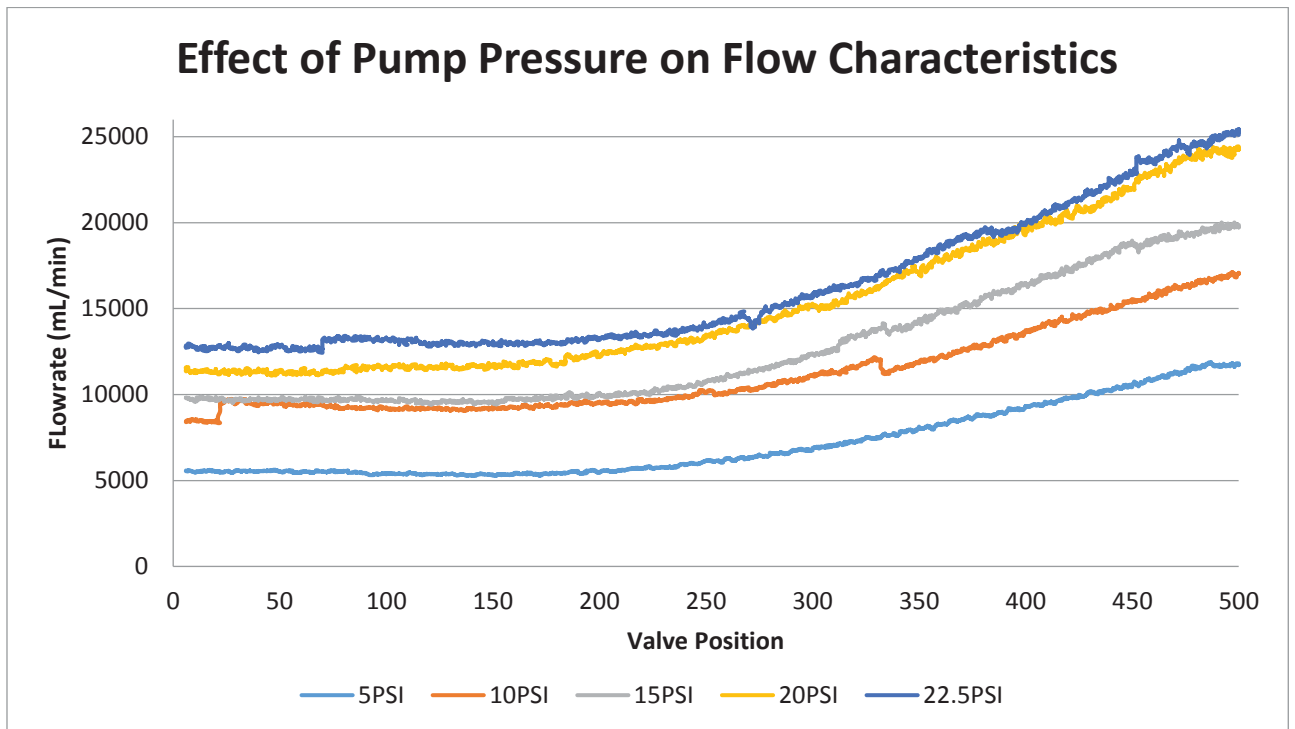


Figure 42 - Effect of Pump Pressure on Nozzle Flow Characteristics

3.3.7 Nozzle Flow Characteristics

The effect of nozzle selection on flow characteristics was determined in a similar way to the pump pressure. The motor speed was set such that the manifold pressure was 20PSI. A nozzle was inserted into the spray head and the flow controller was used again to close the control valve. Figure 43 shows the relationships between flowrate and valve position for three different nozzles and a hose that was used to return fluid back into the tank.

The plots in Figure 43 show a consistent shape between the three nozzles and a slightly altered relationship when the return hose was used.

3.3.8 Testing Diaphragm Valve Consistency

The majority of tests were performed with the diaphragm valve forced open, always allowing flow through the nozzle. A test was performed with the valve in the spray position. When a sufficiently high pressure is reached, the diaphragm opens and fluid begins to flow through the nozzle.

Figure 44 shows the results from the diaphragm valve testing. The valve consistently opened allowing flow at a valve position of 300, except in one test where it was delayed until around 310. This gives a region of 200 units (2/5ths of the butterfly valve range) to modulate flowrate. It is important to note that the spring load on the diaphragm valve can be adjusted to move this cut-off point.

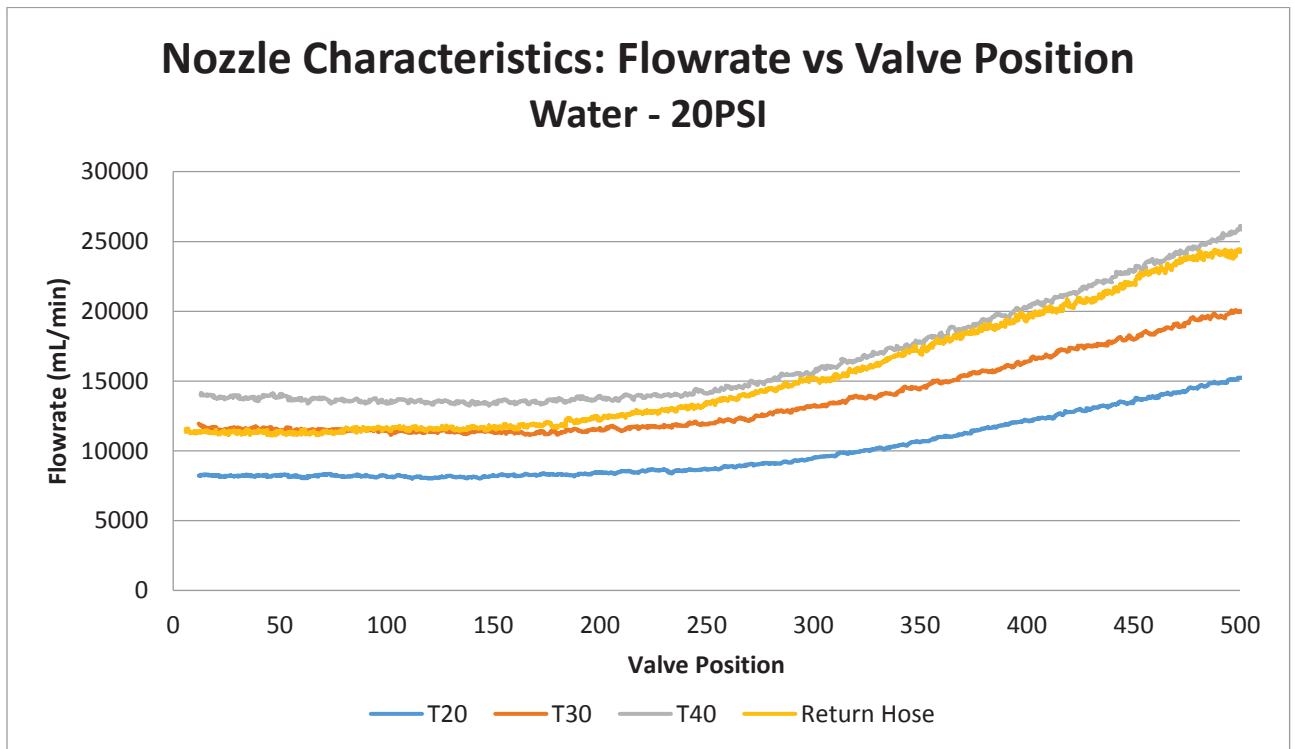


Figure 43 - Nozzle Flow Characteristics

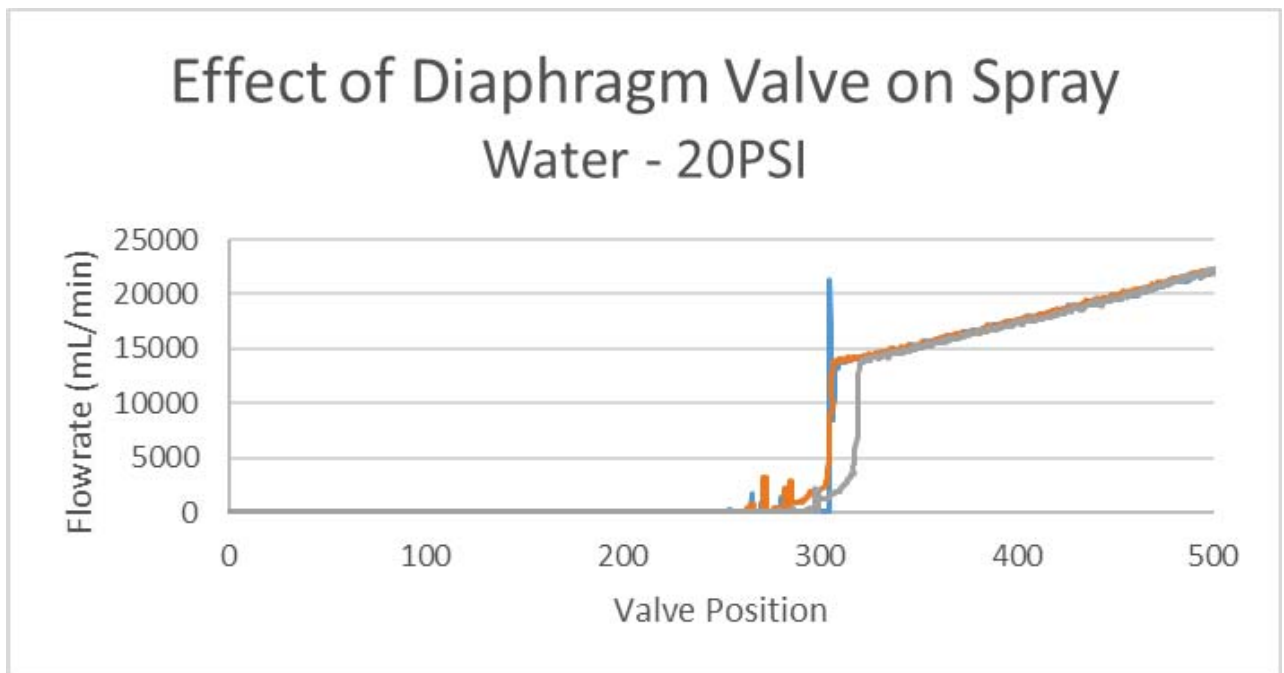


Figure 44 - Diaphragm Valve Testing

4 Hardware and Software Design of Flow Controller

A prototype flow controller was developed for controlling the flow on the Tow and Fert. The controller is intended to monitor the vehicle speed and control the flowrate to ensure the set application rate remains as consistent as possible.

4.1 Controller Design and Specifications:

The prototype controller was initially designed against a certain set of requirements. The controller needed to be able to:

- Communicate with TUF2000M modules for flow control
- Communicate with a computer
- Bidirectional control of a linear actuator
- Measure position of a linear actuator
- Measure vehicle speed
- Flexible enough for modifications and additions during testing

4.1.1 Microcontroller selection (ATmega2560)

A microcontroller was the obvious selection for the basis of the controller given the requirements. Microcontroller selection was a more difficult decision. Eventually it was decided that the Atmel ATmega2560 was the best option for the prototype.

The ATmega2560 is an 8-bit AVR RISC based microcontroller that can run at up to 16MHz.

Key features include:

- 256k Bytes of flash memory
- 32 External Interrupts
- 4 Hardware UART modules for serial communication
- 16 channel 10bit Analog to Digital Converter (ADC)
- 6 Advanced timers with:
 - 16 output compare modules for hardware PWM
 - 4 Input capture modules for advanced timing
- 4096 Bytes of EEPROM for persistent data storage

After the ATmega2560 was chosen, it was decided that the Arduino hardware design and software libraries would be used to decrease development time. The ubiquity and availability of the Arduino platform has many benefits in terms of development. Using the Arduino environment has overheads in both code size and physical size of the controller but in this case, neither will be strained. The Arduino board with an ATmega2560 is known as an Arduino Mega. The board consists of the microcontroller and required circuitry (like external oscillator etc.) as well as voltage regulators for both 5v and 3.3v.

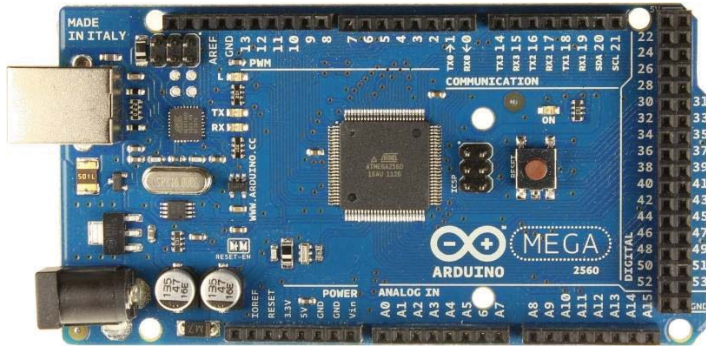


Figure 45 - Arduino Mega Microcontroller Development Board [40]

The board is designed to have additional boards attached to it (referred to as shields) to provide additional functionality. This shield concept was used to create the prototype controller.

4.1.2 Additional Electronics and Modules

While the microcontroller is capable of a lot of the required functionality, several additional modules and electronics were needed.

4.1.2.1 Serial Communication

In order to communicate with the TUF2000M modules described in section 3.2 an RS485 interface was required. RS485 is a balanced multi-drop serial standard that uses differential signalling and typically operates in a half-duplex mode. Commonly a master-slave arrangement is used to control the data transmission to avoid collisions [39].

The ATmega2560 has four UARTs for use with serial communication however, the differential signalling and line drivers are not implemented in the UARTs. In order to drive the RS485 lines an SP483 chip was used.

The SP483 is a half-duplex transceiver capable of meeting the requirements for RS485 communications up to 250kbps [41]. This is the maximum speed that the TUF2000M module is able to achieve, therefore a faster transceiver is not required.

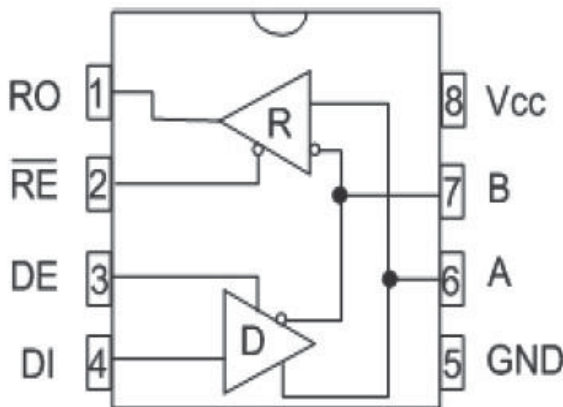


Figure 46 - SP483 Pinout [41]

The pinout of the SP483 is shown in Figure 46. The A and B lines are the RS485 lines. The receiver out (RO) and data in (DI) pins were connected to one of the UARTS of the microcontroller. The not receive enable (RE) and drive enable were tied together and were connected to a GPIO pin of the microcontroller.

4.1.2.2 Motor Driver

To be able to achieve bidirectional control of the linear actuator an H-bridge module was used. H-bridges are circuits commonly used for DC motor control and many drivers are available. In this case, an ST VN12SP30 was used because of its availability and high current limit. This module can operate between 5.5v and 16v and has a continuous current rating of 14A although much higher currents are possible for short periods [42]. The VN12SP30 has current sense ability, thermal protection and can switch up to 20 kHz.

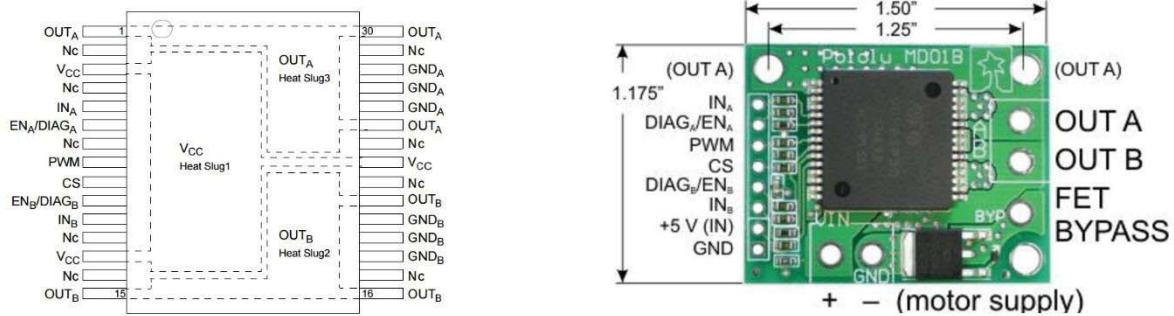


Figure 47 - VN12SP30 pinout and chip as implemented on Pololu MD01B [42]

A Pololu breakout board for the VN12SP30 was used as it provides good thermal dissipation for the chip.

4.1.2.3 Wireless Communication (Bluetooth)

Wireless communication was added to the controller in the form of an HC-05 Bluetooth transceiver module. The HC05 module is based around the Cambridge Silicon Radio BC417 Chip. The HC05 can be used in master or slave mode and at its simplest, can be used as a wireless UART bridge [43].

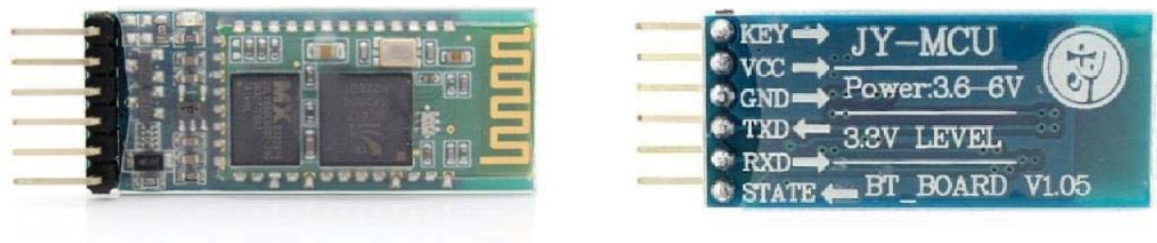


Figure 48 - HC05 Module (front and back) [43]

Once paired, the HC05 can be used as a virtual serial device, allowing programs to interact as if they were connected on a UART or RS232 serial line. This allows for simple programs to be developed on the microcontroller side and for use of existing feature rich programs on the host device.

Adding Bluetooth to the controller allows for testing and debugging during experimentation as well as adding the possibility for future control from wireless devices. A Bluetooth enabled unit would allow for the testing of control using tablets and smartphones for controlling the application rate and monitoring speed and flow rates.

4.1.3 Controller PCB Design

A printed circuit board was designed using Altium Designer. The board was created in the Massey School of Engineering and Advanced Technology Electronics Workshop by electronics technicians. The components were then soldered to the board. Figure 49 shows the PCB layout.

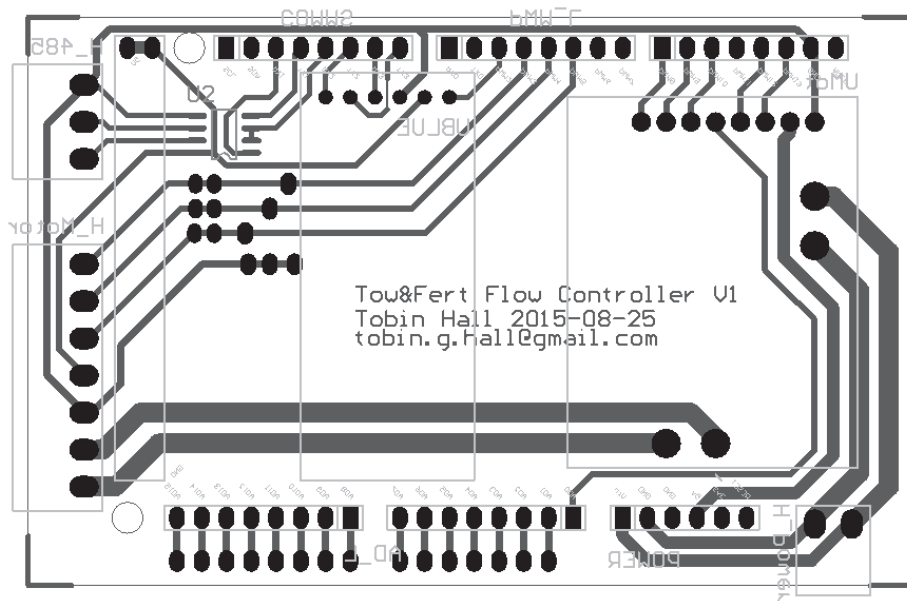


Figure 49 - Flow Controller PCB Layout

The tracks to and from the H-bridge driver are increased to handle the higher current of driving the linear actuator. Extra IO pins were 'broken out' to allow extra functionality to be added later. This greatly increased the versatility of the controller.



Figure 50 - Flow Controller and TUF2000M Meters

4.2 Prototyping Code Development

4.2.1 TUF2000M Communication Library

In order to communicate with the TUF2000M flowmeters a library was created. Communication is over an RS-485 serial line using the Modbus protocol. A C++ class was created to consolidate the code used.

4.2.1.1 Modbus Protocol

Modbus is a digital communication protocol designed for use on RS-232 and RS-485 serial lines. The Modbus protocol is a de facto communications standard in industrial devices. It was designed to integrate programmable computers, logic controllers (PLCs), sensors and actuators [39].

Modbus uses a master/slave model with a single master and up to 247 slave devices. The master is responsible for initialising all communication. Typically, the master will read or write to registers on a slave device. In both cases, the slave will send a response back to the master. The master can also send a broadcast message to all slaves, to which none of the slaves respond.

Two variants of Modbus exist, the ASCII mode, which uses printable characters that start with a colon and end with a line return and RTU mode, which uses binary data. The RTU mode uses half the number of characters of the ASCII mode.

The Modbus protocol uses two error check bytes. For the ASCII mode, these bytes are a longitudinal redundancy check (LRC). For the RTU mode, these bytes are a 16-bit cyclic redundancy check (CRC).

Table 5 shows an example transaction to read the first two registers from slave with id number one:

Table 5 - Modbus Protocol Example Transaction

Master -> Slave (Request)			Slave-> Master (Response)		
Field Name	RTU(Hex)	ASCII	Field Name	RTU(Hex)	ASCII
Header		:	Header		:
Slave Address	0x01	0 1	Slave Address	0x01	0 1
Function	0x03	0 3	Function	0x03	0 3
Register Address (Hi)	0x00	0 0	Byte Count	0x04	0 4
Register Address (Lo)	0x00	6 B	Data0(Hi)	0x00	0 0
Number of Registers(Hi)	0x00	0 0	Data0(Lo)	0x06	0 6
Number of Registers(Lo)	0x02	0 3	Data1(Hi)	0x00	0 0
			Data1(Lo)	0x05	0 5
Error Check (Lo)	0xC4	F	Error Check (Lo)	0xDA	E
Error Check (Hi)	0x0B	A	Error Check (Hi)	0x31	D
Trailer		CR LF	Trailer		CR LF
Total Bytes	8	17	Total Bytes	9	19

4.2.1.2 TUF2000M readReg function

The readReg function is a low-level function used to request data from the registers of a slave device. The function takes three arguments, the id number of the slave device, the address of the first register to read and the number of registers to be read. The data response from the slave is stored into an array for later decoding.

The function first sets up the request data packet with the required information. Then the CRC of the data packet is calculated and appended to the packet. The Drive Enable pin of the SP483 (see section

4.1.2.1) is pulled high to enable data transfer to the slave devices. The data packet is then transferred out to the slaves using the UART connected to the SP483 device. The drive enable pin is set low. Finally, the function waits for the response from the slave device and checks to ensure that the expected number of bytes was received from the slave device. The function returns the number of bytes received from the slave or zero if an error occurred.

4.2.1.3 Decoding slave packet data

Several functions were created to extract useful information from the flowmeters. These functions were used to get the flowrate, difference in transit times, total transit times and signal strength data from the meters. These functions were very similar and had a basic flow as shown in Figure 51:

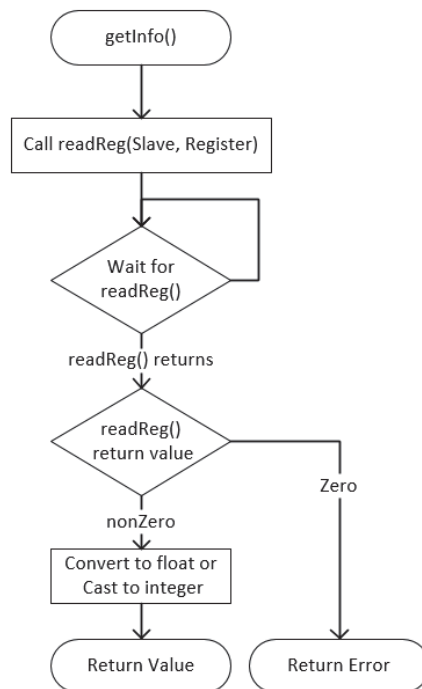


Figure 51 - Basic TUF2000M Query

Table 6 - TUF2000M Relevant Registers

Information	Data Type	Register Address
Flowrate	Float	1
Difference in transit time	Float	83
Total transit time	Float	81
Signal Strength	Integer	91

Table 6 show the register addresses and data types of the relevant information extracted from the flowmeters. Each register is 16bit, the float data type is a 32-bit (4 byte) stored in a Big Endian manner. The ATmega2560 stores floating-point numbers in Little Endian, so a conversion is required. This conversion has been implemented using a C union. The full TUF2000M class code is available in Appendix B.

4.2.2 Linear Actuator Class Development

To consolidate code associated with controlling the linear actuator a class named `Actuator` was created. The class maintains the position of the actuator and can control the speed of the actuator while retracting and extending using pulse width modulated (PWM) signals. The full code listing is in Appendix A.

4.2.2.1 *findLimits()* Function

The Linak LA12 linear actuator fitted to the Tow and Fert has an incremental encoder. The nature of incremental encoders means that on power up the controller is not aware of the position of the actuator. The position must be determined.

The find limit function first drives the linear actuator in slowly in one direction and monitors the pulses from the encoder. If the encoder has not changed state after a certain timeout (100ms) the actuator has reached the limit of travel in that direction. The direction is reversed and this time the number of pulses of the encoder are counted until the timeout is again reached. When the timeout is reached, the limit of travel in the second direction is found. This becomes the new datum for the incremental encoder.

Because the number of pulses of the encoder was counted in the second travel period, the controller knows the full range of the encoder. This allows for actuators with a different number of counts per stroke to be used in the system without modification of the controller code.

The functionality of this function is shown in Figure 52.

4.2.2.2 *setSpeed()* Function

The `setSpeed` function is used to control the power applied to the linear actuator.

A velocity is sent as an argument to the function (ranging from -255 to 255). The function then determines the direction of the velocity and sets the pins to the motor driver direction control accordingly. Finally, the magnitude is loaded into the microcontroller's hardware PWM generation register that modulates the signal going to the motor drivers enable pin.

This function allows for bidirectional control of the linear actuator.

4.2.2.3 *The update() function and PID control*

The `update` function is intended to be called with consistent timing (by a hardware timer interrupt) and implements a PID controller for the linear actuators position.

The function compares the current position of the actuator to the desired position and determines the appropriate action to take to move the actuator toward the desired location. The `setSpeed` is then called to adjust the power to the actuator by setting the PWM signal.

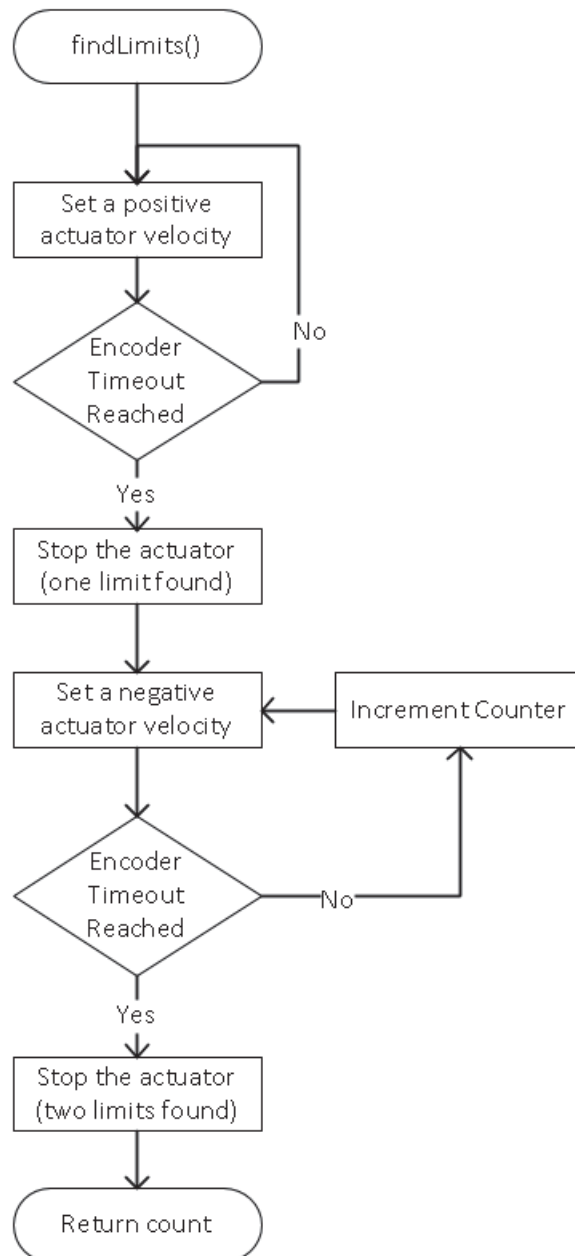


Figure 52 - findLimits() Function Flow

```

/* findLimits
 * this function is used to find
 the upper limit
 * of the linear actuator and set
 the zero point
 */
void Actuator::findLimits() {
    int oldActPos;
    //run backwards
    setSpeed(-32);
    //keep running backwards until
 the actuator stops
    do {
        oldActPos = position;
        delay(100);
    } while (oldActPos != position);

    //found the zero of the actuator
    position = 0;

    //run forward
    setSpeed(32);
    delay(1000);
    //keep running until the
 actuator stops
    do {
        oldActPos = position;
        delay(100);
    } while (oldActPos != position);

    //found the upper limit of
 the actuator
    maxPosition = position;
    //we can stop now
    setSpeed(0);
}
  
```

4.3 Controller Tuning

Two feedback loops are present in the system. One source of feedback is the encoder of the Linak LA12 linear actuator. This provides information about the position of the actuator and therefore the status of the butterfly valve controlling the flowrate. The second source of feedback is the nozzle flowrate measured by the ZD1200 flowmeter discussed in section 3.3.

Using these two feedback loops, control of both the actuator position and flowrate is possible.

4.3.1 Actuator Positioning Tuning

Actuator positioning control is implemented in the linear actuator class code discussed in section 4.2.2.

A major limitation of this control is the single incremental encoder integrated into the linear actuator. Because the encoder generates only one pulse train, it is impossible to determine the direction of travel. Often a second encoder channel 90 degrees out of phase of the original channel is used. This is commonly referred to as a quadrature encoder [39].

Because the linear actuator is self-locking, under normal conditions back driving is not possible. This means that if the encoder position changes it can be assumed that the controller caused that change. If an encoder pulse occurs, the encoder position is incremented or decremented depending on the direction that the controller was last driving the actuator.

Under normal conditions, this assumption holds and the system works fine. However, if the direction of the controller is reversed quickly and an encoder pulse is encountered before the actuator has mechanically stopped and reversed, the encoder pulse will be assumed, incorrectly, to be in the new direction. This will cause the position of actuator to be incorrect permanently.

This issue could be alleviated by the use of speed profiling code, which does not allow the velocity of the actuator to rapidly change directions. This will also have the effect of reducing wear on the mechanics of the actuator. The problem could be entirely overcome by the use of a quadrature encoder.

4.3.2 Flow Control Overview

Two methods of flow control are possible in this system. Controlling the flow by controlling the *position* of the flow valve or by controlling the *power* applied to the flow valve.

Using the valve position would essentially create a cascade control system [39]. One loop would control the valve position and another would control the flowrate by altering the set point of the position controller. This method increases the complexity of tuning the controller. It also suffers a lot from the actuator limitations discussed in section 4.2.2.3 as the controller will constantly be changing direction rapidly to control the flow.

Using the alternative of controlling the flowrate by controlling the power applied to the actuator is a more suitable option. The power applied to the actuator can easily be controlled by using the `setSpeed` function of the linear actuator class (section 4.2.2). This has only a single control loop and tuning the controller is simplified.

Figure 53 shows an overview of the fluid flow path and fluid control loop.

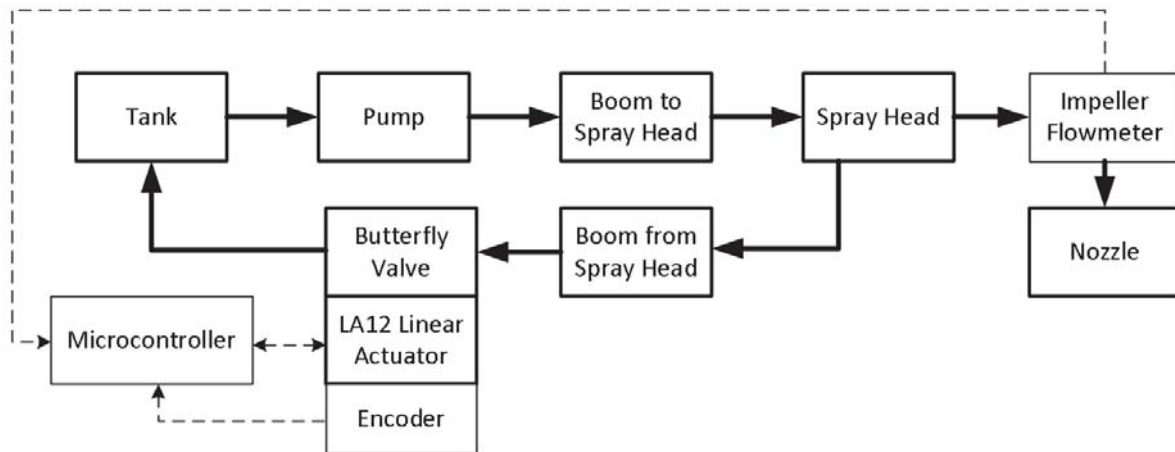


Figure 53 - Control System Overview

4.3.3 Ultimate Gain Tuning

A PID controller was implemented to control the nozzle flowrate using the power applied to the linear actuator that moves the control valve. The power is controlled by a PWM signal to the motor driver (section 4.1.2.2).

A variation of the ultimate gain tuning method was used to tune the controller.

1. The system was setup with a hose connected to the nozzle output to return the flow back into the tank.
2. The motor was set to generate 20 PSI of pressure at the pump output (see section 2.4.2).
3. A low initial proportional gain was set.
4. The controller was programmed to generate step changes from 10litres/min to 18litres/min.
5. After each step, the gain of the system was increased.
6. The testing was continued until the increasing gain caused oscillations of the system.

The plot in Figure 54 shows the set point and actual flowrate during the first tuning process:

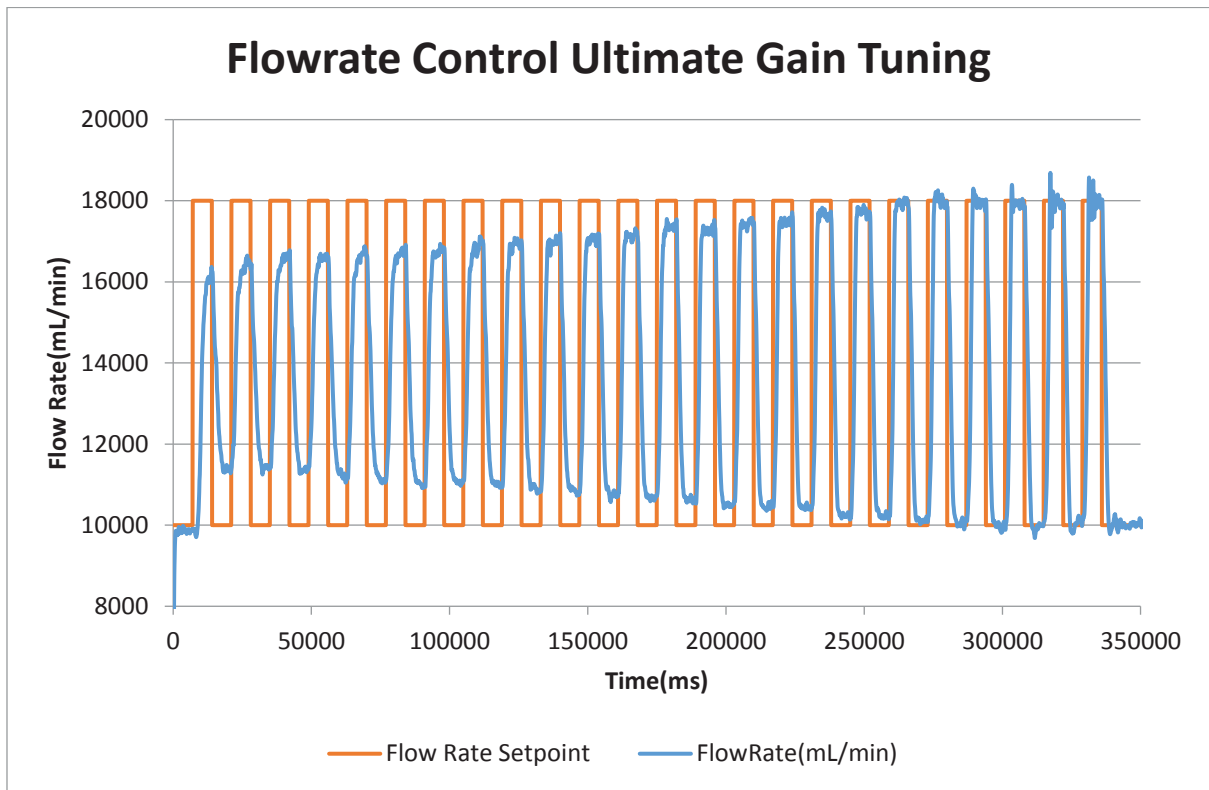


Figure 54 - Flowrate Control – Rough Ultimate Gain Tuning

Figure 55 shows data from the same test with the valve position and gain of the controller plotted.

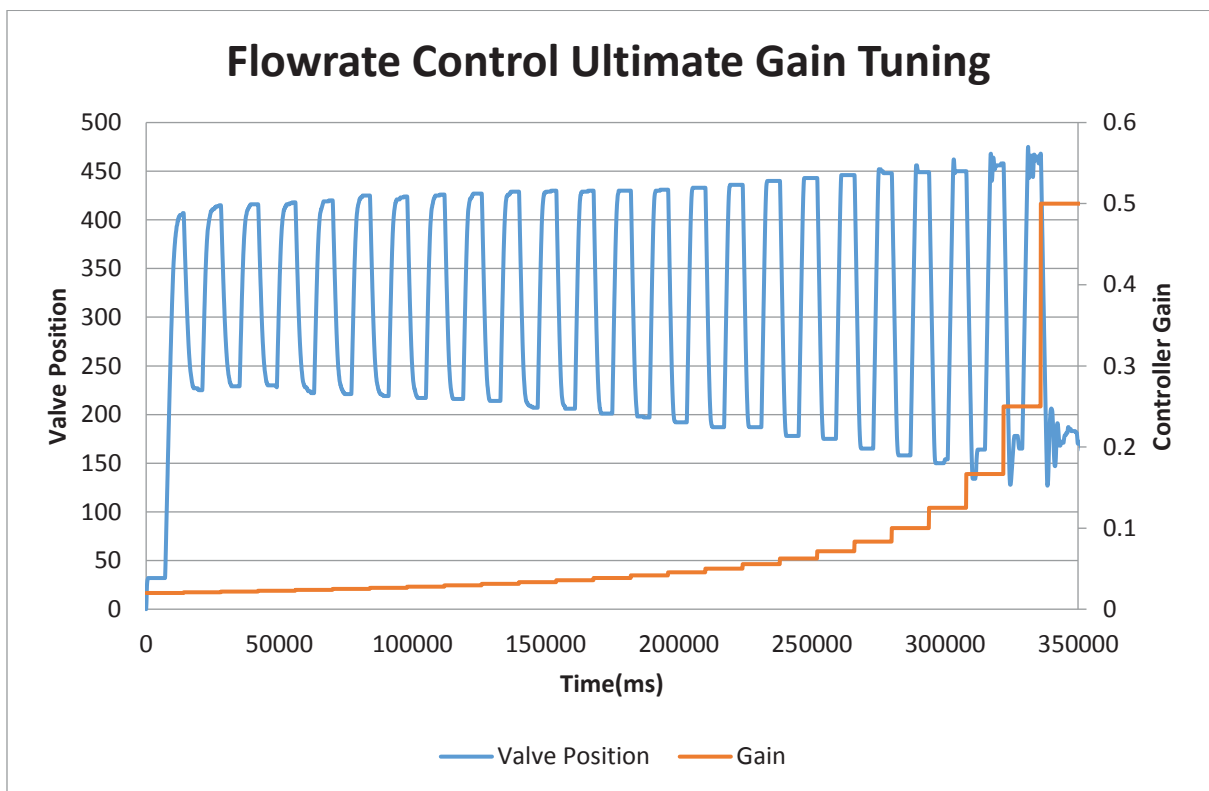


Figure 55 - Flowrate Control - Rough Gain Tuning

The plot shows that the system began to oscillate when the gain was increased to around 0.1.

After the preliminary gain of 0.1 was found, the test was repeated with a finer resolution. This is shown in Figure 56 and Figure 57.

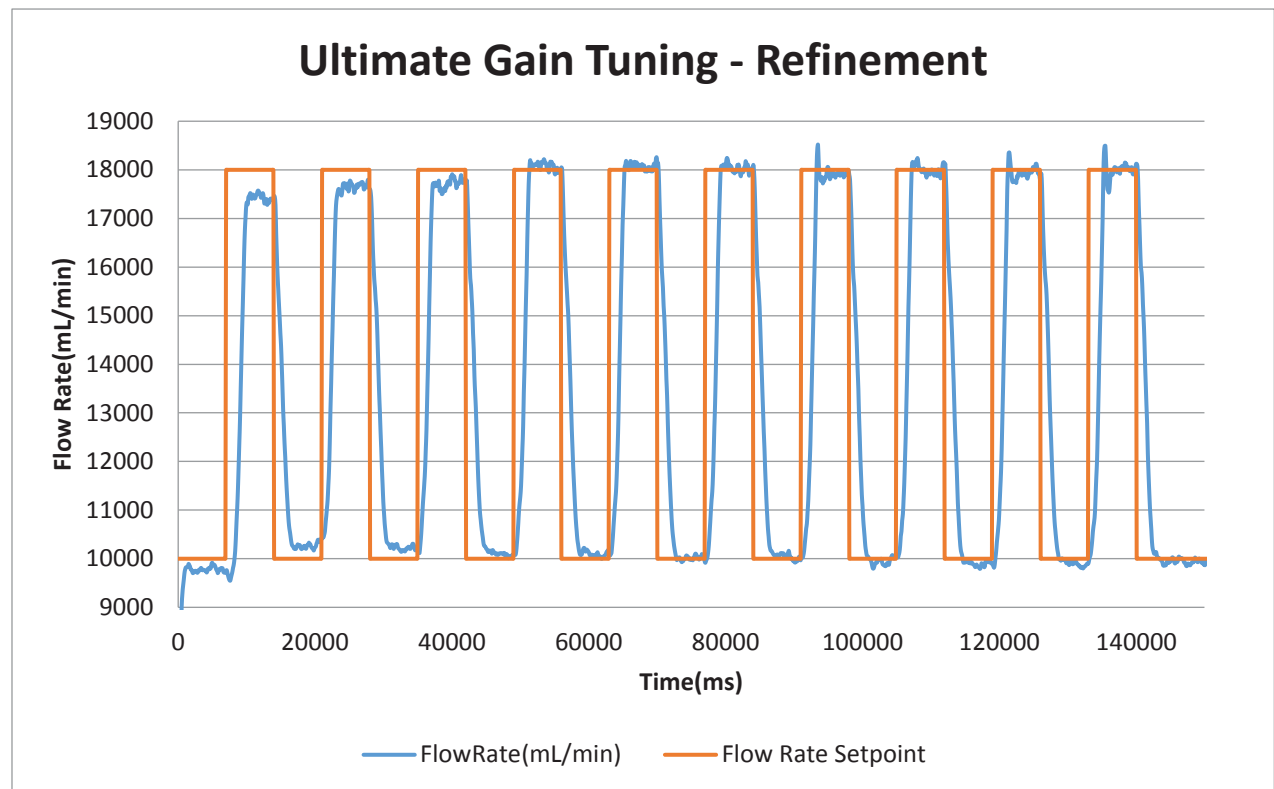


Figure 56 - Flowcontrol Tuning - Refinement

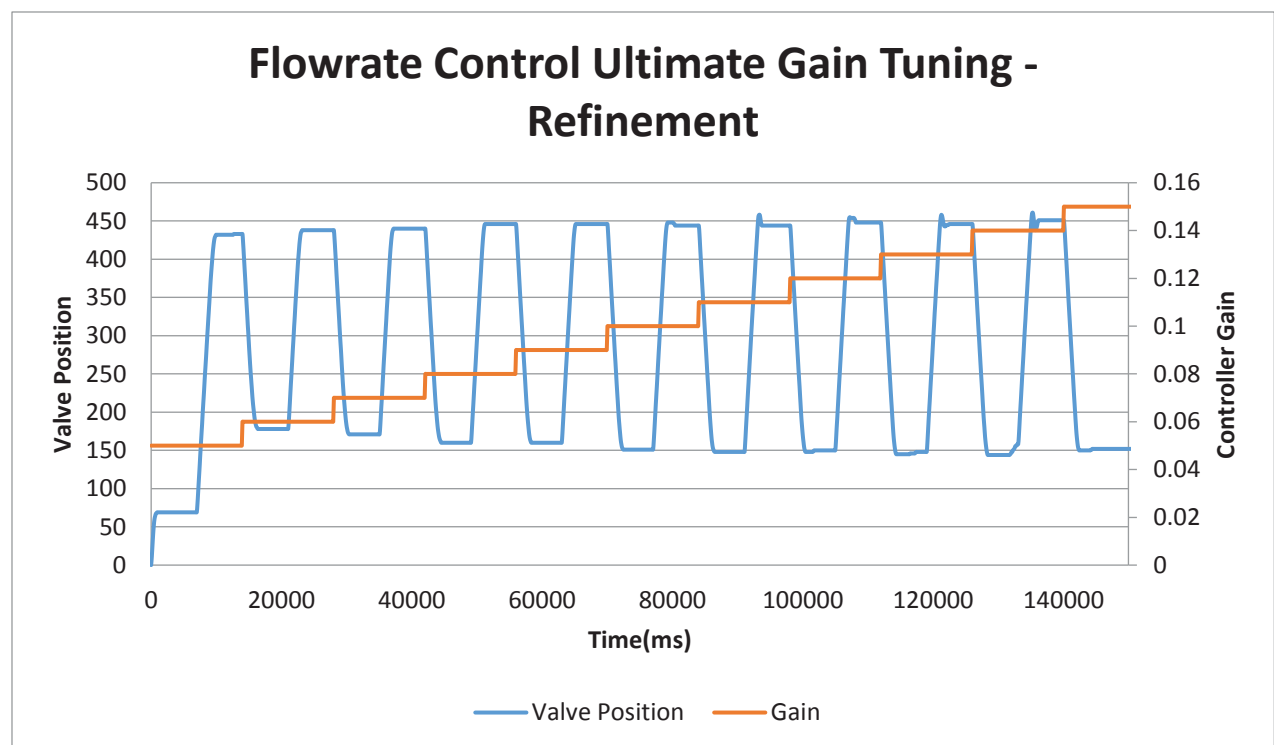


Figure 57 - Flowrate Control Tuning - Refinement

Because of the nature of the system and the use of a linear actuator with a high gear ratio, it is difficult to maintain stable oscillations so the ultimate gain is difficult to identify accurately. Overshooting of the linear actuator begins at a gain of 0.1.

From the plots above the gain of 0.09 was chosen as the ideal gain.

4.3.4 Testing Proportional Flow Control

After the maximum gain with no actuator overshoot was identified, a purely proportional flow controller was tested. The gain used was 0.09.

A function was created to vary the flowrate set point. This was designed to simulate changes in vehicle speed over time.

The function used to generate the simulated required flowrate at time t was:

$$3000 \cdot \sin \frac{t}{60000} + \frac{t}{60} + 1000 \quad (4.1)$$

The constants used in the equation above were generated by a vehicle moving at a speed range of between 5 and 8 km/h and with an application rate of 100L/ha based on a spray area of 20m.

Figure 58 shows the controller response to changing flowrate set point:

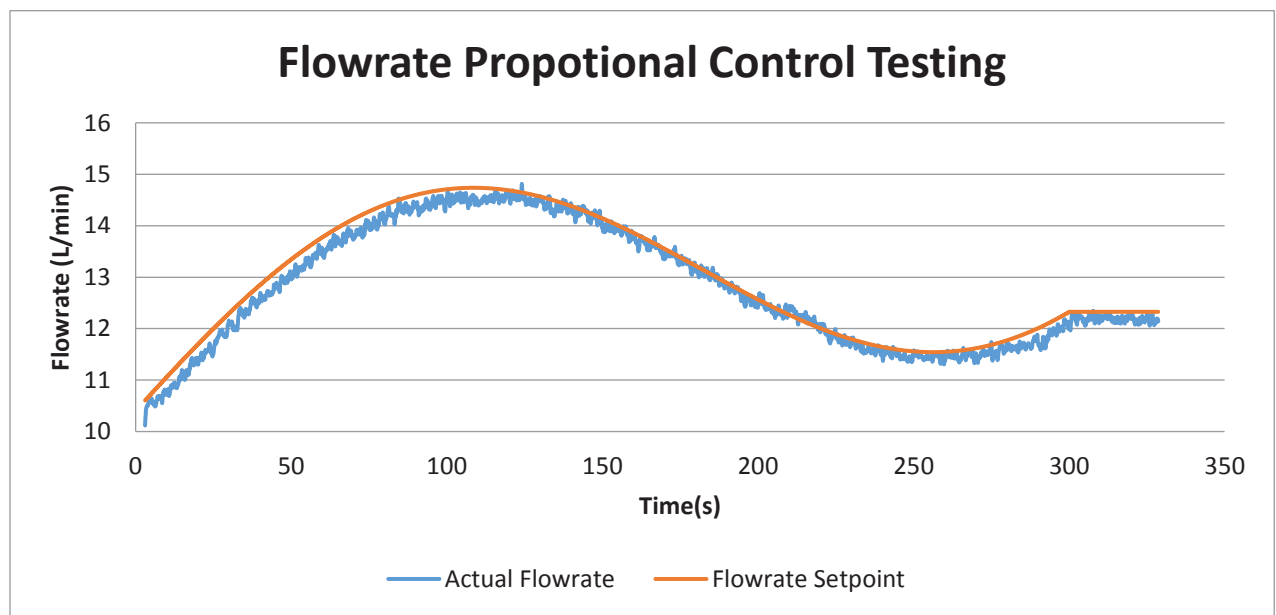


Figure 58 - Flowrate Proportional Control Testing - Simulated Speed Variation

The plot shows a small steady state error caused by using purely proportional control. The controller is able to make the flowrate track the desired flowrate very well.

5 Spray Area Distribution

Another challenge associated with measuring and controlling the flow rate of the Tow and Fert is the consistency of the spray area. To maintain a constant application-rate the flow rate of the product must be changed to compensate for changes in vehicle speed.

The proposed method of flow control is to vary the fluid pressure by means of a butterfly valve controlled with a linear actuator. Given the fixed geometry of the nozzle, as the pressure and volumetric flow rate change the spray area will also change. Fluid with a lower velocity will hit the nozzle with less energy and travel less distance. Therefore, as the vehicle speed reduces, the flow reduces to maintain the application rate and the spray width will decrease. Likewise, if vehicle speed increases the flow will have to increase to compensate which will increase the spray width.



Figure 59 - Ideal Spray Application

An ideal spray application pattern is shown in Figure 59. If the spray width is predictable throughout the application, maintaining constant application is relatively easy. However, if the vehicle speed reduces due to terrain changes for example, the proposed controller would reduce the flow rate. The reduced flow rate would reduce the spray width and if the same path were followed, the result would be an area where no product is sprayed. This is illustrated in Figure 60.

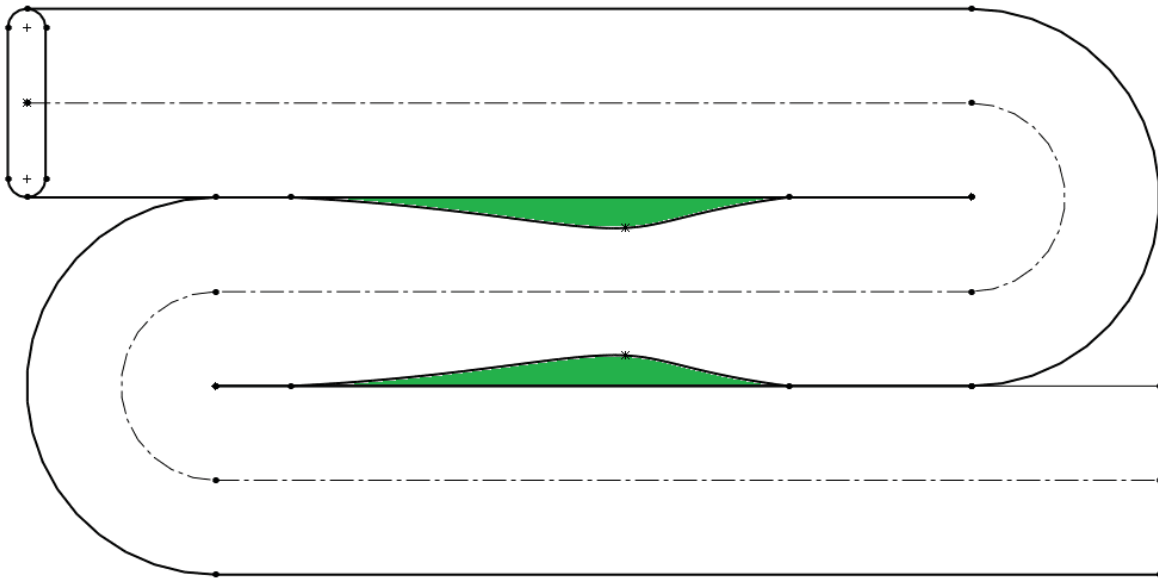


Figure 60 - Areas of no spray caused by reduced spray width

If the vehicle speed increases and the spray width increases following the same path will result in areas of excessive application. An example is shown in Figure 61.

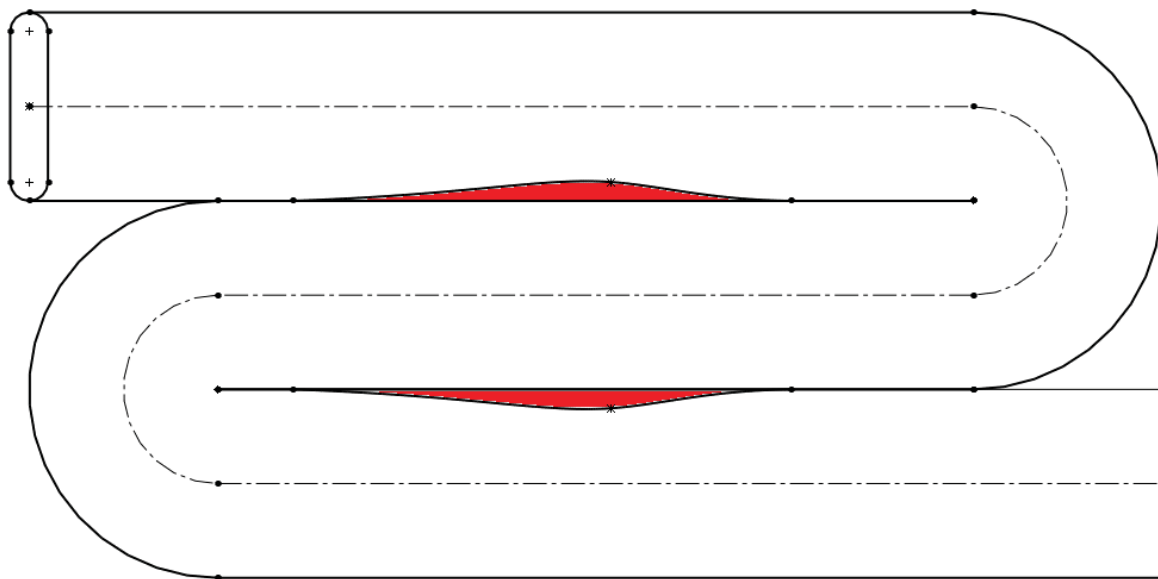


Figure 61 - Areas of excessive spray caused by increased spray width

Given the issues associated with spray area and its effect on application, it is important to be able to quantify the spray width accurately. Because the spray width changes with the nozzle geometry, the manifold pressure of the Tow and Fert and the properties of the fluid, it is critical that the test procedure to measure the spray width is at least semi-automated.

Previously the spray area has been determined by use of plastic plates. The procedure involved laying a line of disposable plastic dinner plates on the ground. The Tow and Fert machine was then driven past the plates in a manner in which the plates were inside the spray. After the machine had passed, the plates were individually weighed to determine the amount of spray collected.

This process is relatively simple and effective. It was used by Metalform to test nozzle design under certain conditions. However, given the number of tests that would need to be performed to quantify the spray area given the changes in flow rate, manifold pressure, fluid properties and nozzle design this test would not be realistic. A continuous or semi-continuous testing method would be needed.

5.1 Spray Area Measurement

Several methods exist for measuring spray area. Typically, these methods are used to measure the spray from a single spray nozzle. These nozzles usually have spray coverages of less than one square meter.

5.1.1 Vision Based Measurement

Vision based measurements use one or more cameras to capture images of the spray or a section of the spray.

Laser sheet imaging uses a laser generator and a divergent lens to create a laser plane. If water droplets enter the plane, they scatter the light of the laser. A camera is used to capture an image of the plane. The camera is often fitted with a bandpass filter to remove all light except that of the wavelength of the laser. The image captured is a snapshot of the spray in that plane at that instant.

This method is often used with water as the spray medium as the light scattered by a sphere of water is predictable. The illumination of the water droplets is proportional to the droplet's surface area. Sometimes an agent is added to the water to enable Laser Induced Fluorescence (LIF). When this occurs, the entire droplet emits light.

5.1.2 Mechanical Patternators

To measure spray distribution mechanical patternators divide the spray into discrete regions. Fluid sprayed into these regions is collected and channelled into calibrated tubes. Typically, the patternators use an inclined plane to channel all fluid to one end of the patternator where it is collected. This results in a one-dimensional distribution. Because the spray usually comes from a moving vehicle, a one-dimensional distribution that is perpendicular to the travel direction sufficiently quantifies the spray distribution.



Figure 62 - Example of Horizontal Spray Patternator [44]

The tubes are typically sealed and have to be manually emptied at the end of each test.

The height of the fluid in each tube indicates the distribution of the spray. Sometimes brightly coloured floats are added so that the level is more obvious with visual inspection.

Variations exist where the height of each tube can be measured electronically typically using ultrasonic range sensors mounted on an axis that moves over each tube.

Experiments have also been performed in two dimensions where a collection grid is used instead of a slanted platform [45].

5.1.3 Scanning Patternators

Similar to traditional patternators, scanning patternators divide fluid flow into discrete areas. Unlike traditional patternators however, the covered area is not the entire spray area. Instead, the patternator is moved under the segments of the spray and characterises only one segment at a time [46]. The patternator is scanned along the spray until the entire spray area has been characterised.



Figure 63 - Scanning Patternator [47]

5.2 Scanning Load Cell Panel

This section describes the design, construction and testing of a variant of the scanning patternators described in section 5.1.3. Two variations to the design were made. The scanning element uses a plate suspended by two load cells and measures the spray impact rather than accumulated flow volume. The second variation is that the scanned element is stationary and in this case, the spray machine and nozzle is scanned past the impact sensitive platform.

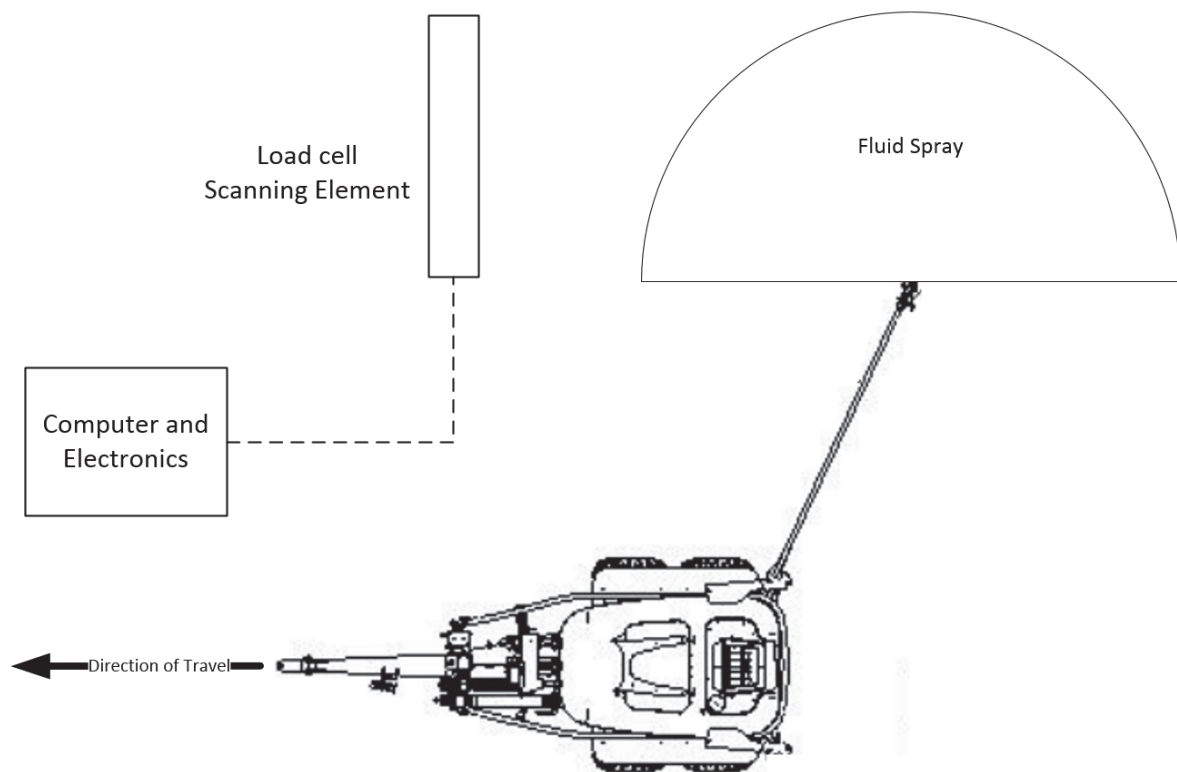


Figure 64 - Scanning Platform Experimental Setup

This scenario is made possible by the ability to rotate the nozzles on the Tow and Fert. Normally the nozzle would be oriented to spray out in a direction perpendicular to the direction of travel. In this case, it is rotated 90 degrees so that the spray width is in the direction of the travel.

Moving the machine rather than the scanning element has two benefits. Firstly, the machine was designed to be moved, it can be moved with many vehicles. Secondly, and more importantly, it removes any noise that would be transmitted by bumps and knocks to the sensitive load cell platform. This removes the need to create a smooth track to move the platform.

5.2.1 Design and Construction

To test this concept a platform was created. The platform consists of an aluminium plate bent centrally along its length to allow water to run off. This bend has the added advantage of increasing the plate stiffness. This plate is suspended by two load cells, one at each end. The load cells anchor to an aluminium base that keeps the suspended plate from the ground. Spacers were created to ensure clearance around the load cells. These spacers were 3D printed with angles that match the bend in the aluminium scan plate.

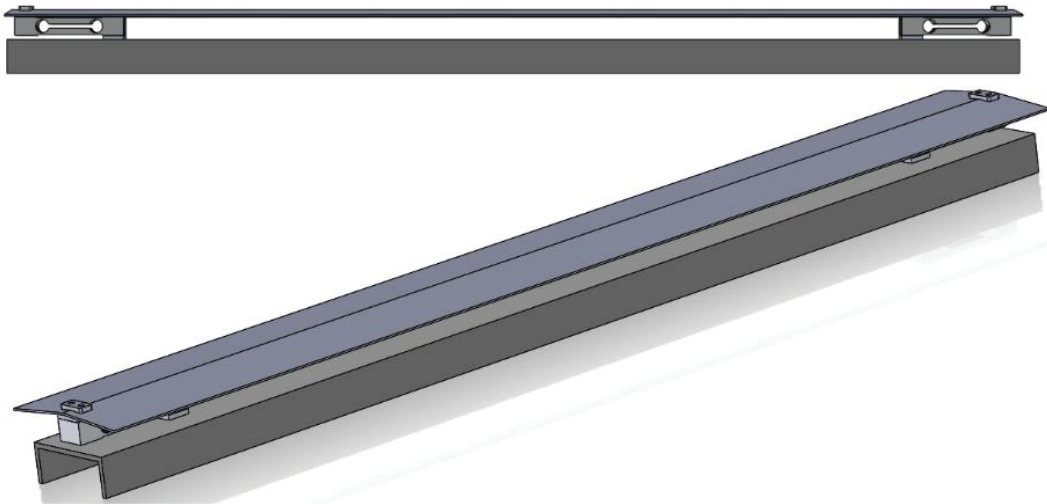


Figure 65 - Scanning Element

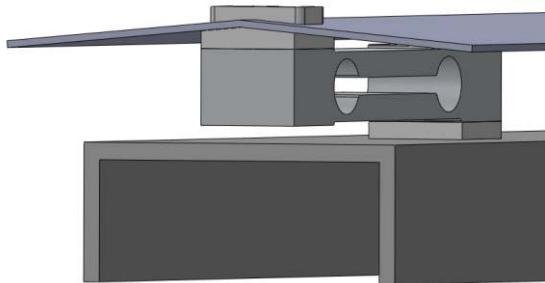


Figure 66 - Scanning Element Spacers

The load cells used were TAL201 wide bar style load cells with a 10kg capacity.



Figure 67 - TAL201 Load Cells

The load cells are 130x30x22mm in dimension.

5.2.2 Electronics and Code Development

An electronic circuit board was developed to measure the load experienced by both load cells. The measurement was based around an AD7190 24-bit sigma-delta analog to digital convertor (ADC). This chip is capable of measuring two differential inputs channels or four pseudo differential input channels. In this application two differential channels are used, one for each load cell. The AD7190 communicates over an SPI serial connection.

To allow communication between a computer and the ADC an Arduino Nano microcontroller was used. The Arduino Nano board has a built in USB to UART serial convertor.

The electronics are powered over the Arduino Nano's USB port. The voltage specification of the USB standard ranges from 4.45 volts to 5.25 volts. In order to supply the ADC and load cells with a stable voltage, the USB power was first stepped up to 8 volts using a boost converter and then regulated down to 5 volts using a linear voltage regulator. The LTC3459 and the ADP3303 integrated circuit chips were used respectively for these functions. This setup provides a very stable voltage for the load cell excitation and the ADC reference. The electronics overview is shown in Figure 68.

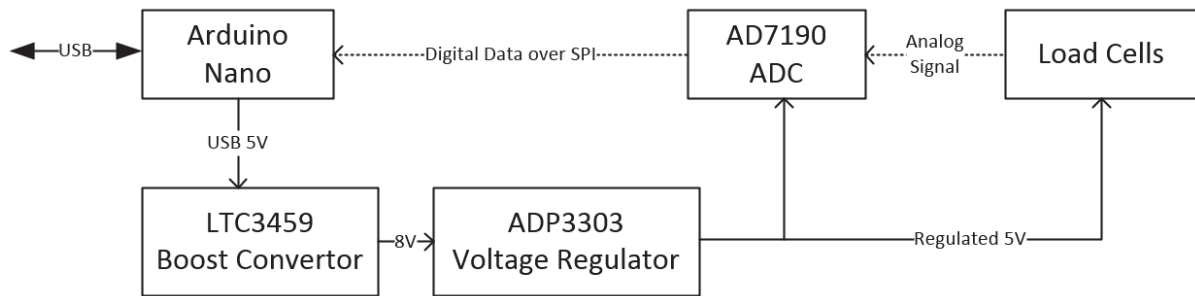


Figure 68 - Load Cell Scanner Electronics Overview

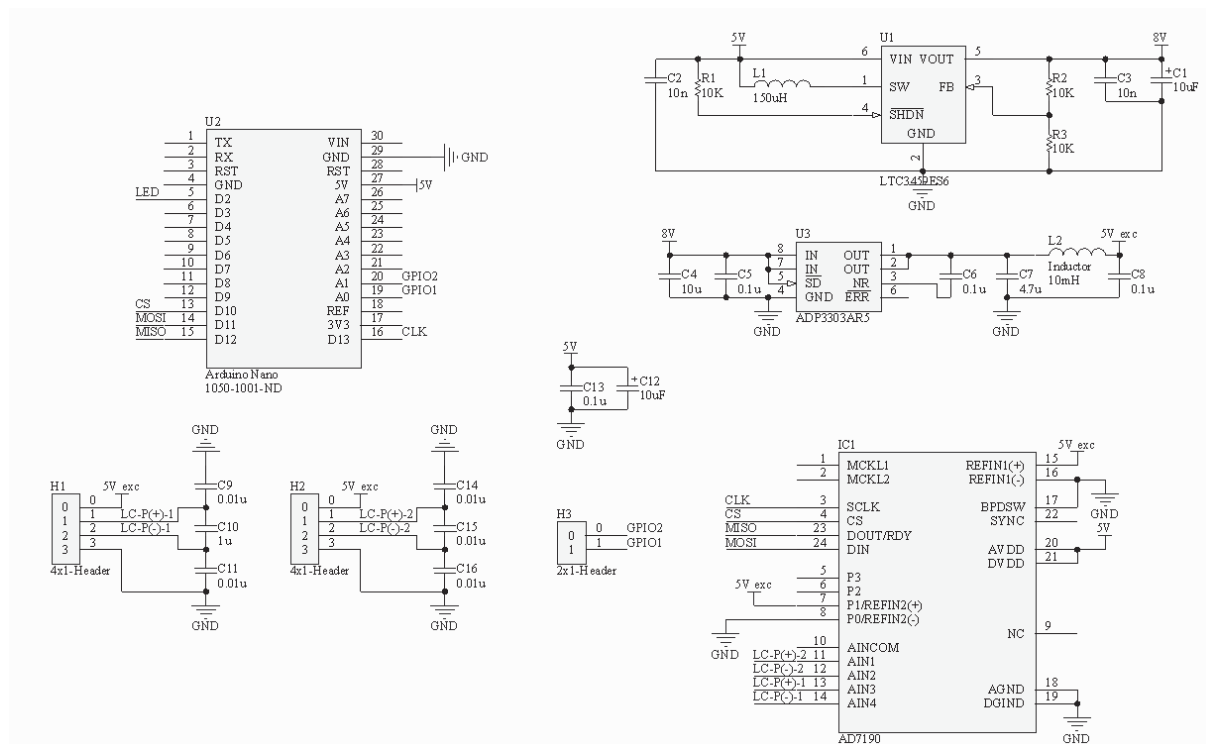


Figure 69 - Load Cell Scanner Electronics Schematic

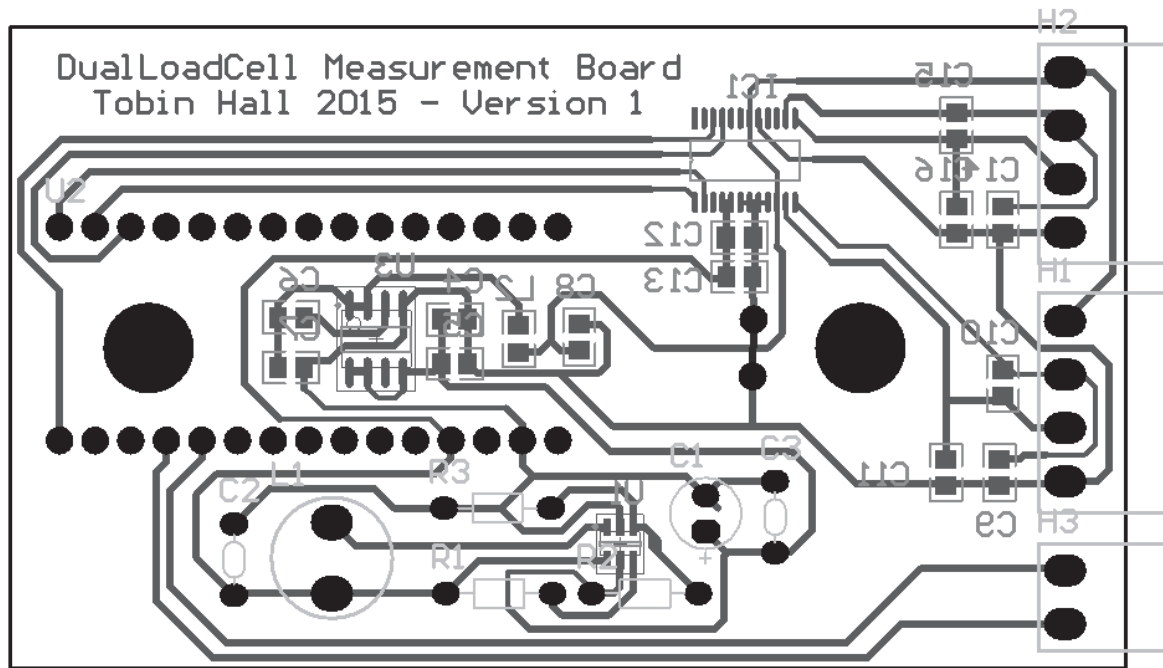


Figure 70 - Load Cell Scanner Electronics PCB Layout

The AD7190 communicates over a SPI serial bus. Code was developed to configure and collect data from the ADC. This code was developed in C.

The AD7190 was configured to use the external reference pin 1 as the voltage reference. This pin is connected to the regulated and stabilised 5-volt supply. The ADC was set to use the internal oscillator as a clock signal and an internal gain of 128. Finally, the ADC was configured for continuous conversion mode on both dual-ended channels. In this mode, the analog to digital convertor is constantly converting the analog voltages to digital values. When a conversion is complete, the Data-Out line of the ADC is brought low and conversion of the next channel is started.

5.2.3 Calibration and Signal Conditioning

Calibration was performed in the platform using two weights with known masses. Each weight was placed in three locations on the platform, at each end directly above each load cell and somewhere near the centre of the platform. The raw data from this test is plotted in Figure 71.

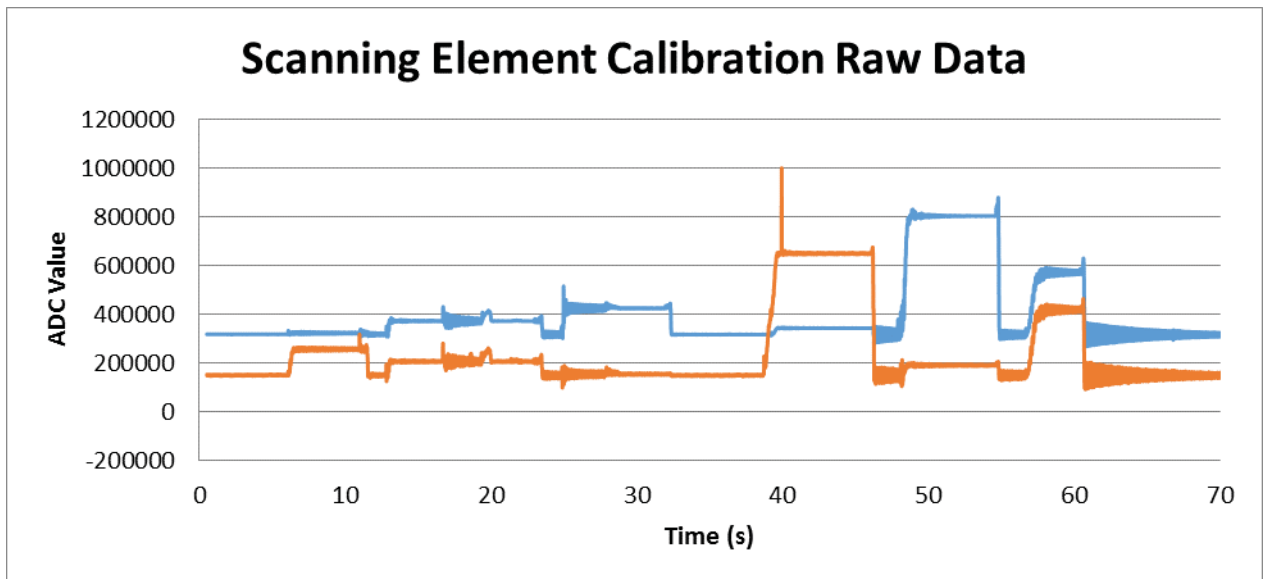


Figure 71 – Load Cell Calibration Raw Data

The offset for each signal was taken from the average value of the initial section where no additional weight was added to the platform. To remove the high frequency, noise a cumulative moving average filter with an n-value of 15 was used. This filter is described in section 3.2.3. Figure 72 show the two signals after correcting for the offset and filtering. The sum of the signals showing the total weight is also shown.

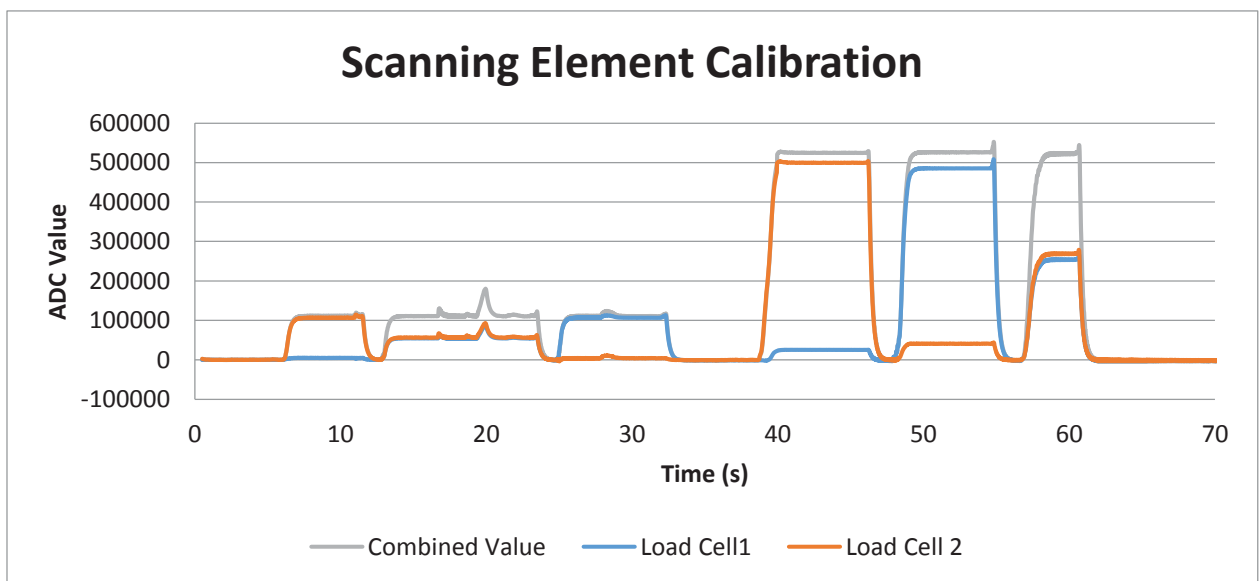


Figure 72 - Load Cell Calibration Filtered Offset-Corrected Data

Data from the combined signal was used to obtain the calibration data. The average value of the combined signal when the larger weight was applied was 524704. The weight of this object was 1258 grams. Dividing the ADC count by the weight of the object yields a calibration value of 417counts per gram. The ADC count of the smaller weight was 111130, dividing this by 417 yields 266.5g. The measured weight of this object was 266.7g, confirming the calibration.

Because of the long thin plate of the platform, the plate has a tendency to vibrate when disturbed. Figure 73 shows the impulse response of the platform. A small rubber ball was dropped into the platform to simulate an impulse.

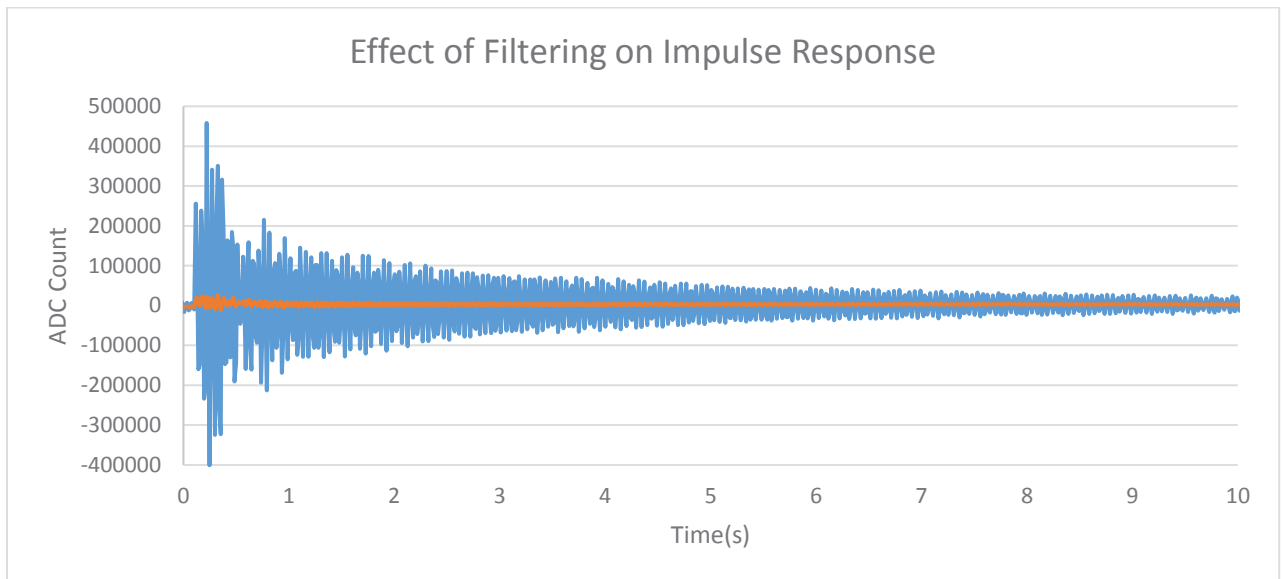


Figure 73 - Effect of Filtering on Impulse Response

The plot shows both the unfiltered values and the data after being filtered by a cumulative moving average with an n value of 15. The filter is very effective at removing the noise caused by the continued vibration of the platform.

5.2.4 Testing and Results

After the scanning element was calibrated, tests were performed with the Tow and Fert machine.

In each of the tests, the scanning element remained stationary on the ground and the sprayer was towed forward over the scanning plate. The machine was then moved around in a loop to perform the next test. This is shown in Figure 74. This allowed for a semi continuous testing process. Because of the space requirements, the test was performed outside. This meant that testing was limited to clear, fine days with little to no wind.

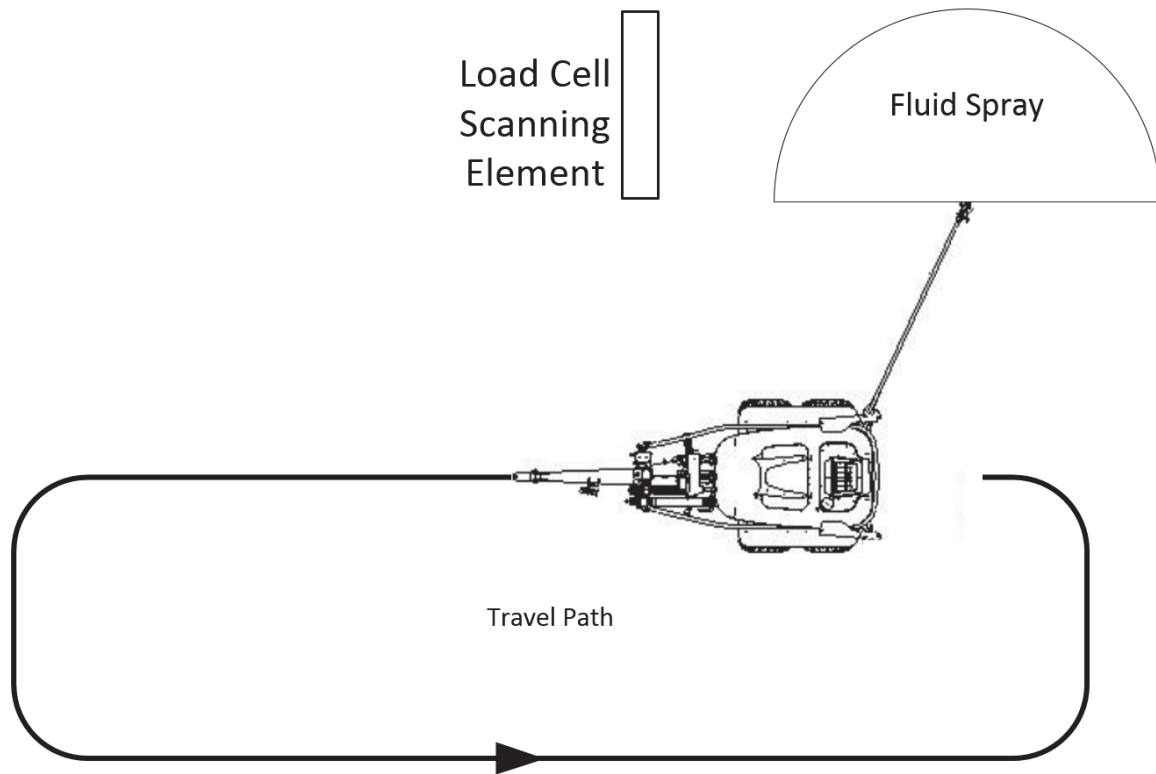


Figure 74 - Scan Platform Test Path

A plot of the first test is shown in Figure 75.

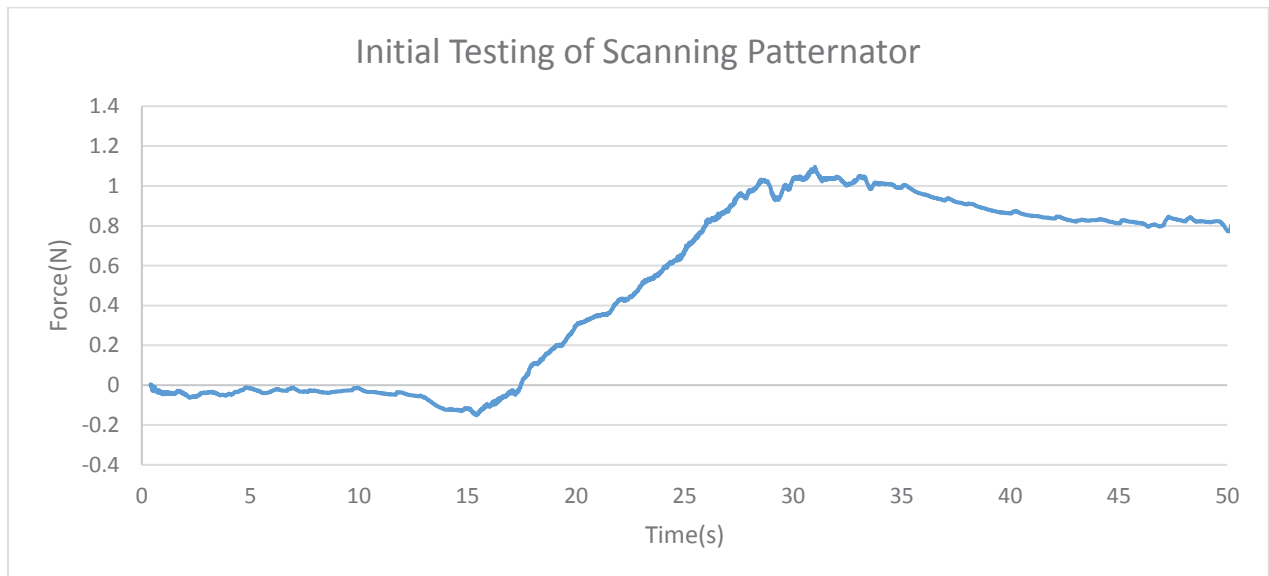


Figure 75 - Initial Scanning Patternator Testing

The plot shows a gradual increase in applied force from around 0N to a peak around 1.2N and then a decrease to around 0.8N where it remains. The reason for this was the accumulation of fluid on the platform as shown in Figure 76.



Figure 76 - Scanning Element Water Accumulation

Figure 75 shows that the signal amplitude was around 0.2N. Compared to the 0.8N of accumulated fluid on the platform this is a very low signal. To reduce the effect of fluid accumulation the surface of the platform was polished and a silicon-based water repellent was applied. This water repellent ("Selleys Water Shield") is typically used on fabrics but preliminary tests showed that it was still effective when applied to aluminium and allowed to dry. After this process, the platform retained significantly less water.

After the polishing and coating of the platform additional testing was performed in the manner described. The tests seemed to provide two distinct styles of spray pattern. Representative plots of the two types are shown in Figure 77 and Figure 78.

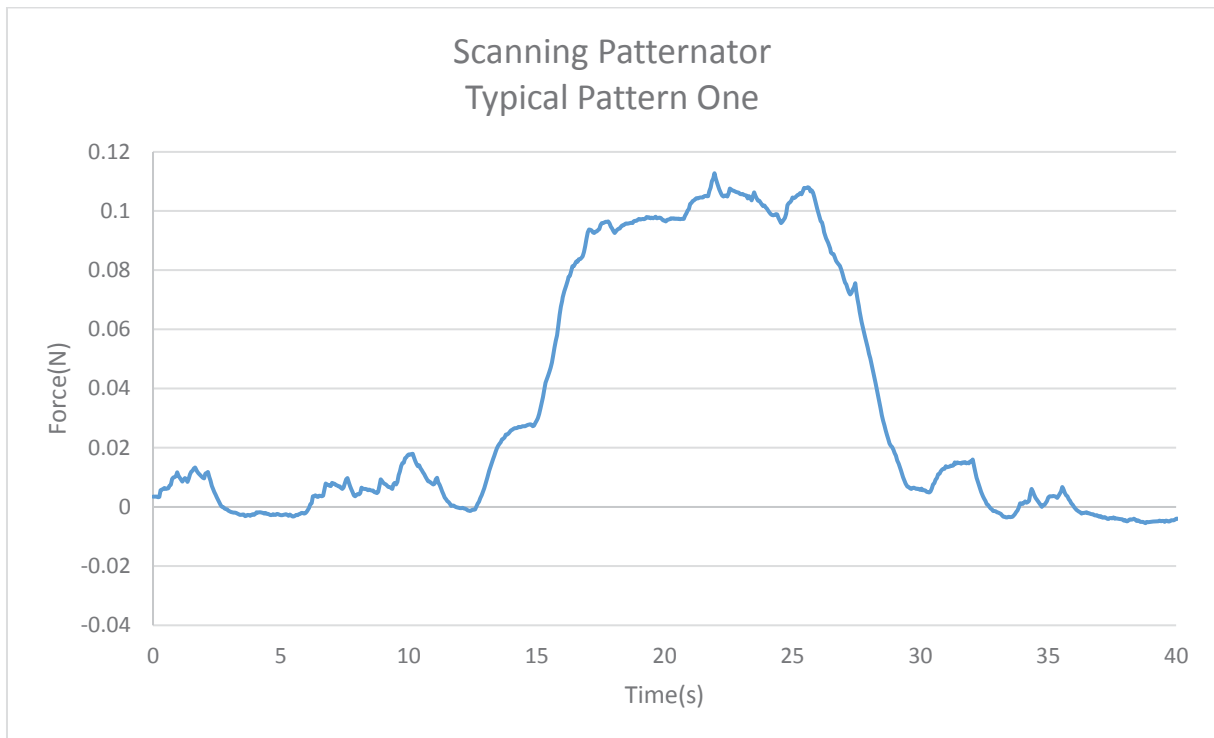


Figure 77 - Scanning Patternator - Typical Pattern One

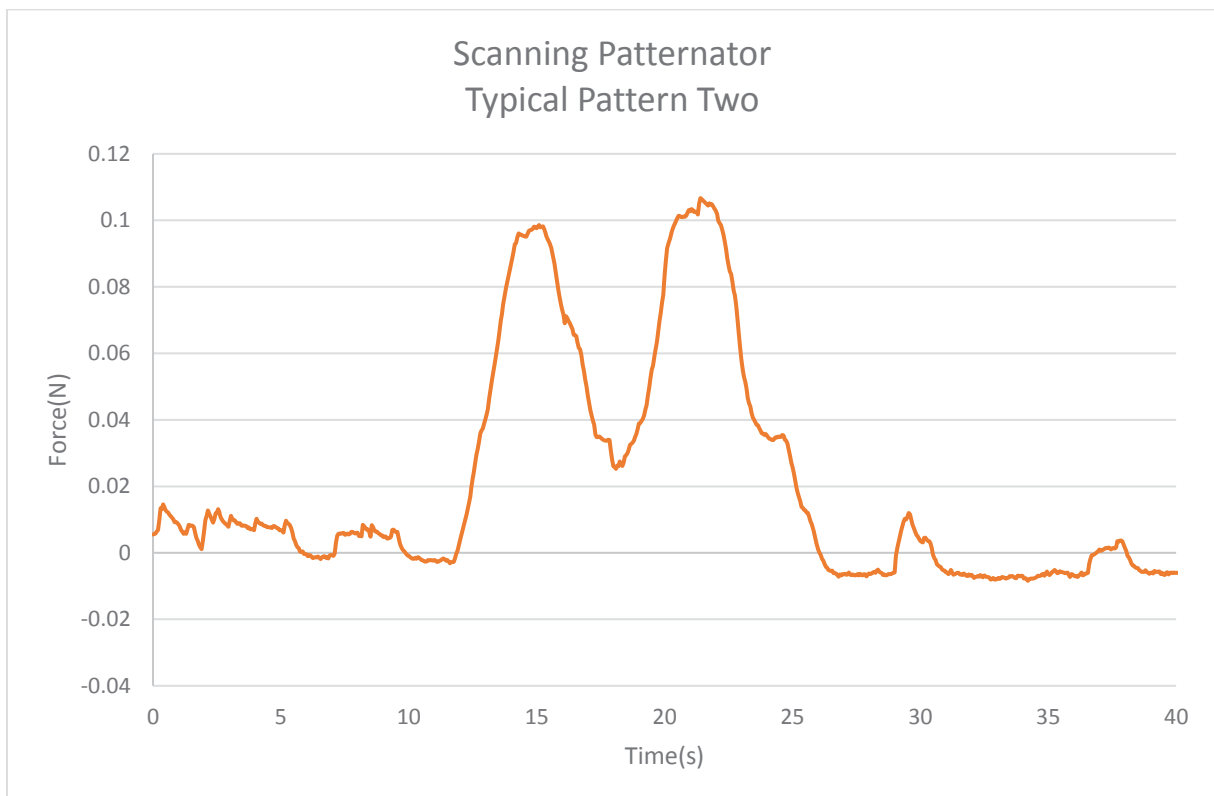


Figure 78 - Scanning Patternator - Typical Pattern Two

The reason for the two distinct patterns in the tests was evident after examining the spray more closely. The spray pattern was not purely elliptical as first thought. To determine what shape of the spray pattern, the machine was used to spray water onto a dry sealed area for a short time. An image of the result is shown in Figure 79.



Figure 79 - Visual Indication of Spray Pattern

There is a blank area in the spray pattern around the nozzle. This test was performed using a TF20 nozzle. The total size of the pattern was measured to be around 12 meters wide and 3 meters deep.

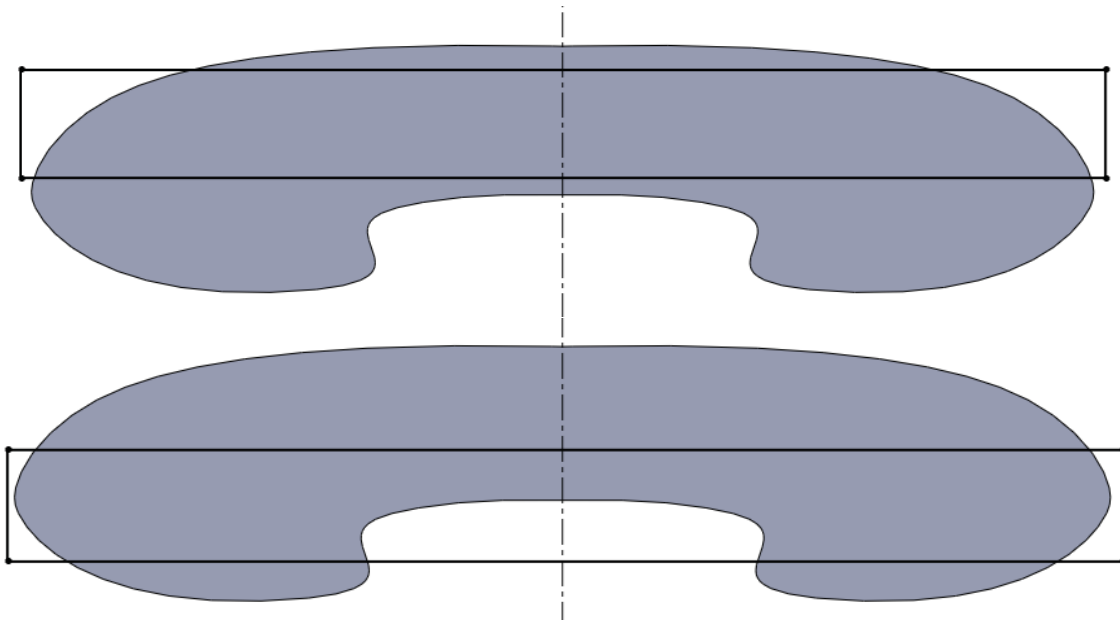


Figure 80 - Segmentation of Spray Pattern by Scanning Element

The scanning element was 1.2 meters long while the spray pattern depth is around 3 meters. Figure 80 shows the spray pattern being segmented by the scanning element in two different locations. This would account for the two distinctive trends in the data. The only way to overcome this would be to expand the length of the platform to cover the entire spray depth. To achieve this either the length of a single panel could be increased, or multiple panels could be used, each with their own load cell sensing elements.

5.2.5 Evaluation and Conclusion

The testing performed using this scanning load cell panel has shown that the method is not ideal for quantifying spray patterns in this situation. The space required to test in a semi-continuous way means that the test could not be performed indoors. This means that the test is influenced heavily by the weather, including even light wind. The consistency of the tests was low, with a relatively low signal to noise ratio.

The platform used was not sufficiently large to capture the entire spray area. This yielded two styles of results, single and twin peaked patterns. It would be possible to build a platform to capture the entire spray area. However, given the other issues with this method of measurement other methods were investigated.

5.3 Stationary Patternator

To allow for continuous spray area testing a stationary patternator was developed. Instead of collecting fluid into closed containers, the fluid is drained through flowmeters.

5.3.1 Design and Construction

The patternator was designed to use standard sheets of corrugated roofing. The roofing has a pitch of 76.2mm. The framing consists of nine individual frames. Each of these frames support exactly one corrugated sheet. The central frame has a pair of legs at each end and is self-supporting. The remaining frames have legs only along one side. These frames are supported on the other side by the adjacent frame. The support is by a pair of brackets mounted to the underside of the framing into which the new frame is slotted. The legs of the patternator fold into the frame for storage.

The overlap of the corrugations is reversed on either side of the central frame in such a way that the outer frames always overlap the inner frames. This means that when the frames are lifted from the supporting brackets the roofing does not interfere with the motion. This allows the patternator to be disassembled easily for storage and transport

The total span of the patternator is around 6m. The pitch of the patternator is 76mm. The corrugations drain into twenty collecting bins. Each collecting bin covers four corrugations for a sampling resolution of 305mm.

Each of the collecting bins drain through a small flowmeter. This allows the flow from each section to be individually measured.

5.3.2 Flow Measurement and Calibration

In order to quantify the flow from each of the collection bins flow sensors were used. The sensors needed to be capable of measuring relatively low flow with very low fluid pressure. The pressure in this case is supplied only the fluid head within the containing bins.

5.3.2.1 YF-S401 Flow Sensors

The YF-S401 flow sensors were selected. These sensors are rated to measure flows between 300mL/min and 6000mL/min at a maximum working pressure of 0.8MPa. The sensors are simple Pelton-wheel style flow sensors. The sensor consists of a plastic body and water rotor with a magnet and Hall Effect sensor. The Hall Effect sensor provides an open collector type output.



Figure 81 - YF-S401 Flow Sensor

The sensors were wired into a loom in pairs. An unshielded four-core cable runs to each pair of sensors. Two of the cores are used to supply a 5v power line to the both of the sensors. The remaining two cores are used to return the signal lines back to the controller, one core per sensor.

The sensors were installed to the patternator using a length of polyurethane tubing. This tubing was inserted with an interference fit into the bottom of each of the collecting bins. The tubing protruded around 2mm into the collecting bins and around 120mm below it. The sensors were then inserted into the tubing. The fit of tubing into the bins and around the connector of the flow sensor is tight enough to suspend the sensor from the bins.

Once fluid has been through the flow sensor, it is drained to the ground.



Figure 82 - Stationary Patternator Flow Sensor Installation

5.3.2.2 Stationary Patternator Flow Sensor Calibration

Once the YF-S401 flow sensors were installed to the patternator, they were calibrated in situ. The calibration was performed using the following procedure:

1. The controller was connected to a computer for data logging.
2. The controller periodically sends a time stamp and the encoder count for each sensor.
3. 1750mL of water is measured using a measuring jug and poured into a collection bin.
4. Water drains through the flow sensor and the encoder pulses are counted by the controller.
5. Step 3 is repeated for each of the 20 bins.

This test was repeated 5 times with 100 total encoder counts collected in total. This data is show plotted in Figure 83.

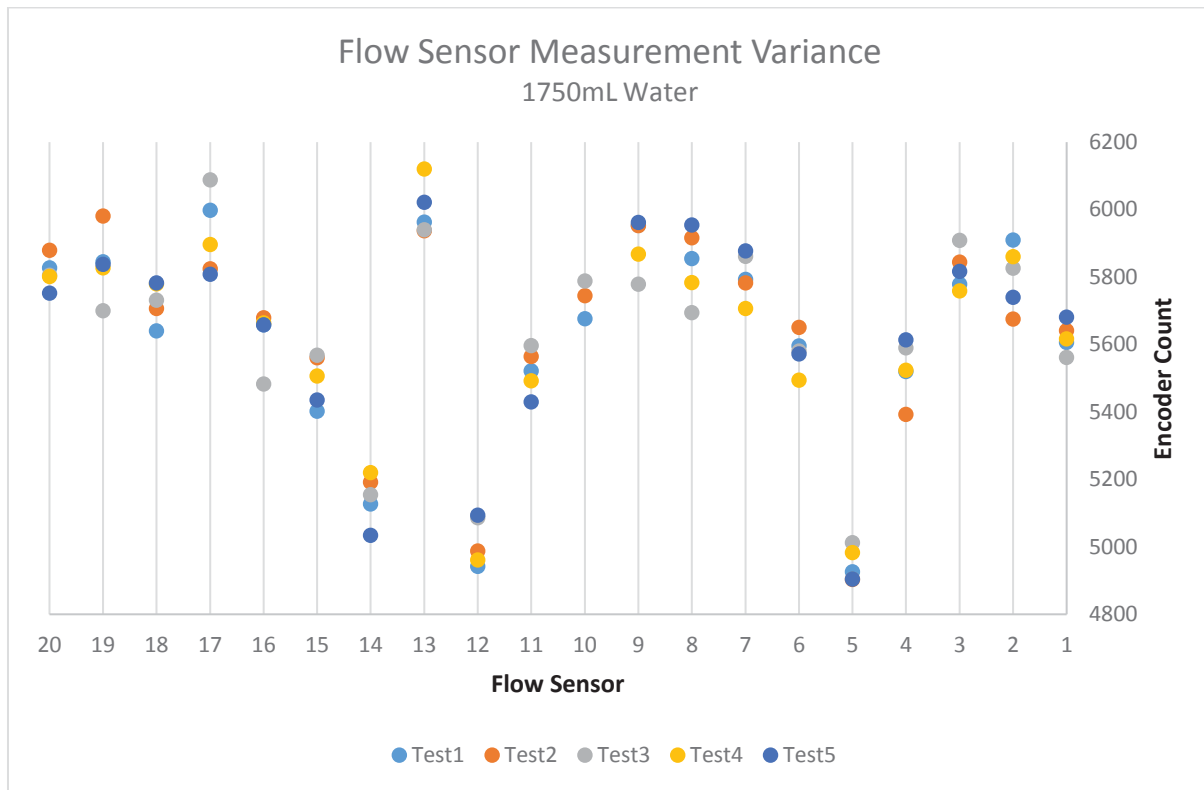


Figure 83 - Patternator Flow Calibration Variance

Figure 83 shows the flow-sensor count variation, both within each flow sensor and between all flow meters. Table 7 shows the mean, standard deviation and range as a percentage of mean, for each of the 20 sensors.

The sensors show a more or less normal distribution around a mean value. The maximum variation came from sensor 17 with a standard deviation of 119. The sensor with the greatest range was sensor 19 with a range (expressed as a percentage of mean reading) of 4.8%.

Table 7 - Patternator Flow Calibration Variance

	S20	S19	S18	S17	S16	S15	S14	S13	S12	S11
Average	5813	5838	5728	5923	5628	5495	5146	5996	5014	5521
Range(%)	2.2	4.8	2.5	4.7	3.5	3.0	3.6	3.1	3.0	3.0
StdDev	46.0	99.6	59.0	119.0	81.7	74.3	71.7	77.1	71.2	64.7

	S10	S9	S8	S7	S6	S5	S4	S3	S2	S1
Average	5038	5903	5841	5804	5579	4946	5528	5822	5802	5621
Range(%)	3.1	3.1	4.5	2.9	2.8	2.2	4.0	2.6	4.1	2.1
StdDev	60.2	79.0	104.2	68.1	56.5	49.3	85.9	58.9	94.3	43.9

Summarising the means of each flowmeter:

Mean: 5599
Range (% of mean): 19
Standard Deviation: 315

The mean value of all the flow meter means was 5599. The range of means expressed as a percentage of the mean was 19. In summary, the variation between meters is around 20%, however the variation within meters is less than 5%. This means each meter must be calibrated individually.

Once this data had been collected, it was possible to determine the calibration factor for each of the flow sensors individually. The known quantity of fluid (1750mL) was divided by the mean value for each of the sensors. This gives a calibration factor with a unit of mL per encoder tick. These values are shown in Table 8.

Table 8 - Sensor Calibration Factors

Sensor	S20	S19	S18	S17	S16	S15	S14	S13	S12	S11
mL/tick	0.30	0.30	0.31	0.30	0.31	0.32	0.34	0.29	0.35	0.32

Sensor	S10	S9	S8	S7	S6	S5	S4	S3	S2	S1
mL/tick	0.35	0.30	0.30	0.30	0.31	0.35	0.32	0.30	0.30	0.31

5.3.2.3 Patternator Discharge Characteristics

While the YF-S401 flow sensor is rated to a maximum flow rate of 6000mL/min, in this setup the maximum flowrate is determined by the maximum discharge rate caused by the water head. In this case, both the container and drain are at atmospheric pressure, so according to [37] the flow rate can be approximated by the equation:

$$Q = a \cdot C \cdot \sqrt{2gh}$$

Where: a is the orifice area, C is the discharge coefficient, g is the gravitation constant (9.81ms) and h is the fluid height. This equation does not take into account the pressure drop across the meter.

The bins are close to rectangular, but they are mounted sloping in two directions. This allows the fluid to flow to toward the flow sensor drain. However, it also means that the relationship between the volume and height of the fluid is not linearly related. Instead the cross section forms a tapered pyramid type shape which varies the cross sectional area with height.

During the calibration process described in section 5.3.2.2, time stamps were included with each of the encoder count data. This meant the flow rate characteristics of the discharge could be determined. Given the relatively low variation in sensor 1, the first test of this sensor was used to create a discharge plot. The encoder flow count was converted to a volume using the calibration factor value of 0.311 found in section 5.3.2.2. A moving average filter of 10 values was used to filter the data to remove high frequency noise. The plot is shown in Figure 84.

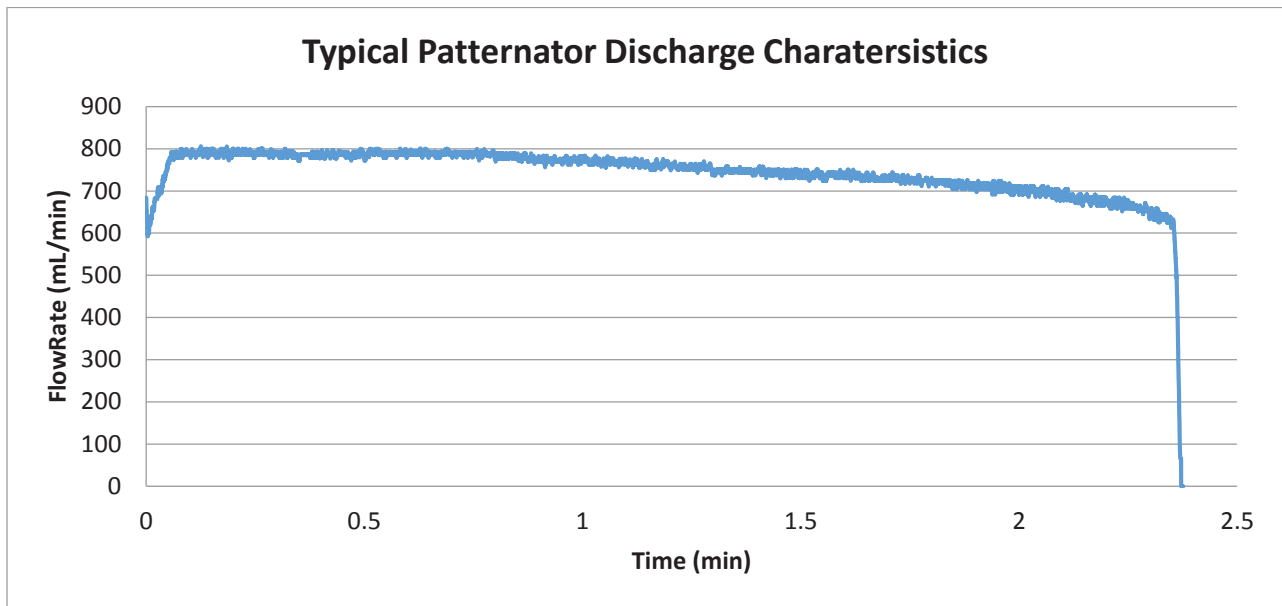


Figure 84 - Patternator Discharge Characteristics

The plot shows a gradual decay of flowrate from around 800mL/min to around 600mL/min then a sudden decrease in flowrate to zero.

The plot shows that the maximum flow rate is around 800mL/min. The patternator can handle this maximum flow rate in every 304mm section. That means that the patternator is capable of handling around 2.6L/min per meter, which equates to 16L/min spread uniformly across the 6.1m span.

From nozzle data obtained by Metalform (listed in table Table 2 from section 0) the spray density of each nozzle in their range was approximated. This is shown in Table 9.

Assuming a uniform spray distribution from each nozzle, the patternator is capable of quantifying the spray from the TF10 to TF40. However, the TF60, TF70 and TF80 would cause the containing bins to overflow.

Table 9 - Tow and Fert Nozzle Spray Density

Nozzle	Spray Rate(L/min)	Spread Width(metres)	Spray Density(L/min/meter)
TF10	10	14	0.71
TF15	15	14.5	1.03
TF20	20	15	1.33
TF30	30	16	1.88
TF40	40	17	2.35
TF50	50	18	2.78
TF60	60	19	3.16
TF70	70	20	3.50
TF80	80	21	3.81

5.3.3 Spray Characterisation Testing and Results

Initial tests were performed on the platform using a TF20 nozzle. The spray nozzle was positioned such that exactly half of the spray was collected by the platform. This was achieved with the nozzle midpoint over one edge of the platform because of nozzle symmetry. The entire half spray was captured by the platform. The testing process involved using the flow controller to maintain a flowrate for a period of two minutes and then step up the flow rate. This flow was tested on the TF20 nozzle for flowrates of 10, 12, 14, 16, and 18 litres per minute. These correspond to flowrates of 5,6,7,8 and 9 litres per minute on the platform.

The tests involved logging the flowmeter count for each flow sensor and a time stamp. From this data, the flowrate from each meter can be obtained. The totalised flowrate from each of the meters is shown in Figure 85 compared to the data obtained from the Tow and Fert machine.

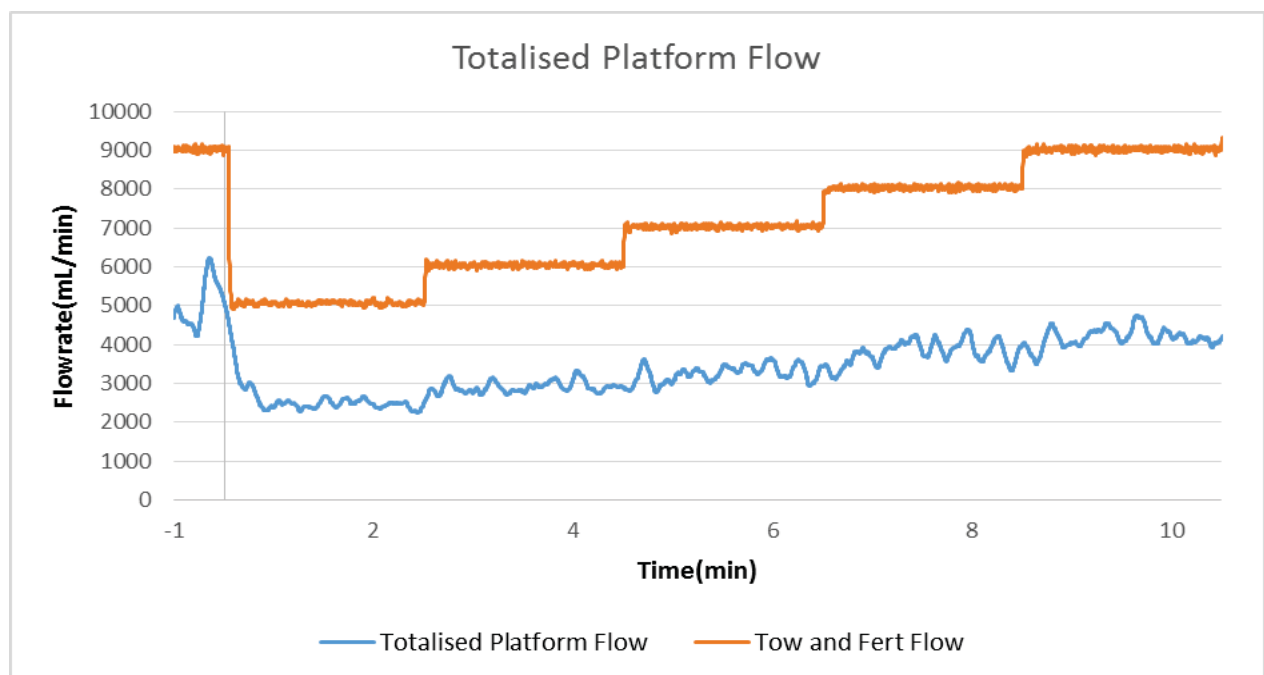


Figure 85 - Totalised Patternator Platform Flow

The plot shows that the reported flow rate does not come close to matching the actual flowrate. The totalised flow signal does increase with the expected data. However, the discrete steps of the input are not present in the signal.

When looking at the individual flow rates for the meters, it becomes more obvious why the totalised flowrate is not representative of the flow of the platform. The flowmeters are numbered away from the nozzle, therefore meter one corresponds to the 304mm section closest to the centre of the nozzle. Figure 86 shows the flowrates for the first six sections. During the tests, these sections had fluid flow. However, the flow in these six sections was not sufficient to allow for a continuous flow into the flowmeter. This intermittent flow means that the turbine in the flowmeter is not always spinning. When the turbine stops spinning more energy is needed to start it spinning again. This means that the encoder value no longer corresponds to the flow in the same way as the calibration data described in section 5.3.2. In Figure 86, the flow rate was calculated over a ten-second period.

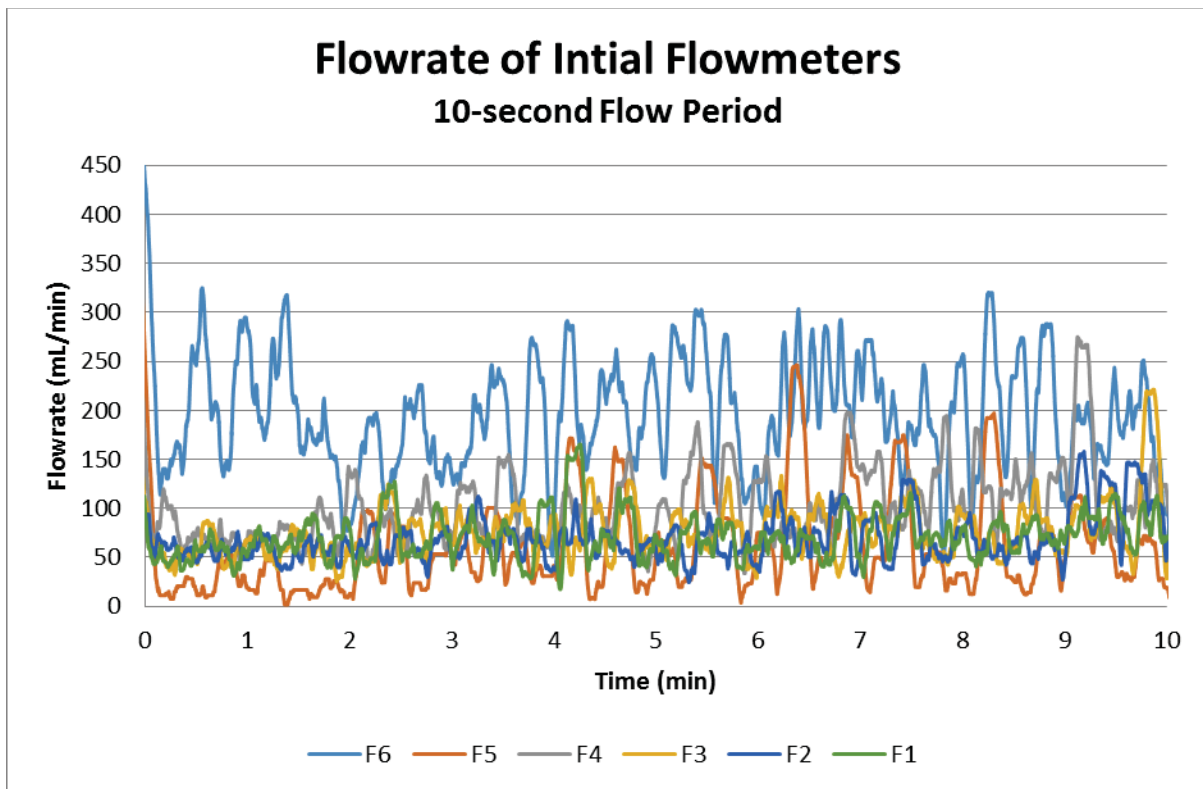


Figure 86 - Flowrate of first six spray sections

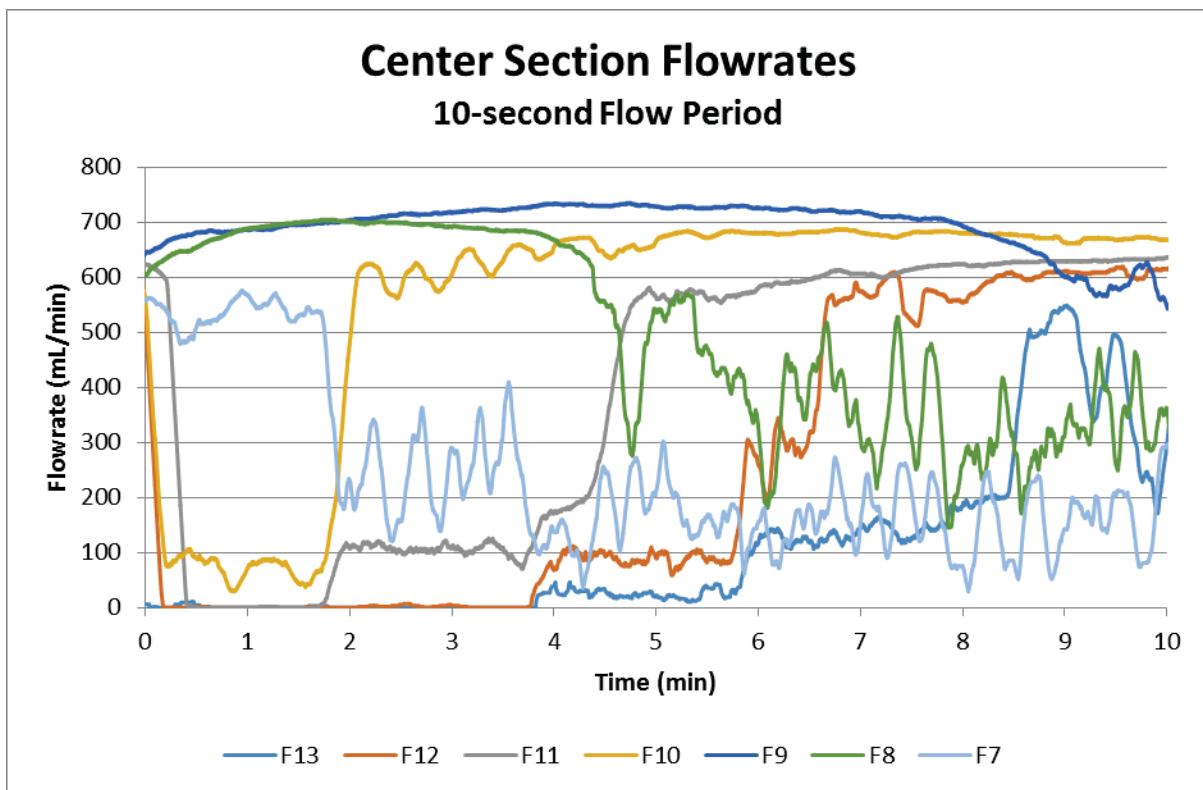


Figure 87 - Flowrate of central spray sections

Figure 87 shows the central sections of the platform for the same test. In these sections, the obtained data is quite different. The flow in these sections is sufficiently high to keep the flowmeters spinning.

Several interesting patterns are shown in Figure 87. Around the two-minute mark, the flow from section 7 reduces drastically while section 10 increases. Likewise, after the 4-minute mark the flow from section 8 drops off and the flow in section 11 increases. After the 6-minute mark the flow in section 12 increases. Finally, after the 8-minute mark the flow in section 13 increases and a slight decrease is shown in section 9.

This trend suggested there is a region in the spray that has a significantly higher flow and is around three sections (912mm) wide. This seems to be particularly prominent at lower flowrates.

To estimate the spray distribution, the flowrate was calculated using a period of 60 seconds instead of 10. This has the effect of reducing higher frequency noise, smoothing the pulsations. The flowrates of each section at each of the one, three, five, seven, and 9-minute marks were obtained. These times were chosen to give sufficient time for the flowrate to come to a steady state, after changing on the even minute marks.

These flowrates should correspond to the distributions at nozzle flow rates of 10, 12, 14, 16, and 18 litres per minute.

These distributions are shown in Figure 88.

It is important to note that the reported flow rates are highly nonlinear. The lower flowrates are underestimated. Table 10 shows the totalised values for each flowrate and compares it to the flowrate that was being applied to the platform.

Table 10 -Proportion of Flow Measured

Nozzle Flowrate	5021	6010	7012	8014	9005
Totalised Flowrate	2481	2906	3304	3918	4263
Percentage	49	48	47	49	47

The nozzle flowrate in this table is half of the flowrate measured by the Tow and Fert flow controller.

The table shows that only around 48% of the fluid being applied to the patternator is being accounted for in by the flowmeters. The majority of the discrepancy is likely to come from the meters with small, intermittent flows.

There are several ways this issue could be remedied. One possibility is that a biasing flow could be added to each section to ensure the flowmeters are always spinning. This flow bias could be removed from the reported flow rates to obtain the spray rate in each section. This method could work well for low flows. However, it would further reduce the upper limit of flow measurement discussed in section 5.3.2.3.

Another possibility would be the use of another style of flowmeter such as a tilting bucket flowmeter. This style of flow meter is particularly good for extremely low flow rates with a very low pressure requirement. However, these meters are not particularly good at higher flow rates [27]. A hybrid approach may be possible where the paddle wheel meters are used in conjunction with tilting bucket meters.

Spray Distributions of Different Flowrates

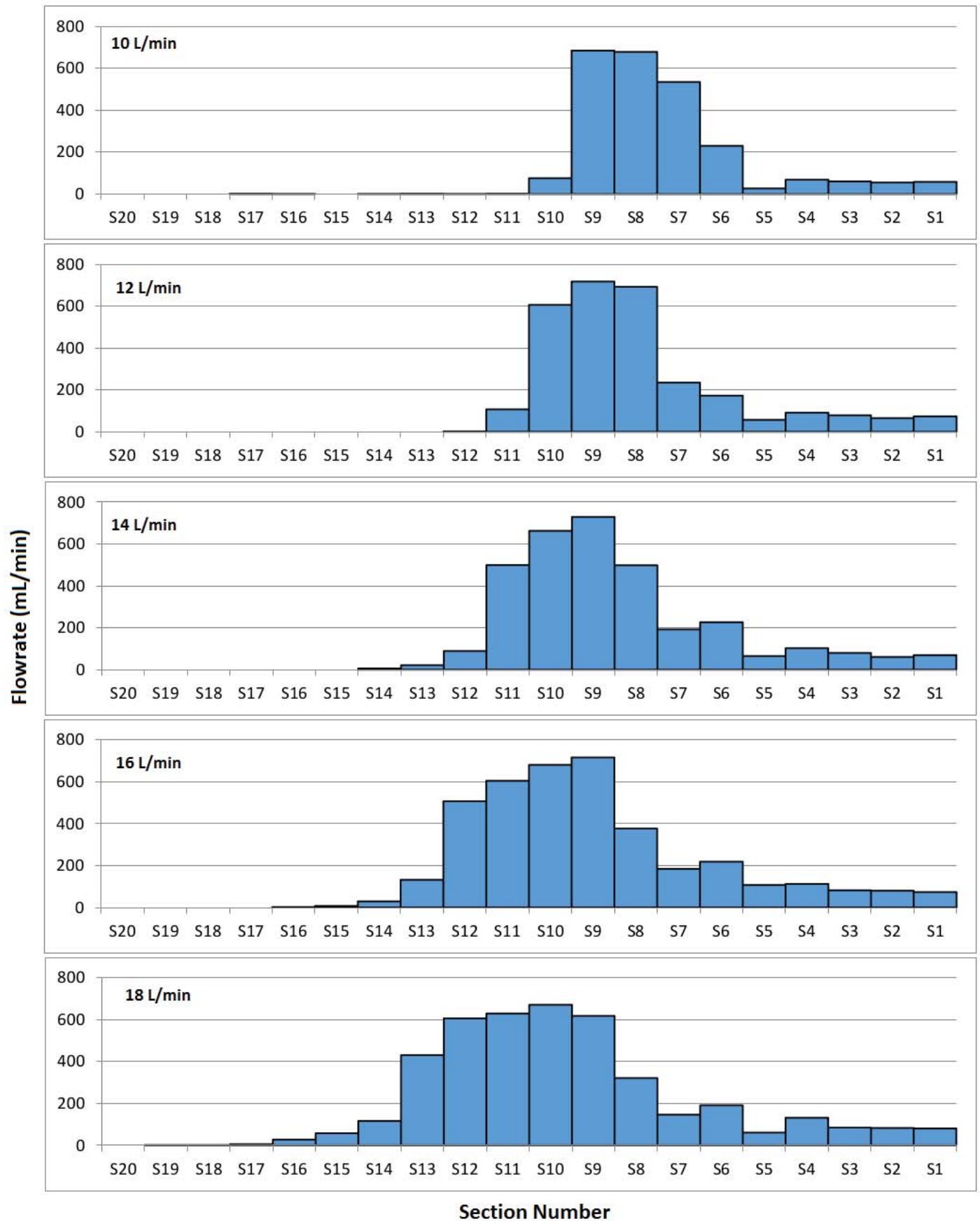


Figure 88 - Reported Spray Distributions – TF20 Nozzle at 10, 12, 14, 16 and 18 Litres per minute

6 Conclusions and Future Work

A pair of TUF2000M ultrasonic transit time flowmeters was tested to determine their suitability for the measurement of nozzle flowrate on the Tow and Fert machines. There are numerous advantages to these meters, including their low cost, their unobstructive nature and their theoretical independence on fluid properties. In practice, the signal to noise ratio was too low to allow for reliable flow measurement in this application. The source of this noise was investigated but could not be definitively located. After testing the TUF2000M meters, a ZD1200 flowmeter was installed into the machine. This is a turbine-based flowmeter and would not be suitable for use with the wide variety of fluids and suspensions the Tow and Fert machines are capable of spraying. These erosive and potentially corrosive mixtures mean that this meter is not suitable in any commercial application of the machines. However, it was suitable for testing and research purposes. It is possible these meters could be used to create models of the flow of different fluids. If the models can accurately describe the fluid flowrates given the fluid properties and flow valve position, a controller without feedback may be possible.

A flowrate controller has been developed to fit onto the existing Tow and Fert machines with minimal modification. This controller is capable of communicating with the TUF2000M meters and measuring flowrates from the ZD1200 sensors. It is also capable of serial communication using RS485 lines, USB and Bluetooth. Preliminary tuning of the controller has been performed. This tuning was performed using water as the spraying fluid. Though a full PID controller has been implemented, this initial tuning found that purely proportional control was sufficient for testing. The software implementation means that the controller can easily be modified. Speed measurement of the machine was not installed during testing. However, the controller was designed to be able to accept speed signals from various common speed measurement devices. This would require minimal modification to the existing controller code.

Several methods of continuously measuring the spray distribution were investigated. A modified version of the scanning patternator was then tested. In this case, the 'scanning' element was kept stationary and the machine was scanned over it. The scanning element used sensitive load cells to measure the force applied by the fluid spray. There were several issues with this approach. Firstly, the platform was not sufficiently large to capture the entire fluid spray. This caused two different patterns of spray to appear in the test results. The second issue was the effect of noise. Because the testing required a large area in which to manoeuvre the testing was conducted outside. The scanning element was extremely sensitive to wind. Even when tests were conducted on calm days, the noise was significant.

Finally, a stationary patternator was developed. This patternator uses an array of small paddle wheel meters, which measure the flowrates of each section of the patternator. Because the machine is stationary in this test setup, the testing could be conducted indoors. The patternator is approximately 6m wide and 3m deep. This is sufficiently large to capture an entire half of the spray from every nozzle. Because of the symmetry of each nozzle, capturing half the spray pattern will fully define the distribution. After calibrating each flowmeter of the patternator individually, the maximum flow the patternator could handle was determined. This maximum flow was found to be around 2.6 Litres per minute per meter. This allows testing of 5 of the 9 nozzles in the range. This could be remedied by increasing the height of each fluid collection unit.

Testing the stationary patternator revealed that there was intermittent flow in sections of low flow. This intermittent flow cannot be accurately measured by the paddle wheel meters. Because of this, the flow being measured by the patternator was only around 50% of the flow being applied. This

issue could be resolved in a couple of ways. A biasing flow could be used to ensure that the meters continue to spin regardless of the low flowrate. However, this would further reduce the number of nozzles that could be tested. Another option is to investigate other flow meter types such as tipping bucket meters.

Despite this issue, it was obvious from the testing that the nozzles are not uniformly distributing fluid within the spray. There are lobes of higher spray at the edge of the spray pattern.

This work represents a good first step toward the development of the Tow and Fert range into precision agricultural machines.

References

- [1] C. Trampusch and D. C. Spies, "Agricultural Interests and the Origins of Capitalism: A Parallel Comparative History of Germany, Denmark, New Zealand, and the USA," *New Political Economy*, pp. 918-942, 2014.
- [2] Statistics New Zealand, "Topic 5: Land use," in *Measuring New Zealand's Progress Using a Sustainable Development Approach: 2008*, Wellington, Statistics New Zealand, 2008.
- [3] F. R. Troeh and L. M. Thompson, *Soils and Soil Fertility*, Ames: Blackwell Publishing, 2005.
- [4] Waikato Regional Council, "Fertiliser use on farms," 21 September 2016. [Online]. Available: <http://www.waikatoregion.govt.nz/Environment/Environmental-information/Environmental-indicators/Land-and-soil/Soil/fertiliser-use-report-card/>.
- [5] A. Srinivasan, Ed., *Handbook of Precision Agriculture - Principles and Applications*, New York: The Haworth Press, 2006.
- [6] T. Brase, *Precision Agriculture*, New York: Thomson Delmar Learning, 2006.
- [7] A. Sharda, J. P. Fulton, T. P. McDonald and C. J. Brodbeck, "Real-time nozzle flow uniformity when using automatic section control on agricultural sprayers," *Computers and Electronics in Agriculture*, vol. 79, pp. 169-179, 2011.
- [8] R. N. Klein, "Spray Boom Set-up on Field Sprayers," *University of Nebraska-Lincoln Extension*, September 2004.
- [9] TeeJet Technologies, "Teejet Boom Components," [Online]. Available: http://www.teejet.com/literature_pdfs/catalogs/C51A-M/boom_components.pdf. [Accessed 20 October 2016].
- [10] Ballance Agri-Nutrients, "Foliar uptake of nitrogen," 04 April 2014. [Online]. Available: <http://www.ballance.co.nz/Our-Science/Library/Articles/Dairy/Foliar-uptake-of-nitrogen>. [Accessed 20 October 2016].
- [11] R. Grisso, P. Hipkins, S. D. Askew, L. Hipkins and D. McCall, "Nozzles: Selection and Sizing," *Virginia Cooperative Extension P442-032*, May 2013.
- [12] Y. Guan, D. Chen, H. Ketai, Y. Liu and L. Li, "Review on Research and Application of Variable Rate Spray in Agriculture," in *10th IEEE Conference On Industrial Electronics And Applications*, Auckland, 2015.
- [13] D. Nuytens, K. Baetens, M. De Schamphelleire and B. Sonck, "Effect of nozzle type, size and pressure on spray droplet characteristics," *Biosystems Engineering*, vol. 97, no. 3, pp. 333-345, 2007.
- [14] H. Liu, H. Zhu, Y. Shen, Y. Chen and H. E. Ozkan, "Development of digital flow control system for multi-channel variable-rate sprayer," *Transactions Of The Asabe*, vol. 57, no. 1, pp. 273-281, 2014.
- [15] D. K. Giles and J. A. Comino, "Droplet size and spray pattern characteristics of an electronic flow controller for spray nozzles," *Journal of Agricultural Engineering Research*, vol. 47, no. 1, pp. 249-267, 1990.
- [16] H. R. Ghasemzadeh and D. D. Humburg, "Using variable spray angle fan nozzle on long spray booms,"

Agricultural Engineering International: Cigr Journal, vol. 18, no. 1, pp. 82-90, 2016.

- [17] W. M. Porter, J. A. Rascon, Y. Shi, R. K. Taylor and P. A. Weckler, "Laboratory Evaluation of a Turn Compensation Control System for a Ground Sprayer," in *Applied engineering in agriculture*, Kansas City, 2013.
- [18] C-Dax Ltd, "Goldline 1500L Trailed Sprayer," [Online]. Available: http://www.c-dax.co.nz/index.php?page=shop/flypage&product_id=17301. [Accessed 20 October 2016].
- [19] C-Dax Ltd, "Goldline Hi-Spec," [Online]. Available: http://www.c-dax.co.nz/index.php?page=shop/flypage&product_id=1000193. [Accessed 20 October 2016].
- [20] Metalform (Dannevirke) Ltd, "Tow and Fert - The Product Series," [Online]. Available: <http://towandfarm.co.nz/shop/tow-and-fert/>. [Accessed 20 October 2016].
- [21] Metalform (Dannevirke) Ltd, "Tow and Fert Multi 1000," [Online]. Available: <http://towandfarm.co.nz/product/multi-1000/>. [Accessed 20 October 2016].
- [22] D. Johnson, "Differential Flowmeters: Simple Can Be Better," *Control Engineering*, pp. 91-92, September 2000.
- [23] E. L. Upp and P. J. LaNasa, *Fluid Flow Measurement : A Practical Guide to Accurate Flow Measurement*, Boston: Gulf Professional Publishing, 2002.
- [24] T. W. Lee, *Thermal and Flow Measurements*, Boca Raton: CRC Press, 2008.
- [25] R. C. Baker, "Turbine and related flowmeters: I. Industrial practice," *Flow Measurement and Instrumentation*, pp. 147-161, 1991.
- [26] EnggCyclopedia, "Mechanical flow measurement devices," [Online]. Available: <http://www.enggcyclopedia.com/2011/07/mechanical-flow-measurement-devices/>. [Accessed 20 October 2016].
- [27] R. C. Baker, *Flow Measurement Handbook*, Cambridge: Cambridge University Press, 2005.
- [28] Blue-White Industries Ltd, "Paddlewheel Flowmeters and why they are popular," [Online]. Available: <http://blue-white.com/paddlewheel-flowmeters-and-why-they-are-popular/>. [Accessed 16 October 2016].
- [29] Pioneer Systems, "Micro Hydro," [Online]. Available: http://pioneer-sys.net/_borders/bottom.htm. [Accessed 12 October 2016].
- [30] D. Ginesi and C. Annarummo, "Application and installation guidelines for volumetric and mass flowmeters," *ISA Transactions*, pp. 61-72, 1994.
- [31] Univeristy of Michigan - Chemical Engineering Department, "ENCYCLOPEDIA OF CHEMICAL ENGINEERING EQUIPMENT," [Online]. Available: <http://encyclopedia.che.engin.umich.edu/Pages/Flowmeters/PositiveDisplacement/PositiveDisplacement.html>. [Accessed 13 October 2016].
- [32] R. A. Furness, "The principles of flowmeter selection," *Flow Measurement and Instrumentation*, pp. 233-242, 1991.
- [33] ABB, "Electromagnetic flowmeters," [Online]. Available: <http://new.abb.com/products/measurement->

- products/flow/electromagnetic-flowmeters. [Accessed 17 October 2016].
- [34] Engineering Measurements Company, "Sono-Trak Operation and Maintenance Manual," [Online]. Available: <http://www.helgem.com.tw/EMCO/990632%20Rev.%20A.pdf>. [Accessed 18 October 2016].
- [35] N. Heywood, "On-line Monitoring of Slurry Flows in the Process Industries," in *10th T&S Conference*, Wroclaw, 2000.
- [36] TUF, "Ultrasonic Flow Meter User Manual - TUF2000M," [Online]. Available: <https://github.com/gambit-labs/tuf-2000m/blob/master/docs/tuf-2000m.pdf>. [Accessed 21 Jul 2016].
- [37] V. L. Steeter, E. B. Wylie and K. W. Bedford, *Fluid mechanics*, Boston: WCB/McGraw Hill, 1998.
- [38] Jaycar Electronics, "ZD1200 Flow Sensor," [Online]. Available: https://www.jaycar.com.au/medias/sys_master/images/h83/h55/8840881373214/ZD1200-dataSheetMain.pdf. [Accessed 26 August 2016].
- [39] B. Drury, *Control Techniques Drives and Controls Handbook*, 2 ed., London: The Institution of Engineering and Technology, 2009.
- [40] Arduino, "Arduino MEGA 2560," [Online]. Available: <https://www.arduino.cc/en/Main/arduinoBoardMega2560>. [Accessed 26 August 2016].
- [41] Exar Corporation, *SP483 / SP485 Low Power Half-Duplex RS-485 Transceivers*, Freemont CA: Exar Corporation, 2006.
- [42] Pololu Corporation, "VNH2SP30 Motor Driver Carrier MD01B," [Online]. Available: <https://www.pololu.com/product/706>. [Accessed 01 Oct 2016].
- [43] Itead Studio, "Serial Port Bluetooth Module (Master/Slave) : HC-05," [Online]. Available: [https://www.itead.cc/wiki/Serial_Port_Bluetooth_Module_\(Master/Slave\)_:_HC-05](https://www.itead.cc/wiki/Serial_Port_Bluetooth_Module_(Master/Slave)_:_HC-05). [Accessed 2 Oct 2016].
- [44] King Saud University, "Spray Patternator," [Online]. Available: <http://faculty.ksu.edu.sa/21293/Picutre%20Library/Forms/DispForm.aspx?ID=18>. [Accessed 9 October 2016].
- [45] C. Zhai, C. Zhao, X. Wang, N. Wang, W. Zou and W. Li, "Two-Dimensional Automatic Measurement for Nozzle Flow Distribution Using Improved Ultrasonic Sensor," *Sensors*, pp. 26353-26367, 2015.
- [46] G. Matthews, R. Bateman and P. Miller, in *Pesticide Application Methods, Fourth Edition*, Hoboken, Wiley-Blackwell, 2014, pp. 125-157.
- [47] Advanced Agricultural Measurement Systems, "AAMS spray scanner," [Online]. Available: <http://www.aams.be/engels/product.asp?product=34>. [Accessed 10 October 2016].

Appendices

Appendix A Actuator Class Code:

```
#include "actuator.h"

Actuator::Actuator() {
    position = 0;
}

int Actuator::setPos(int pos) {
    long pPos = ((long)maxPosition * pos) / 500;
    if (pPos < 0)
        pPos = 0;
    else if (pPos > maxPosition)
        pPos = maxPosition;

    desiredPosition = pPos;
    return pPos;
}

int Actuator::getPos() {
    return ((long)position * 500) / maxPosition;
}

void Actuator::setSpeed(int speed) {
    if (speed > 0)
        direction = 1;
    else if (speed == 0)
        //direction = 0;
    else {
        direction = -1;
        speed = -speed;
    }
    if (speed > MAXPWM)
        speed = MAXPWM;
    digitalWrite(MOTA, direction == 1);
    digitalWrite(MOTB, direction == -1);
    analogWrite(PWM, speed);
}

/* findLimits
 * this function is used to find the upper limit of the linear actuator
and set the zero point
*/
void Actuator::findLimits() {
    int oldActPos;
    //run backwards
    setSpeed(255);
    Serial.println("Running backward");
    //keep running backwards until the actuator stops
    do {
        oldActPos = position;
        delay(100);
    } while (oldActPos != position);

    //found the zero of the actuator
    position = 0;

    //run forward
    setSpeed(-255);
    Serial.print("Running forward:  ");
    delay(1000);
    //keep running until the actuator stops
```

```

do {
    oldActPos = position;
    delay(100);
} while (oldActPos != position);
//found the upper limit of the actuator
maxPosition = -position;
position = 0;
Serial.println(maxPosition);
//we can stop now
setSpeed(0);
}

int Actuator::update()
{
    float posError = (desiredPosition - position);
    int output;
    //intPosError += (posError > 0) - (posError < 0);
    output = posError / PGAIN ;//+ intPosError / IGAIN;

    if (output > 0 && output < MINPWM)
        output = MINPWM;
    else if (output < 0 && output > -MINPWM)
        output = -MINPWM;

    setSpeed(output);
    return output;
}

```

Appendix B: TUF2000M Class Code:

```
#include "tuf2000m.h"
#include <util/crc16.h>

uint8_t Tuf2000m::readReg(uint8_t networkId, uint16_t regAdd, uint16_t
regCount) {
    uint16_t ul6CRC = 0xFFFF;
    packet[0] = networkId;
    //modbus command to read a register
    packet[1] = 3;
    //two bytes for register address and register count
    packet[2] = highByte(regAdd);
    packet[3] = lowByte(regAdd);
    packet[4] = highByte(regCount);
    packet[5] = lowByte(regCount);
    //calculate the CRC:
    for (int i = 0; i < 6; i++)
        ul6CRC = _crc16_update(ul6CRC, packet[i]);
    //append the CRC to the packet
    packet[6] = lowByte(ul6CRC);
    packet[7] = highByte(ul6CRC);

    //Serial.print("\nSending: "); for (int i = 0; i < 8;
i++){Serial.print(packet[i]);Serial.print(" "); }

    digitalWrite(DE_485, HIGH);
    delay(2);
    s485.write(packet, 8);
    s485.flush();
    digitalWrite(DE_485, LOW);

    uint8_t receivedBytes = s485.readBytes(packet, 2 * regCount + 5);
    dataLength = packet[DATALENGTH];
    //Serial.print("\nReceiving: "); for ( int i = 0; i < 2 * regCount + 5;
i++) {Serial.print(packet[i]);Serial.print(" "); }Serial.println();

    //check to see if we got any data and then see if we got what we asked
for
    if (receivedBytes != 0 && dataLength == 2 * regCount)
        return dataLength;
    else
        Serial.print("Error getting register data from");
        Serial.println(networkId);
        return 0;
}

float Tuf2000m::getFlowRate(uint8_t networkId) {
    union Data {
        double f;
        byte b[4];
    } data;

    if (readReg(networkId, 1, 2))
    {
        data.b[0] = packet[DATASTART + 3];
        data.b[1] = packet[DATASTART + 2];
        data.b[2] = packet[DATASTART + 1];
    }
}
```

```

        data.b[3] = packet[DATASTART];
        return data.f;
    }
}

float Tuf2000m::getDeltaTransitTime(uint8_t networkId) {
    union Data {
        double f;
        byte b[4];
    } data;

    if (readReg(networkId, 83, 2))//could be 82
    {
        data.b[0] = packet[DATASTART + 3];
        data.b[1] = packet[DATASTART + 2];
        data.b[2] = packet[DATASTART + 1];
        data.b[3] = packet[DATASTART];
        return data.f;
    }
    else
        return 0.0;
}

float Tuf2000m::getTotalTransitTime(uint8_t networkId) {
    union Data {
        double f;
        byte b[4];
    } data;

    if (readReg(networkId, 81, 2))//could be 80
    {
        data.b[0] = packet[DATASTART + 3];
        data.b[1] = packet[DATASTART + 2];
        data.b[2] = packet[DATASTART + 1];
        data.b[3] = packet[DATASTART];
        return data.f;
    }
    else
        return 0.0;
}

int Tuf2000m::getSignal(uint8_t networkId) {
    if (readReg(networkId, 91, 1))
    {
        return packet[DATASTART + 1];
    }
}

int Tuf2000m::getScreen(uint8_t networkId) {
    if (readReg(networkId, 256, 32))
    {
        for (int i = 0; i < 32; i+=2) {
            Serial.write(packet[DATASTART + i+1]);
            Serial.write(packet[DATASTART + i]);
        }
        Serial.print('\n');
        for (int i = 32; i < 64; i+=2) {
            Serial.write(packet[DATASTART + i+1]);

```

```
        Serial.write(packet[DATASTART + i]);  
    }  
    Serial.print("\n\n");  
    //return packet[DATASTART+1];  
}  
}
```